nature communications

Article

https://doi.org/10.1038/s41467-022-34355-w

Global and regional ecological boundaries explain abrupt spatial discontinuities in avian frugivory interactions

Received: 10 March 2022

Accepted: 20 October 2022

Published online: 14 November 2022

Check for updates

A list of authors and their affiliations appears at the end of the paper

Species interactions can propagate disturbances across space via direct and indirect effects, potentially connecting species at a global scale. However, ecological and biogeographic boundaries may mitigate this spread by demarcating the limits of ecological networks. We tested whether large-scale ecological boundaries (ecoregions and biomes) and human disturbance gradients increase dissimilarity among plant-frugivore networks, while accounting for background spatial and elevational gradients and differences in network sampling. We assessed network dissimilarity patterns over a broad spatial scale, using 196 quantitative avian frugivory networks (encompassing 1496 plant and 1004 bird species) distributed across 67 ecoregions, 11 biomes, and 6 continents. We show that dissimilarities in species and interaction composition, but not network structure, are greater across ecoregion and biome boundaries and along different levels of human disturbance. Our findings indicate that biogeographic boundaries delineate the world's biodiversity of interactions and likely contribute to mitigating the propagation of disturbances at large spatial scales.

Abiotic gradients underlie the existence of a wide array of natural ecosystems, which are the cornerstone of biological diversity on Earth[1,2]. Ecoregions, defined as regional-scale terrestrial ecosystems[1], delineate regional discontinuities in the environment and in species composition[3,4], whereas biomes mark ecological boundaries at a global scale, such that ecoregions are nested within biomes[1,3] (Supplementary Fig. 1). Accordingly, ecoregion and biome maps have been widely used for guiding conservation planning[3,5], but it has only recently been shown that distinct ecoregions truly represent sharp boundaries for species composition across several taxa[4].

There has been growing recognition that interactions among species are critical for biodiversity and ecosystem functioning[6] and represent an important component of biodiversity themselves, such that interactions may disappear well before the species involved[7]. Species interactions also provide a pathway for the propagation of disturbances via direct and indirect effects, such as secondary extinctions and apparent competition[8,9], with indirect effects of species on others potentially being as important as direct effects[10]. Moreover, adjacent habitats can share many interactions and function as a single dynamic unit[9,11], suggesting that the habitat boundaries typically used by ecologists to delineate interaction networks may not represent true boundaries[11]. Thus, both natural and human disturbances in local communities of interacting species might reverberate and affect ecosystem functioning at multiple sites[12,13], with widespread interactions potentially connecting species at a global scale[12]. However, the spread of disturbances may be hindered when ecological interactions are arranged discontinuously into distinct compartments[14]. Despite this importance, we are only beginning to understand the connections among ecological networks at very large scales[12,13], and it remains unknown whether predictable, large-scale discontinuities in interaction network composition (i.e., the identity of interactions that comprise a local network) exist across ecoregions and biomes. Such discontinuities would mark true network boundaries, and could thus act as a barrier to the global spread of disturbances.

Because species tend to be replaced across ecosystems[2,4] and environmental conditions can favor some types of interactions over

e-mail: martinslucas.p@gmail.com; jason.tylianakis@canterbury.ac.nz

others (e.g., by altering the quality and detectability of interaction partners)[15], we hypothesize that ecoregions and biomes delineate the large-scale distribution of species interactions. Specifically, we expect to find sharp differences in the composition of species interactions when crossing ecoregion and biome boundaries, beyond what would be expected from spatial processes alone—which are known to drive gradual changes in species and interaction composition[15]. Indeed, distance–decay relationships have been demonstrated across spatial and elevational gradients not only for species[16], but also for ecological networks[17–19], and likely result from dispersal limitation and increasing environmental dissimilarity with increasing geographic distance[15,16]. Alternatively, ecological boundaries might be blurred by the processes of species and interaction homogenization (i.e., increasing similarity among biological communities), which accompany human disturbances such as land-use change and biotic invasions[12,20]. Thus, an alternative hypothesis would be that shared interactions and biotic homogenization prevent any sharp discontinuities in interaction composition. If this is true, we expect to find a gradual decrease in the similarity of interactions with increasing spatial distance, but no abrupt differences in the identity of interactions from networks located at distinct ecoregions and biomes.

Here we evaluate whether significant changes in the composition of species, the composition of interactions, and the structure of local networks of avian frugivory are explained by large-scale ecological boundaries (ecoregions and biomes) and human disturbance gradients, while accounting for background spatial and elevational effects. Given known patterns of species turnover across environmental gradients[16], we hypothesize a similar pattern of turnover in interaction composition (hereafter, interaction dissimilarity), which could lead to changes in the whole structure of networks (i.e., changes in the arrangement of interactions among species), represented here by a metric combining several descriptors of network architecture, which we call network structural dissimilarity (see "Methods" for more details). Notably, environmental conditions may also affect niche partitioning and interaction specialization, potentially explaining further structural differences among ecological networks from distinct habitats and biogeographical regions[15,21,22]. We focused on avian frugivory networks, that is, local communities of interacting bird and fruiting plant species, because of their importance for seed dispersal[23], promoting species diversity[24] and regenerating degraded ecosystems[25]. As such, mapping the global distribution of plant-frugivore interactions will be crucial to ensure ecosystem functioning and resilience in a context of increasing global changes.

In this study, we show that both ecoregion and biome boundaries explain abrupt spatial discontinuities in the composition of species and their interactions within plant-avian frugivore networks. These effects are detectable on top of the effects of spatial and elevational gradients and after accounting for differences in sampling effort and methods. Similarly, we find evidence that human disturbance gradients also promote large-scale shifts in species and interaction composition. Interestingly, despite the large (often complete) changes observed in the composition of species and interactions, the structure of avian frugivory networks is relatively consistent across large-scale environmental gradients. Our results reveal that ecoregion and biome boundaries delineate the world's biodiversity of interactions and may therefore contribute to mitigating the spread of disturbances across the global network of avian frugivory.

Results

Overview of the analysis

To test our hypotheses, we assembled a large-scale database comprising 196 quantitative local networks of avian frugivory (with 9819 links between 1496 plant and 1004 bird species) distributed across 67 ecoregions, 11 biomes, and 6 continents (Supplementary Figs. 1 and 2; Supplementary Table 1). Local networks are composed of nodes—plant and bird species, connected by links whenever two species interact with each other. Each local network is represented by a matrix, with plants and birds on rows and columns, respectively, and cell values describing the weighted network links—the number of fruit-feeding events (i.e., interaction frequency) between a plant and bird species. To ensure that our results would not be driven by taxonomic uncertainty, we standardized the taxonomy of plant and bird species in our local networks. For this, we extracted the frugivore and plant species lists from all networks and performed a series of filters to remove non-existent species names (e.g., morphospecies labels) and standardize synonymous names according to reference databases (steps and examples are presented graphically in Supplementary Figs. 3–6). To account for sampling differences between networks, we controlled statistically for network sampling metrics (i.e., hours, months, years, intensity and methods) in our analyses (see Network sampling dissimilarity section in "Methods"; relationships among sampling variables and network metrics are presented in Supplementary Figs. 7 and 8; variables are described in Supplementary Tables 2 and 3).

We generated several distance matrices ($N \times N$, where N is the number of local networks in our dataset) to be our variables in the statistical models. Specifically, we used ecoregion, biome, local human disturbance (measured using the human footprint index[26]), spatial, elevation and sampling-related distance matrices as predictor variables, and facets of network dissimilarity (i.e., species turnover, interaction dissimilarity, and network structural dissimilarity) as response variables (see a summary of our methods in Fig. 1). By evaluating these three different facets of network dissimilarity, we were able to assess the extent to which changes in species composition are associated with changes in both the identity of component interactions (interaction dissimilarity) and the architecture of local networks (network structural dissimilarity, which may remain the same despite turnover of species and interactions[27,28]). Together these facets contribute to greater understanding of the scale at which one ecological network ends and another begins, and how/why networks vary across large spatial scales[15,27]. We tested the significance of our predictor variables by employing a combination of Generalized Additive Models (GAMs, to allow for non-linear relationships among variables)[29] and Multiple Regression on distance Matrices (MRM, to account for the non-independence associated with pairwise comparisons of local networks)[30]. Essentially, this analysis is equivalent to a GAM, but where the predictor and response variables are distance matrices and the non-independence of distances from each local network is accounted for in the hypothesis testing by permuting the response matrix (see more details in the Statistical analysis section in "Methods"). Finally, we used deviance partitioning analyses to explore the unique and shared contributions of our predictor variables to explaining the variance in network dissimilarity. We did this by fitting reduced models (i.e., GAMs where one or more predictor variables of interest were removed) and comparing the explained deviance.

Species turnover across networks

Using a binary approach—in which two ecological networks located within the same ecoregion/biome were given a value of zero, otherwise a one—to generate our ecoregion and biome distance matrices, we found that the turnover of plant and frugivorous-bird species composition was strongly affected by ecoregion ($t = -38.093$; $P = 0.001$) and biome ($t = -8.799$; $P = 0.001$) boundaries (Supplementary Table 4). Trends were qualitatively similar when we assessed the effect of these ecological boundaries using a quantitative approach based on the environmental dissimilarity between ecoregions and biomes (Supplementary Table 5; Supplementary Figs. 9a-b). Similarly, there was an overall trend of networks located at different positions along the human disturbance gradient having different species composition

https://doi.org/10.1038/s41467-022-34355-w

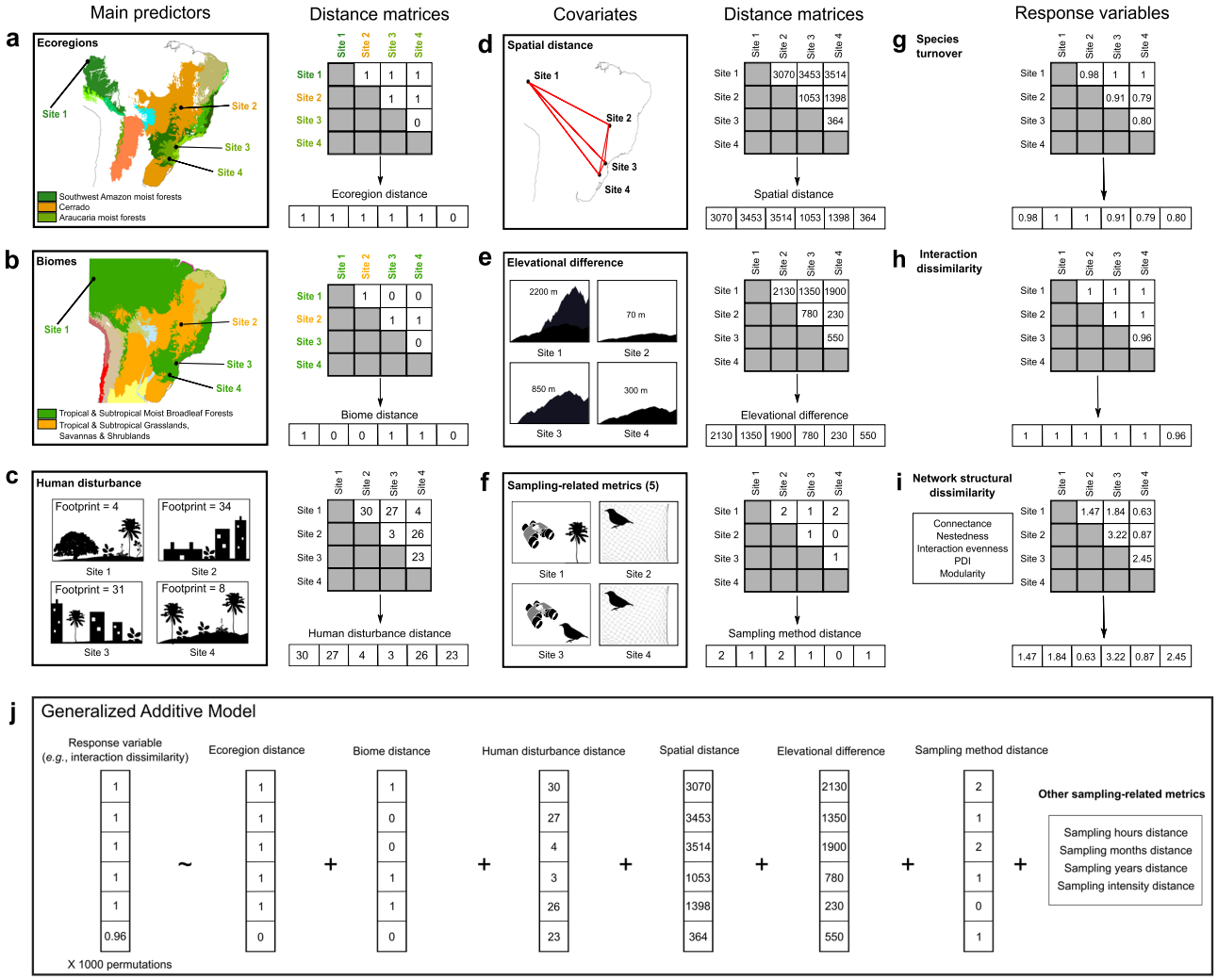

Fig. 1 | Our approach for evaluating the multiple predictors of network dissimilarity at large spatial scales. We used several distance matrices ($N \times N$, where N is the number of local networks in our dataset) as variables in the statistical models. **a**, **b** Maps show examples of ecoregions and biomes (colors of shaded areas) represented in our dataset. Points indicate the locations of four network sites used to illustrate how we generated our distance matrices (see Fig. 2 to visualize the locations of all network sites in our dataset). Ecoregion and biome distance matrices were generated using both a binary (shown in the figure) and a quantitative approach (generated by measuring the environmental dissimilarity between ecoregions/biomes; see "Methods"). Because ecoregions are nested within biomes, network sites located within the same ecoregion are always within the same biome, but the opposite is not necessarily true; see, for example, the comparison between network site 1 and network site 3, which involves two ecoregions (Southwest Amazon moist forest and Araucaria moist forest) from the same biome (Tropical & Subtropical Moist Broadleaf Forests). **c** The human disturbance distance matrix was generated by calculating the absolute difference between local-scale human footprint values around each network site. **d**–**f** Spatial distance, elevational difference and sampling-related distance metrics (i.e., sampling methods, hours, months, years, and intensity) were used as covariates in our models to control for distance-decay effects and differences in network sampling. Note that even though we only depict the sampling method distance matrix in **f**, all sampling-related metrics were used as predictors in the models. **g**–**i** We used three different facets of network dissimilarity (i.e., species turnover, interaction dissimilarity and network structural dissimilarity) as response variables (see Network dissimilarity section in "Methods"). **j** We tested the significance of our predictor variables by employing a combination of Generalized Additive Models (GAM) and Multiple Regression on distance Matrices (MRM). In this analysis, the non-independence of distances from each local network is accounted for by performing 1000 permutations of the response matrix. Ecoregions and biomes were defined based on the map developed by Dinerstein et al.[3] (available at https://ecoregions.appspot.com/ under a CC-BY 4.0 license). Bird and plant silhouettes were obtained from http://phylopic.org under a Public Domain license.

($F = 28.504$; $P = 0.001$) (Supplementary Fig. 9c). As expected, spatial and elevational gradients also promoted species turnover across networks (Supplementary Tables 4 and 5), with spatial distance alone accounting for the greatest proportion of deviance explained in species turnover (12.9%), followed by the shared contribution of spatial distance and ecoregion boundaries (11.2%) (Supplementary Fig. 10).

Interaction dissimilarity

Plant-frugivore interaction dissimilarity increased significantly across ecoregions ($t = -36.401$; $P = 0.001$), biomes ($t = -3.323$; $P = 0.044$) and different levels of human disturbance ($F = 29.988$; $P = 0.001$), even after accounting for the effects of spatial distance, elevational differences, and sampling-related metrics (Table 1). Similar results were found when we performed the analyses using quantitative versions of ecoregion and biome distance matrices (Supplementary Table 6). These findings provide strong support to the hypothesis that large-scale ecological boundaries mark spatially abrupt discontinuities in plant-frugivore interactions (Figs. 2 and 3; Supplementary Fig. 11). Importantly, a great proportion of the deviance explained by biomes was shared with ecoregions (see the overlapping areas between ecoregions and biomes in Fig. 4 and Supplementary Fig. 12), which suggests that changes in interaction dissimilarity across biome boundaries

Table 1 | Multiple predictors of plant-frugivore interaction dissimilarity (β_{WN})

Parametric coefficients	Estimate	t	P
Intercept	0.997	2964.191	**0.001**
Ecoregion (same)	−0.070	−36.401	**0.001**
Biome (same)	−0.002	−3.323	**0.044**
Smooth Terms	**EDF**	**F**	**P**
s (human disturbance distance)	8.534	29.988	**0.001**
s (spatial distance)	8.785	65.378	**0.001**
s (elevational difference)	6.168	47.707	**0.001**
s (hours distance)	1.558	5.449	0.290
s (months distance)	5.482	6.902	0.075
s (years distance)	7.208	11.848	**0.019**
s (sampling intensity distance)	1.018	5.182	0.259
s (methods distance)	8.632	16.002	**0.005**

Here, we used the binary version of ecoregion and biome distance matrices. *P* values were calculated using a two-tailed statistical test that combines Generalized Additive Models (GAM) and Multiple Regression on distance Matrices (MRM). In this approach, the non-independence of distances from each local network is accounted for in the hypothesis testing by performing 1000 permutations of the response matrix (see "Methods"). EDF represents the effective degrees of freedom for each smooth term in the model. *N* pairs of networks = 19,110.
Bold *P* values indicate statistically significant results ($P < 0.05$).

mostly reflect the variation occurring at a finer (ecoregion) scale. Specifically, crossing an ecoregion boundary induced an average 7% increase in interaction dissimilarity, while crossing a biome boundary only induced an additional 0.2% change. As with species turnover, we found a strong effect of human disturbance gradients on interaction composition ($F = 29.998$; $P = 0.001$), such that networks at opposite ends of the human disturbance continuum usually exhibited very different interactions, even if they were located within the same ecoregion or biome (Fig. 5; Supplementary Fig. 13).

In addition to the importance of ecological boundaries and human disturbance gradients for driving plant-frugivore interaction dissimilarity, these effects were observed against a background of increasing interaction dissimilarity through space. Indeed, interaction dissimilarity increased sharply until a threshold distance of around 2500 km between network sites, beyond which few networks shared any interactions and dissimilarity remained close to its peak (Fig. 6; Supplementary Fig. 14). In the cases where spatially distant networks shared interactions, these typically involved species that had been introduced in at least one location. For instance, the interaction between the Blackbird *Turdus merula* and the Blackberry *Rubus fruticosus* was shared between networks located more than 18,000 km apart: while both species are native in Europe, they have been introduced by humans to Aotearoa New Zealand. Similarly, networks from Asia were connected to Hawai'i mostly through interactions involving introduced species in the latter, such as the Red-whiskered Bulbul *Pycnonotus jocosus* and the Java Plum *Syzygium cumini* (Fig. 2).

Deviance partitioning revealed that the shared effect of crossing ecoregion boundaries and spatial distance explained the greatest proportion of the variance in plant-frugivore interaction dissimilarity (6.41%), followed by the unique contributions of each of these two variables (ecoregion boundaries = 4.22%; spatial distance = 1.90%; Fig. 4). This relatively high contribution of both ecoregion and spatial distance indicates that gradual increases in interaction dissimilarity over space are made significantly steeper when crossing ecoregion boundaries.

Network structural dissimilarity

Despite significant turnover in species and interaction composition, structural dissimilarity of frugivory networks did not change significantly across large-scale ecological boundaries and human disturbance gradients, being only affected by spatial distance ($F = 20.408$; $P = 0.021$) and differences in sampling intensity ($F = 238.987$; $P = 0.002$) (Supplementary Table 7). These findings held true when evaluating both the binary and quantitative versions of ecoregion and biome distance matrices (Supplementary Tables 7 and 8).

All our main results were robust to different processes of assigning uniqueness to problematic species in local networks, that is, species without a valid epithet that could not be considered as unique species in our dataset (see Supplementary Methods and Supplementary Tables 9–32). Finally, tests of our key hypotheses were not affected by the removal of individual studies (Supplementary Figs. 15 and 16; Supplementary Tables 33 and 34) or small networks (i.e., up to 10 species) from the dataset (see Sensitivity analysis section in the Supplementary Methods).

Discussion

Our results support the hypothesis that large-scale ecological boundaries drive abrupt differences in species and interaction composition of avian frugivory networks. Specifically, on top of the gradual effect of spatial distance on interaction dissimilarity (whereby networks >2500 km apart had very few interactions in common), transitions across ecoregions and biomes promoted divergence in species interactions. These results show that ecoregions and biomes, classically defined based on environmental conditions and species occurrences[1,3,4], also carry a signature within biotic interactions. Indeed, because the large-scale distribution of both species and interactions is punctuated by ecoregion and biome boundaries (Fig. 2 and Supplementary Fig. 17), our findings suggest that species biogeography is matched by a higher-order biogeography of interactions. In parallel, differences in human disturbance led sites to have significantly different species and interaction composition, which might be partly attributed to the filtering of sensitive species and their interactions from disturbed sites[17,31]. In fact, while networks from natural ecosystems usually contain interactions between native species, which better reflect natural biogeographic patterns[12] and are more susceptible to human disturbances[31], interactions from high-disturbance regions are generally performed by generalist and introduced species[17,31,32]. Nevertheless, despite these differences in composition, we found that the structure of avian frugivory networks was relatively consistent across large-scale environmental gradients. Similar results have been reported at smaller spatial scales[32], indicating that assembly rules may generate common structural patterns in plant-frugivore networks[33] despite the shifts in species and interaction composition that usually accompany environmental changes[15].

Because most of the variation in interaction dissimilarity across biome borders can be explained by ecoregion boundaries, preserving the distinctness of ecoregions[3,4] will likely contribute to maintaining the natural barriers that limit the spread of disturbances across the global network of frugivory. Unfortunately, the unique species assemblages that comprise ecoregions have been increasingly threatened by global changes[3,5]. In fact, the global frugivory network is connected not only through natural processes, such as bird migration[34], but also through human-related processes. Biotic homogenization, in particular, has contributed to blurring biogeographical signatures[12,20] and mitigating the effect of spatial processes on interaction dissimilarity[12]. This notion is reinforced by the fact that all long-distance (>10,000 km) connections (shared interactions) between local networks of frugivory involved at least one region where novel interactions performed by introduced species have largely replaced those performed by declining or already extinct native species, such as Aotearoa New Zealand and Hawai'i[32,35] (see, for example, the shared

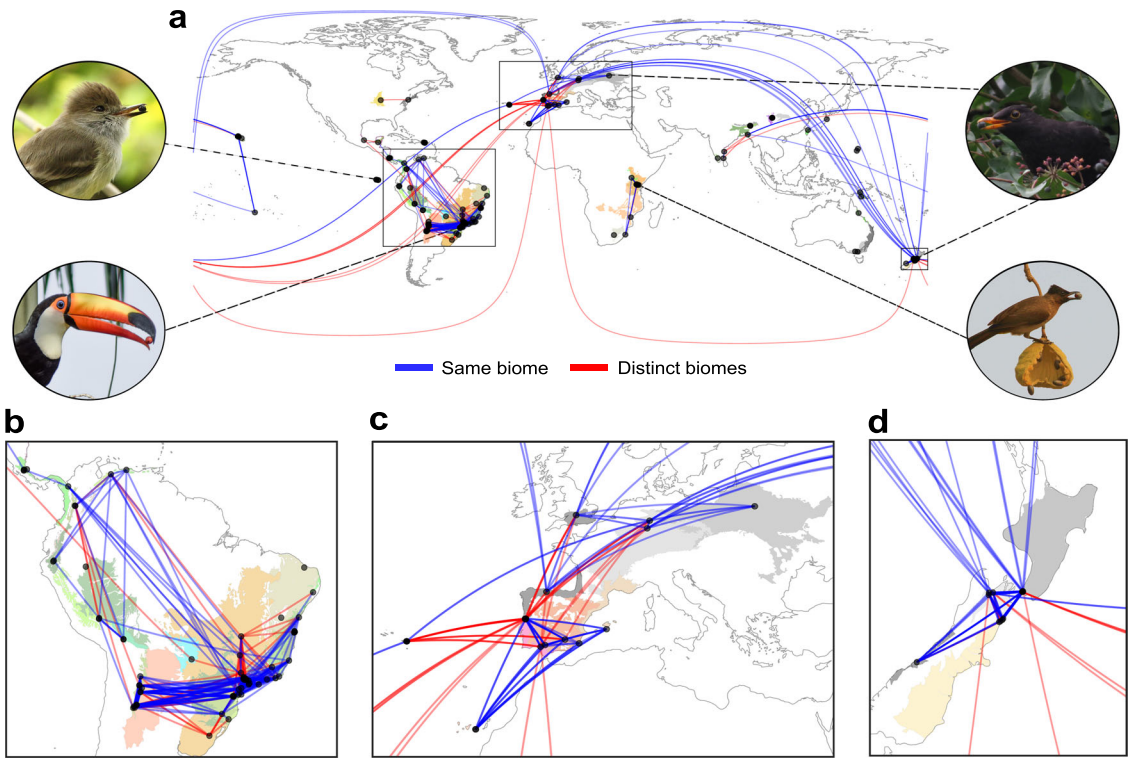

Fig. 2 | Plant–frugivore interactions shared among local networks, ecoregions, and biomes. a World map with points representing the 196 avian frugivory networks in our dataset. Colors of shaded areas represent the 67 ecoregions where networks were located, with similar colors indicating ecoregions that belong to the same biome. Lines represent the connections (shared interactions) plotted along the great circle distance between networks, with most of these connections occurring within (blue lines) rather than across (red lines) biomes. Stronger color tones of lines indicate higher similarity of interactions (1-β_{WN}) between networks. Connections across continents were mostly attributed to introduced species in one of these regions. Lines disappearing at the side edges of the world map are connected to those from the opposite edge. Photos show some of the frugivorous birds present in our dataset. Inset maps depict three regions with many networks and connections (especially within biomes). **b** South America. **c** Europe. **d** Aotearoa New Zealand. Photo credits: R. Heleno (top left and bottom right); R. B. Missano (bottom left); J. M. Costa (top right). Ecoregions and biomes were defined based on the map developed by Dinerstein et al.[3] (available at https://ecoregions.appspot.com/ under a CC-BY 4.0 license). Source data are provided as a Source Data file.

interactions connecting networks from Europe and Aotearoa New Zealand in Fig. 2). Interestingly, these long-distance connections tend to occur more frequently within than across biomes, despite a greater proportion of network comparisons being cross-biome (Supplementary Fig. 18). This indicates that biomes may represent meaningful boundaries not only for species, but also for novel interactions resulting from species introductions around the world[12]. Notably, because species interactions provide the pathways across which direct and indirect effects (such as dynamic impacts of population declines, apparent competition and trophic cascades) may propagate, spatially-separated networks that share interactions may have coupled dynamics and respond similarly to disturbance[9,36]. In fact, findings that ecological networks in adjacent habitats may function as a single dynamic unit[9] raises questions around the scale over which two networks can be considered truly distinct. As a step to answering this question, we provide empirical evidence for the existence of large-scale boundaries between ecological networks. Consequently, our results suggest that disturbances in local frugivory networks are much less likely to impact networks from distant sites or elevations, especially if they are located within distinct ecoregions and biomes.

Although species turnover and interaction dissimilarity responded to similar ecological drivers, species might interact differently across environmental gradients not only because of changes in species composition, but also because of partner switching associated with shifts in species abundance (i.e., the probability of random encounters), foraging behavior and co-evolutionary patterns[15]. Indeed, while interactions necessarily differ when the species involved differ[27], it is possible that shared species interact differently across sites, potentially decoupling the relationship between species turnover and interaction dissimilarity. To evaluate whether interaction rewiring (i.e., the extent to which shared species interact differently[27]) increases across large-scale environmental gradients, we used data limited to pairs of networks sharing plant and bird species (*N* pairs of networks = 1314) (see Rewiring analysis section in "Methods"). We found that interaction rewiring increased significantly across human disturbance, spatial, and elevational gradients (Supplementary Table 35), partially explaining why interactions tend to turn over faster than species at large spatial scales (Supplementary Figs. 9d and 14c). In fact, networks shared considerably more species than interactions (Fig. 2 and Supplementary Fig. 17), reinforcing previous findings that plant and bird species are flexible and tend to switch among their potential partners, even when networks have similar species composition[32]. Surprisingly, we did not find an effect of ecoregion boundaries on interaction rewiring (Supplementary Table 35). This effect only became significant when ecoregion and biome distances were the only predictors in the model (Supplementary Table 36), probably because of their collinearity with our other predictor variables (Supplementary Fig. 19).

As with other large-scale studies of ecological networks[12,37], our data were not evenly spread across the globe, which likely affected the observed patterns. For instance, around 59% of our networks were located within a single biome—the Tropical & Subtropical Moist Broadleaf Forests (Supplementary Fig. 2). Because ecoregions tend to be more distinct in tropical than in temperate zones[38], the greater number of networks from tropical ecosystems (which also possess

https://doi.org/10.1038/s41467-022-34355-w

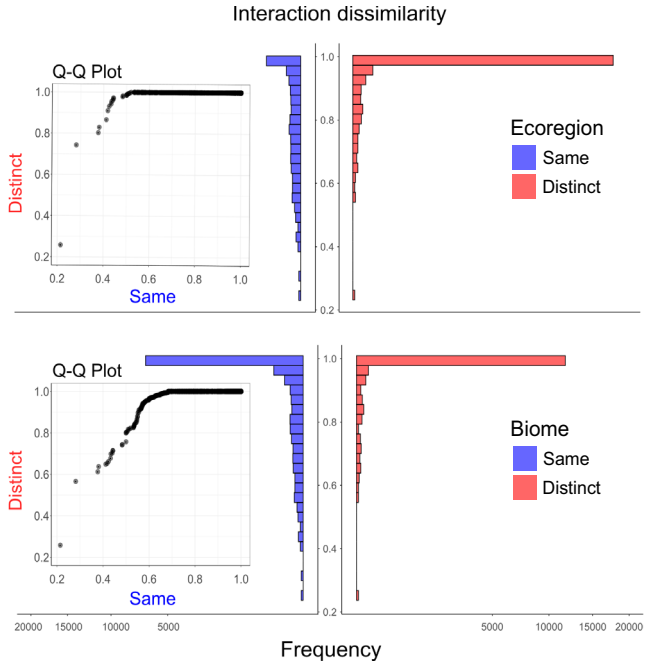

Fig. 3 | The effects of ecological boundaries on interaction dissimilarity (β_{WN}). Histograms and inset quantile-quantile (*Q*–*Q*) plots showing differences in the distributions of interaction dissimilarity values between pairs of networks located within ("same") and across ("distinct") ecoregions and biomes. The effects of ecoregion and biome boundaries were significant, even after controlling for the other predictor variables in the model (Table 1). We square root transformed the x-axis scale to allow a better visualization of the distribution of data points (pairs of networks) with interaction dissimilarity values <1. Source data are provided as a Source Data file.

most of the world's ecoregions[3]) may have contributed to the strong observed effect of ecoregion boundaries on interaction dissimilarity. Nevertheless, both species richness and the proportion of frugivorous birds reach their peaks in the Tropics[39], suggesting that the distribution of networks in our dataset partially mirrors the global distribution of avian frugivory. We also highlight that the ecoregions and biomes represented in our dataset cover around 20% and 69%, respectively, of the world's ice-free land surface. As such, network sampling in data deficient regions[37], especially at the ecoregion scale, may contribute greatly to our understanding of macroecological patterns in avian frugivory networks. Importantly, the extent to which our results apply for other frugivorous taxa (such as mammals and reptiles) and interaction types remains to be investigated. Previous findings, however, indicate that less-mobile taxa tend to show a stronger adherence to ecological boundaries[38], a pattern that is likely to be reflected in species interactions. This is corroborated here by the fact that networks located at distinct ecoregions and biomes tended to share more bird than plant species (Supplementary Fig. 17).

This work provides evidence that ecological boundaries and human disturbance gradients delineate the large-scale spatial distribution of species and their interactions. Nevertheless, network structure remained relatively consistent across broad-scale environmental gradients. This suggests that the processes underlying the architecture of frugivory networks, such as ecological specialization[40] and species' functional roles[41], may be reasonably independent of the identity of interacting species[19]. By demonstrating the validity of the ecoregion-based approach[1,3] for species interactions, our results have important implications for maintaining the world's biodiversity of interactions and the myriad ecological functions they provide.

Methods

Dataset acquisition

Plant-frugivore network data were obtained through different online sources and publications (Supplementary Table 1). Only networks that met the following criteria were retrieved: (i) the network contains quantitative data (a measure of interaction frequency) from a location, pooling through time if necessary; (ii) the network includes avian frugivores. Importantly, we removed non-avian frugivores from our analyses because only 28 out of 196 raw networks (before data cleaning) sampled non-avian frugivores, and not removing non-avian frugivores would generate spurious apparent turnover between networks that did vs. did not sample those taxa. In addition, the removal of non-avian frugivores did not strongly decrease the number of frugivores in our dataset (Supplementary Fig. 20a) or the total number of links in the global network of frugivory (Supplementary Fig. 20b). Furthermore, non-avian frugivores, as well as their interactions, were not shared across ecoregions and biomes (Supplementary Fig. 21), so their inclusion would only strengthen the results we found (though as noted above, we believe that this would be spurious because they are not as well sampled); (iii) the network (after removal of non-avian frugivores) contains greater than two species in each trophic level. Because this size threshold was somewhat arbitrary, we used a sensitivity analysis to assess the effect of our network size threshold on the reported patterns (see Sensitivity analysis section in the Supplementary Methods and Supplementary Figs. 22–24); and (iv) network sampling was not taxonomically restricted, that is, sampling was not focused on a specific taxonomic group, such as a given plant or bird family. Note, however, that authors often select focal plants or frugivorous birds to be sampled, but this was not considered as a taxonomic restriction if plants and birds were not selected based on their taxonomy (e.g., focal plants were selected based on the availability of fruits at the time of sampling, or focal birds were selected based on previous studies of bird diet in the study site). The first source for network data was the Web of Life database[42], which contains 33 georeferenced plant-frugivore networks from 28 published studies, of which 12 networks met our criteria.

We also accessed the Scopus database on 04 May 2020 using the following keyword combination: ("plant-frugivore*" OR "plant-bird*" OR "frugivorous bird*" OR "avian frugivore*" OR "seed dispers*") AND ("network*" OR "web*") to search for papers that include data on avian frugivory networks. The search returned a total of 532 studies, from which 62 networks that met the above criteria were retrieved. We also contacted authors to obtain plant-frugivore networks that were not publicly available, which provided us a further 110 networks. The remaining networks ($N = 12$) were obtained by checking the database from a recently published study[12]. In total, 196 quantitative avian frugivory networks were used in our analyses.

Generating the distance matrices to serve as predictor and response variables

Ecoregion and biome distances. We used the most up-to-date (2017) map of ecoregions and biomes[3], which divides the globe into 846 terrestrial ecoregions nested within 14 biomes, to generate our ecoregion and biome distance matrices. Of these, 67 ecoregions and 11 biomes are represented in our dataset (Supplementary Figs. 1 and 2). We constructed two alternative versions of both the ecoregion and biome distance matrices. In the first, binary version, if two ecological networks were from localities within the same ecoregion/biome, a dissimilarity of zero was given to this pair of networks, whereas a dissimilarity of one was given to a pair of networks from distinct ecoregions/biomes (this is the same as calculating the Euclidean distance on a presence–absence matrix with networks in rows and ecoregion/biomes in columns).

In the second, quantitative version, we estimated the pairwise environmental dissimilarity between our ecoregions and biomes using

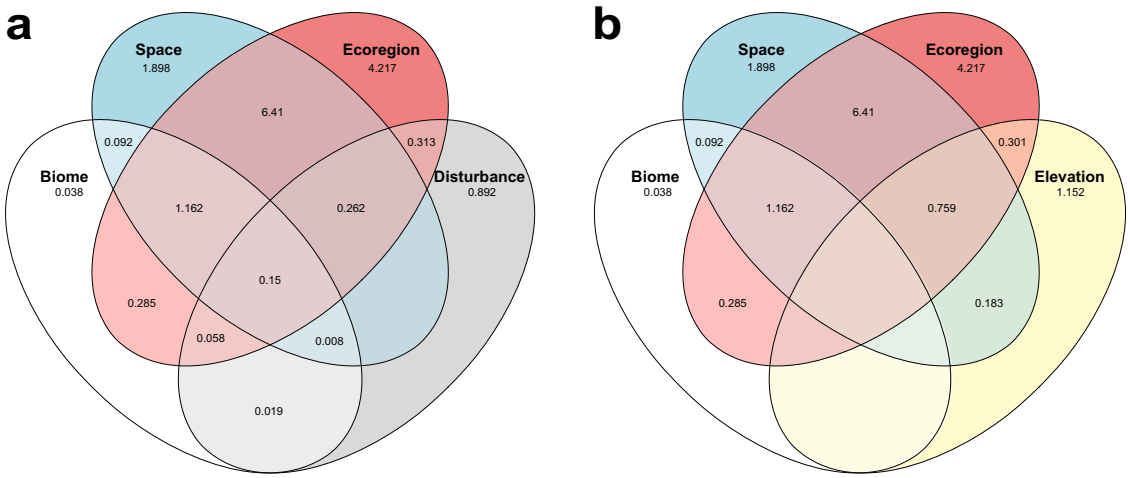

Fig. 4 | Venn diagrams showing the relative contributions (%) of our main predictor variables to explaining the variation in interaction dissimilarity (β_{WN}), calculated using deviance partitioning. Overlapping areas represent deviance that is jointly explained by one or more predictor variables. **a** The relative contributions of ecoregion, biome, spatial and human disturbance (i.e., footprint) distances. In **b**, we replace human disturbance distance with elevational difference; we show these two separate diagrams for visualization purposes, but Supplementary Fig. 12 shows the effect of all our main predictor variables together. Note that we only plot our predictor variables of interest (i.e., not those used for controlling sampling effects). Terms that reduce explanatory power are not shown. Source data are provided as a Source Data file.

six environmental variables recently demonstrated to be relevant in predicting ecoregion distinctness, namely mean annual temperature, temperature seasonality, mean annual rainfall, rainfall seasonality, slope and human footprint[38]. We obtained climatic and elevation data from WorldClim 2.1[43] at a spatial resolution of 1-km^2. We transformed the elevation raster into a slope raster using the *terrain* function from the raster package[44] in R[45]. As a measure of human disturbance, we used human footprint—a metric that combines eight variables associated with human disturbances of the environment: the extent of built environments, crop land, pasture land, human population density, night-time lights, railways, roads and navigable waterways[26]. The human footprint raster was downloaded at a 1-km^2 resolution[26]. Because human footprint data were not available for one of our ecoregions (Galápagos Islands xeric scrub), we estimated human footprint for this ecoregion by converting visually interpreted scores into the human footprint index. We did this by analyzing satellite images of the region and following a visual score criterion[26]. Given the previously demonstrated strong agreement between visual score and human footprint values[26], we fitted a linear model using the visual score and human footprint data from 676 validation plots located within the Deserts and xeric shrublands biome - the biome in which the Galápagos Islands xeric scrub ecoregion is located - and estimated the human footprint values for our own visual scores using the *predict* function in R[45].

We used 1-km^2 resolution rasters and the *extract* function from the raster package[44] to calculate the mean value of each of our six environmental variables for each ecoregion in our dataset. Because biomes are considerably larger than ecoregions (which makes obtaining environmental data for biomes more computationally expensive) we used a coarser spatial resolution of 5-km^2 for calculating the mean values of environmental variables for each biome. Since a 5-km^2 resolution raster was not available for human footprint, we transformed the 1-km^2 resolution raster into a 5-km^2 raster using the *resample* function from the same package.

To combine these six environmental variables into quantitative matrices of ecoregion and biome environmental dissimilarity, we ran a Principal Component Analysis (PCA) on our scaled multivariate data matrix (where rows are ecoregions or biomes and columns are environmental variables). From this PCA, we selected the scores of the four and three principal components, which represented 89.6% and 88.7% of the variance for ecoregions and biomes, respectively, and converted it into a distance matrix by calculating the Euclidean distance between pairs of ecoregions/biomes using the *vegdist* function from the vegan package[46]. Finally, we transformed the ecoregion or biome distance matrix into a $N \times N$ matrix where N is the number of local networks. In this matrix, cell values represent the pairwise environmental dissimilarity between the ecoregions/biomes where the networks are located. The main advantage of using this quantitative approach is that, instead of simply evaluating whether avian frugivory networks located in distinct ecoregions or biomes are different from each other in terms of network composition and structure (as in our binary approach), we were also able to determine whether the extent of network dissimilarity depended on how environmentally different the ecoregions or biomes are from one another.

Local-scale human disturbance distance. To generate our local human disturbance distance matrix, we extracted human footprint data at a 1-km^2 spatial resolution[26] and calculated the mean human footprint values within a 5-km buffer zone around each network site. For the networks located within the Galápagos Islands xeric scrub ecoregion ($N = 4$), we estimated the human footprint index using the same method described in the previous section for ecoregion- or biome-scale human footprint. We then calculated the pairwise Euclidean distance between human footprint values from our network sites. Thus, low cell values in the local human disturbance distance matrix indicate pairs of network sites with a similar level of human disturbance, while high values represent pairs of network sites with very different levels of human disturbance.

Spatial distance. The spatial distance matrix was generated using the Haversine (i.e., great circle) distance between all pairwise combinations of network coordinates. In this matrix, cell values represent the geographical distance between network sites.

Elevational difference. We calculated the Euclidean distance between pairwise elevation values (estimated as meters above sea level) of network sites to generate our elevational difference matrix. Elevation values were obtained from the original sources when available or using Google Earth[47]. In the elevational difference matrix, low cell values

https://doi.org/10.1038/s41467-022-34355-w

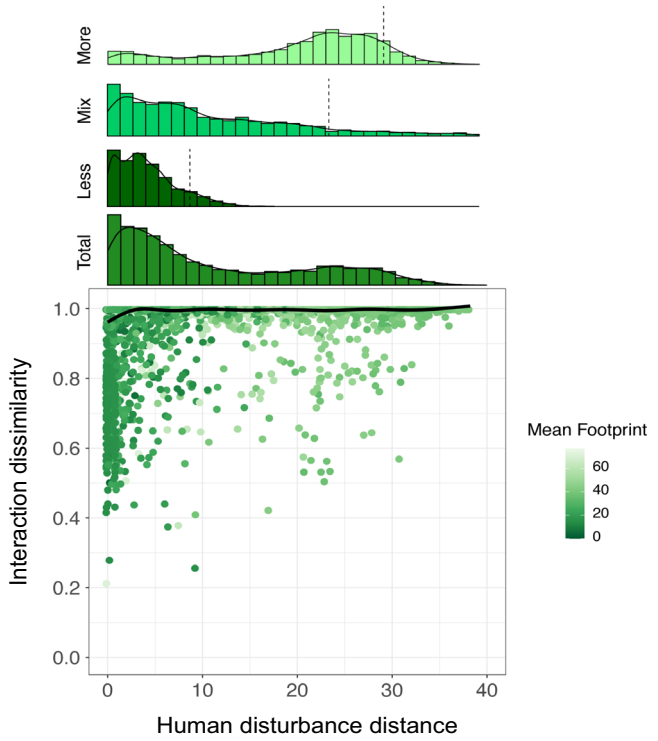

Fig. 5 | The effect of human disturbance gradients on interaction dissimilarity (β_{WN}). The relationship between human disturbance distance and interaction dissimilarity, with a fitted line obtained from a Generalized Additive Model (GAM) with human disturbance distance as the only predictor variable (Supplementary Fig. 13 shows the partial effects plot for the model including all predictors). Human disturbance distance was calculated as the absolute difference in human footprint values between a pair of network sites. Each data point (pair of networks) is colored according to the mean of the human footprint values from the two networks. The histogram above the plot shows the distribution of data points across the human disturbance gradient. To explore whether disturbance distance and the mean intensity of disturbance are related, we further divided our data into three equal sized groups (top three histograms) based on their mean (of the site pair) footprint values: "Less" disturbed (low mean footprint), 'Mix' (medium mean footprint) and 'More' disturbed (high mean footprint). Dashed lines mark the 90th percentile position in each histogram. Note that data points from less disturbed site pairs are skewed towards low values of human disturbance distance, whereas pairs of more disturbed sites also had a larger average distance. Source data are provided as a Source Data file.

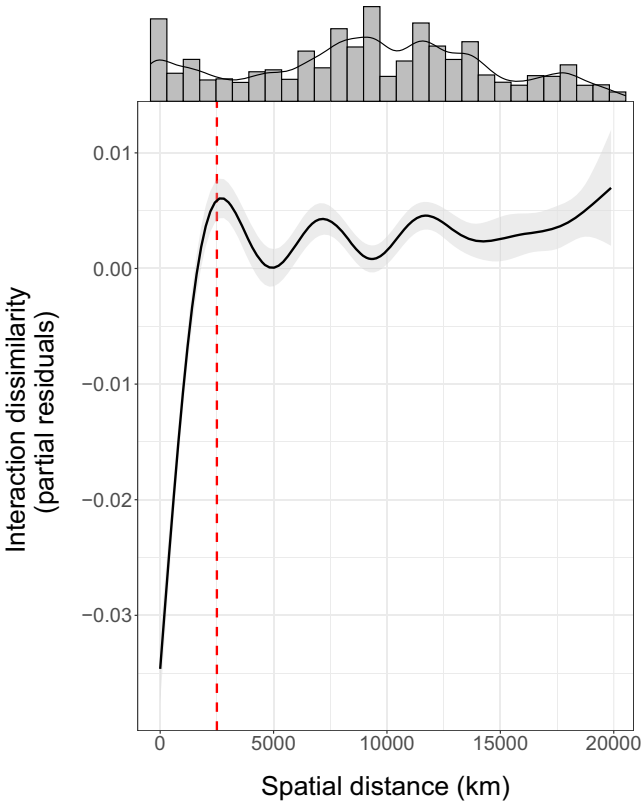

Fig. 6 | Partial effects plot of the relationship between spatial distance and interaction dissimilarity (β_{WN}). Here, we show the fit (solid line) of a Generalized Additive Model (GAM) with interaction dissimilarity as the response variable and all our predictor variables included. Thus, this plot shows the effect of spatial distance on interaction dissimilarity, while controlling for the effect of the other predictor variables in the model. Partial residuals remain on the same scale as the original data, but the sign of values indicates how they differ from what would be expected (i.e., from the fitted values) based on the other predictor variables in the model. The gray area represents two standard errors above and below the estimate of the smooth being plotted. The histogram above the plot shows the distribution of data points across the spatial gradient. Note the sharp increase in interaction dissimilarity until a threshold distance of around 2500 km (dotted red line), beyond which few networks shared interactions (a similar pattern can be seen in Supplementary Fig. 14c). Source data are provided as a Source Data file.

represent pairs of network sites within similar elevations, whereas high values represent pairs of network sites within very different elevations.

Network sampling dissimilarity. We used the metadata retrieved from each of our 196 local networks to generate our network sampling dissimilarity matrices, which aim to control statistically for differences in network sampling. There are many ways in which sampling effort could be quantified, so we began by calculating a variety of metrics, then narrowed our options by assessing which of these was most related to network metrics. We divided the sampling metrics into two categories: time span-related metrics (i.e., sampling hours and months) and empirical metrics of sampling completeness (i.e., sampling completeness and sampling intensity), which aim to account for how complete network sampling was in terms of species interactions (Supplementary Table 2).

We selected the quantitative sampling metrics to be included in our models based on (i) the fit of generalized linear models evaluating the relationship between number of sampling hours and sampling months of the study and network-level metrics (i.e., bird richness, plant richness and number of links), and (ii) how well time span-related metrics, sampling completeness and sampling intensity predicted the proportion of known interactions that were sampled in each local network (hereafter, ratio of interactions) for a subset of the data. This latter metric, defined as the ratio between the number of interactions in the local network and the number of known possible interactions in the region involving the species in the local network, captures raw sampling completeness. Therefore, ratio of interactions estimates, for a given set of species, the proportion of all their interactions known for a region that are found to occur among those same species in the local network. To calculate this metric, we needed high-resolution information on the possible interactions, so we used a subset of 14 networks sampled in Aotearoa New Zealand, since there is an extensive compilation of frugivory events recorded for this country[48]. After this process, we selected number of sampling hours, number of sampling months and sampling intensity for inclusion in our statistical models (Supplementary Figs. 7 and 8; Supplementary Table 2). We generated the corresponding distance matrices by calculating the Euclidean distance between metric values. Similarly, we generated a Euclidean distance matrix for differences in sampling year between pairs of networks, which aims to account for long-term changes in the environment, species composition and network sampling methods. We obtained the sampling year of our local networks from the original

sources and calculated the mean sampling year value for those networks sampled across multiple years.

Because sampling methods, such as sampling design, focus (i.e., focal taxa, which determines whether a zoocentric or phytocentric method was used), interaction frequency type (i.e., how interaction frequency was measured) and coverage (total or partial) might also affect the observed plant-frugivore interactions[49], we combined these variables into a single distance matrix to estimate the overall differences in sampling methods between networks. Because most of these variables were categorical with multiple levels (Supplementary Table 3), we generated our method's dissimilarity matrix by using a generalization of Gower's distance method[50], which allows the treatment of different types of variables when calculating distances. For this, we used the *dist.ktab* function from the ade4 package[51]. We ran a Principal Coordinates Analysis (PCoA) on this distance matrix, selected the first four axes, which explained 81.2% of the variation in method's dissimilarity, and calculated the Euclidean distance between pairs of networks using the *vegdist* function from the vegan package[46] in R[45].

Network dissimilarity. We generated three network dissimilarity matrices to be our response variables in the statistical models. In the first, cell values represent the pairwise dissimilarity in species composition between networks (beta diversity of species; β_S)[27]. Second, we measured interaction dissimilarity (beta diversity of interactions; β_{WN}), which represents the pairwise dissimilarity in the identity of interactions between networks[27]. Importantly, we did not include interaction rewiring (β_{OS}) in our main analysis because this metric can only be calculated for networks that share interaction partners (i.e., it estimates whether shared species interact differently)[27], which limited the number and the spatial distribution of networks available for analysis (but see the Rewiring analysis section for an analysis on the subset of our dataset for which this was possible). Metrics were calculated using the *network_betadiversity* function from the betalink package[52] in R[45].

Finally, we calculated a third dissimilarity matrix to capture overall differences in network structure. We recognize that there are many potential metrics of network structure, and that many of these are strongly correlated with one another[53–56]. We therefore chose a range of metrics that captured the number of links, their relative weightings (including across trophic levels), and their arrangement among species, then combined these into a single distance matrix. Specifically, we quantified network structural dissimilarity using the following metrics: weighted connectance, weighted nestedness, interaction evenness, PDI and modularity.

Weighted connectance represents the number of links relative to the number of possible links, weighted by the frequency of each interaction[55], and is therefore a measure of network-level specialization (higher values of weighted connectance indicate lower specialization). Importantly, it has been suggested that connectance affects persistence in mutualistic systems[54]. We measured nestedness (i.e., the pattern in which specialist species interact with proper subsets of the species that generalist species interact with) using the weighted version of nestedness based on overlap and decreasing fill (wNODF)[57]. Notably, nested structures have been commonly reported in plant-frugivore networks[33]. Interaction evenness is Shannon's evenness index applied for species interactions and represents how evenly distributed the interactions are in the network[21,58]. This metric has been previously demonstrated to decline with habitat modification as a consequence of some interactions being favored over others in high-disturbance environments[21]. PDI (Paired Difference Index) is a measure of species-level specialization on resources and a reliable indicator not only of specialization, but also of absolute generalism[59]. Thus, this metric contributes to understanding of the ecological processes that drive the prevalence of specialists or generalists in ecological networks[59]. In order to obtain a network-level PDI, we calculated the weighted mean PDI for each local network. Finally, we calculated modularity (i.e., the level of compartmentalization within networks) using the DIRTPLAwb+ algorithm[60]. Modularity estimates the extent to which species within modules interact more with each other than with species from other modules[61], and it has been demonstrated to affect the persistence and resilience of mutualistic networks[54]. All the selected network metrics are based on weighted (quantitative) interaction data, as these have been suggested to be less biased by sampling incompleteness[62] and to better reflect environmental changes[21]. All network metrics were calculated using the bipartite package[63] in R[45].

We ran a Principal Component Analysis (PCA) on our scaled multivariate data matrix ($N \times M$ where N is the number of local networks in our dataset and M is the number of network metrics), selected the scores of the three principal components, which represented 89.9% of the variance in network metrics, and converted it into a network structural dissimilarity matrix by calculating the Euclidean distance between networks. In this distance matrix, cell values represent differences in the overall architecture of networks (over all the network metrics calculated), and therefore provide a complementary approach for evaluating how species interaction patterns vary across large-scale environmental gradients.

Statistical analysis

We employed a two-tailed statistical test that combines Generalized Additive Models (GAM)[29] and Multiple Regression on distance Matrices (MRM)[30] to evaluate the effect of each of our predictor distance matrices on our response matrix. With this approach, we were able to fit GAMs where the predictor and responsible variables are distance matrices, while accounting for the non-independence of distances from each local network by permuting the response matrix[30]. The main advantage of using GAMs is their flexibility in modeling non-linear relationships through smooth functions, which are represented by a sum of simpler, fixed basis functions that determine their complexity[29]. Using GAM-based MRM models allowed us to obtain F values for each of the smooth terms (i.e., smooth functions of the predictor variables in our model), and test statistical significance at the level of individual variables. The binary versions of ecoregion and biome distance matrices (with two levels, "same" or "distinct") were treated as categorical variables in the models, and t values were used for determining statistical significance. We fitted GAMs with thin plate regression splines[64] using the *gam* function from the mgcv package[29] in R[45]. Smoothing parameters were estimated using restricted maximum likelihood (REML)[29]. Our GAM-based MRM models were calculated using a modified version of the *MRM* function from the ecodist package[65], which allowed us to combine GAMs with the permutation approach from the original *MRM* function (see Code availability). All the models were performed with 1000 permutations (i.e., shuffling) of the response matrix.

We explored the unique and shared contributions of our predictor variables to network dissimilarity using deviance partitioning analyses. These were performed by fitting reduced models (i.e., GAMs where one or more predictor variables of interest were removed) using the same smoothing parameters as in the full model and comparing the explained deviance. We fixed smoothing parameters for comparisons in this way because these parameters tend to vary substantially (to compensate) if one of two correlated predictors is dropped from a GAM.

Assessing the influence of individual studies on the reported patterns

Because our dataset comprises 196 local frugivory networks obtained from 93 different studies, and some of these studies contained multiple networks, we needed to evaluate whether our results were strongly biased by individual studies. To do this, we followed the approach from a previous study[66] and tested whether F values of smooth terms and t values of categorical variables (binary version of

ecoregion and biome distances) changed significantly when jackknifing across studies. We did this by dropping one study from the dataset and re-fitting the models, and then repeating this same process for all the studies in our dataset.

We found a number of consistent patterns within different subsets of the data (Supplementary Figs. 15 and 16); however, some of the patterns we observed appear to be driven by individual studies with multiple networks, and hence are less representative. For instance, the study with the greatest number of networks in our dataset (study ID = 76), which contains 35 plant-frugivore networks sampled across an elevation gradient in Mt. Kilimanjaro, Tanzania[67], had an overall high influence on the results when compared with the other studies. By re-running our GAM-based MRM models after removing this study from our dataset, we found that the effect of biome boundaries on interaction dissimilarity is no longer significant, whereas the effects of ecoregion boundaries, human disturbance distance, spatial distance and elevational differences remained consistent with those from the full dataset (Supplementary Table 33). Nevertheless, all the results were qualitatively similar to those obtained for the entire dataset when using network structural dissimilarity as the response variable (Supplementary Table 34).

Rewiring analysis

Interaction rewiring (β_{OS}) estimates the extent to which shared species interact differently[27]. Because this metric can only be calculated for networks that share species from both trophic levels, we selected a subset of network pairs that shared plants and frugivorous birds ($N = 1314$) to test whether interaction rewiring increases across large-scale environmental gradients. Importantly, since not all possible combinations of network pairs contained values of interaction rewiring (i.e., not all pairs of networks shared species), a pairwise distance matrix could not be generated for this metric. Thus, we were not able to use the same statistical approach used in our main analysis, which is based on distance matrices (see Statistical analysis section). Instead, we performed a Generalized Additive Mixed-effects Model (GAMM) using ecoregion, biome, human disturbance, spatial, elevational, and sampling-related distance metrics as fixed effects and network IDs as random effects (to account for the non-independence of distances) (Supplementary Table 35). We also performed a reduced model with only ecoregion and biome distance metrics as predictor variables (Supplementary Table 36). The binary version of ecoregion and biome distance metrics (with two levels, "same" or "distinct") were used as categorical variables in both models. Interaction rewiring (β_{OS}) was calculated using the *network_betadiversity* function from the betalink package[52] in R[45]. Although it has been recently argued that this metric may overestimate the importance of rewiring for network dissimilarity[68], our main focus was not the partitioning of network dissimilarity into species turnover and rewiring components, but rather simply detecting whether the sub-web of shared species interacted differently. In this case, β_{OS} (as developed by ref. 27) is an adequate and useful metric[68]. We fitted our models using the *gamm4* function from the gamm4 package[69] in R[45]. Smoothing parameters were estimated using restricted maximum likelihood (REML)[29].

Reporting summary

Further information on research design is available in the Nature Research Reporting Summary linked to this article.

Data availability

The data necessary to reproduce the analyses of this manuscript have been deposited in the Dryad database: https://doi.org/10.5061/dryad.mcvdnck4d (ref. 70). Metadata of the plant-frugivore networks, and predictor and response variables used in our analyses are provided with this paper as Supplementary Data. The Ecoregions 2017 © Resolve map developed by ref. 3 is available at https://ecoregions.appspot.com/ under a CC-BY 4.0 license. Human footprint data are publicly available at https://doi.org/10.5061/dryad.052q5 (ref. 71). The WorldClim 2.1 database[43] is publicly available at https://www.worldclim.org/. The following taxonomic databases were used for standardizing the taxonomy of plant and bird species in our dataset: Global Names Resolver (GNR) (available at https://resolver.globalnames.org/), National Center for Biotechnology Information (NCBI) (available at https://ncbi.nlm.nih.gov/), BirdLife International (available at http://datazone.birdlife.org/species/taxonomy), Avibase (available at https://avibase.bsc-eoc.org/), Integrated Taxonomic Information System (ITIS) (available at https://itis.gov/), International Plant Names Index (IPNI) (available at https://www.ipni.org/), Tropicos (available at https://www.tropicos.org/), and the iPlant Taxonomic Name Resolution Service[72] (available at https://tnrs.biendata.org/). Source data are provided with this paper.

Code availability

R scripts for reproducing the analyses of this manuscript are available at https://doi.org/10.5061/dryad.mcvdnck4d (ref. 70).

References

1. Olson, D. M. et al. Terrestrial ecoregions of the world: a new map of life on Earth. *Bioscience* **51**, 933–938 (2001).
2. Gaston, K. J. Global patterns in biodiversity. *Nature* **405**, 220–227 (2000).
3. Dinerstein, E. et al. An ecoregion-based approach to protecting half the terrestrial realm. *Bioscience* **67**, 534–545 (2017).
4. Smith, J. R. et al. A global test of ecoregions. *Nat. Ecol. Evol.* **2**, 1889–1896 (2018).
5. Dinerstein, E. et al. A global deal for nature: guiding principles, milestones, and targets. *Sci. Adv.* **5**, eaaw2869 (2019).
6. Schleuning, M., Fründ, J. & García, D. Predicting ecosystem functions from biodiversity and mutualistic networks: an extension of trait-based concepts to plant-animal interactions. *Ecography* **38**, 380–392 (2015).
7. Valiente-Banuet, A. et al. Beyond species loss: the extinction of ecological interactions in a changing world. *Funct. Ecol.* **29**, 299–307 (2015).
8. Schleuning, M. et al. Ecological networks are more sensitive to plant than to animal extinction under climate change. *Nat. Commun.* **7**, 13965 (2016).
9. Frost, C. M. et al. Apparent competition drives community-wide parasitism rates and changes in host abundance across ecosystem boundaries. *Nat. Commun.* **7**, 12644 (2016).
10. Menge, B. A. Indirect effects in marine rocky intertidal interaction webs: patterns and importance. *Ecol. Monogr.* **65**, 21–74 (1995).
11. Timóteo, S., Correia, M., Rodríguez-Echeverría, S., Freitas, H. & Heleno, R. Multilayer networks reveal the spatial structure of seed-dispersal interactions across the Great Rift landscapes. *Nat. Commun.* **9**, 140 (2018).
12. Fricke, E. C. & Svenning, J. C. Accelerating homogenization of the global plant–frugivore meta-network. *Nature* **585**, 74–78 (2020).
13. Albouy, C. et al. The marine fish food web is globally connected. *Nat. Ecol. Evol.* **3**, 1153–1161 (2019).
14. Stouffer, D. B. & Bascompte, J. Compartmentalization increases food-web persistence. *Proc. Natl. Acad. Sci. USA* **108**, 3648–3652 (2011).
15. Tylianakis, J. M. & Morris, R. J. Ecological networks across environmental gradients. *Annu. Rev. Ecol. Evol. Syst.* **48**, 25–48 (2017).
16. Qian, H. & Ricklefs, R. E. Disentangling the effects of geographic distance and environmental dissimilarity on global patterns of species turnover. *Glob. Ecol. Biogeogr.* **21**, 341–351 (2012).
17. Emer, C. et al. Seed-dispersal interactions in fragmented landscapes – a metanetwork approach. *Ecol. Lett.* **21**, 484–493 (2018).

18. Quitián, M. et al. Elevation-dependent effects of forest fragmentation on plant-bird interaction networks in the tropical Andes. *Ecography* **41**, 1497–1506 (2018).
19. Dehling, D. M. et al. Similar composition of functional roles in Andean seed-dispersal networks, despite high species and interaction turnover. *Ecology* **101**, e03028 (2020).
20. Capinha, C., Essl, F., Seebens, H., Moser, D. & Pereira, H. M. The dispersal of alien species redefines biogeography in the Anthropocene. *Science* **348**, 1248–1251 (2015).
21. Tylianakis, J. M., Tscharntke, T. & Lewis, O. T. Habitat modification alters the structure of tropical host-parasitoid food webs. *Nature* **445**, 202–205 (2007).
22. Dugger, P. J. et al. Seed-dispersal networks are more specialized in the Neotropics than in the Afrotropics. *Glob. Ecol. Biogeogr.* **28**, 248–261 (2019).
23. Jordano, P. *Fruits and Frugivory* in *Seeds: The Ecology of Regeneration in Plant Communities,* 3nd edn. (ed. Gallagher, R.S.) 18–61 (CABI, Wallingford, UK, 2014).
24. Onstein, R. E. et al. Frugivory-related traits promote speciation of tropical palms. *Nat. Ecol. Evol.* **1**, 1903–1911 (2017).
25. Wunderle, J. M. The role of animal seed dispersal in accelerating native forest regeneration on degraded tropical lands. *Ecol. Manag.* **99**, 223–235 (1997).
26. Venter, O. et al. Global terrestrial Human Footprint maps for 1993 and 2009. *Sci. Data* **3**, 160067 (2016).
27. Poisot, T., Canard, E., Mouillot, D., Mouquet, N. & Gravel, D. The dissimilarity of species interaction networks. *Ecol. Lett.* **15**, 1353–1361 (2012).
28. Petanidou, T., Kallimanis, A. S., Tzanopoulos, J., Sgardelis, S. P. & Pantis, J. D. Long-term observation of a pollination network: fluctuation in species and interactions, relative invariance of network structure and implications for estimates of specialization. *Ecol. Lett.* **11**, 564–575 (2008).
29. Wood, S. N. *Generalized Additive Models: An Introduction with R,* 2nd edn. (Chapman and Hall/CRC, London, 2017).
30. Lichstein, J. W. Multiple regression on distance matrices: a multivariate spatial analysis tool. *Plant Ecol.* **188**, 117–131 (2007).
31. McConkey, K. R. et al. Seed dispersal in changing landscapes. *Biol. Conserv.* **146**, 1–13 (2012).
32. Vizentin-Bugoni, J. et al. Structure, spatial dynamics, and stability of novel seed dispersal mutualistic networks in Hawai'i. *Science* **364**, 78–82 (2019).
33. Bascompte, J., Jordano, P., Melian, C. J. & Olesen, J. M. The nested assembly of plant-animal mutualistic networks. *Proc. Natl. Acad. Sci. USA* **100**, 9383–9387 (2003).
34. Viana, D. S., Santamaría, L. & Figuerola, J. Migratory birds as global dispersal vectors. *Trends Ecol. Evol.* **31**, 763–775 (2016).
35. García, D., Martínez, D., Stouffer, D. B. & Tylianakis, J. M. Exotic birds increase generalization and compensate for native bird decline in plant-frugivore assemblages. *J. Anim. Ecol.* **83**, 1441–1450 (2014).
36. García-Callejas, D., Molowny-Horas, R., Araújo, M. B. & Gravel, D. Spatial trophic cascades in communities connected by dispersal and foraging. *Ecology* **100**, e02820 (2019).
37. Poisot, T. et al. Global knowledge gaps in species interaction networks data. *J. Biogeogr.* **48**, 1552–1563 (2021).
38. Smith, J. R., Hendershot, J. N., Nova, N. & Daily, G. C. The biogeography of ecoregions: descriptive power across regions and taxa. *J. Biogeogr.* **47**, 1413–1426 (2020).
39. Kissling, W. D., Böhning-Gaese, K. & Jetz, W. The global distribution of frugivory in birds. *Glob. Ecol. Biogeogr.* **18**, 150–162 (2009).
40. K. Schleuning, M. et al. Specialization and interaction strength in a tropical plant—frugivore network differ among forest strata. *Ecology* **92**, 26–36 (2011).
41. Dehling, D. M., Jordano, P., Schaefer, H. M., Böhning-Gaese, K. & Schleuning, M. Morphology predicts species' functional roles and their degree of specialization in plant–frugivore interactions. *Proc. R. Soc. B Biol. Sci.* **283**, 20152444 (2016).
42. Fortuna, M. A., Ortega, R. & Bascompte, J. The web of life. Preprint at https://arxiv.org/abs/1403.2575 (2014).
43. Fick, S. E. & Hijmans, R. J. WorldClim 2: new 1-km spatial resolution climate surfaces for global land areas. *Int. J. Climatol.* **37**, 4302–4315 (2017).
44. Hijmans, R. J. raster: geographic data analysis and modeling. R package version 3.1-5. https://CRAN.R-project.org/package=raster (2020).
45. R Core Team. R: a language and environment for statistical computing (R Foundation for Statistical Computing, Vienna, Austria, 2020).
46. Oksanen J. et al. vegan: community ecology package. R package version 2.5-3. http://CRAN.R-project.org/package=vegan (2020).
47. Google Earth. https://www.google.com/earth/ (2020).
48. Peralta, G., Perry, G. L. W., Vázquez, D. P., Dehling, D. M. & Tylianakis, J. M. Strength of niche processes for species interactions is lower for generalists and exotic species. *J. Anim. Ecol.* **89**, 2145–2155 (2020).
49. Jordano, P. Sampling networks of ecological interactions. *Funct. Ecol.* **30**, 1883–1893 (2016).
50. Pavoine, S., Vallet, J., Dufour, A. B., Gachet, S. & Daniel, H. On the challenge of treating various types of variables: application for improving the measurement of functional diversity. *Oikos* **118**, 391–402 (2009).
51. Dray, S. & Dufour, A. B. The ade4 package: implementing the duality diagram for ecologists. *J. Stat. Softw.* **22**, 1–20 (2007).
52. Poisot, T. betalink: beta-diversity of species interactions. R package version 2.2.1. https://CRAN.R-project.org/package=betalink (2016).
53. Banašek-Richter, C. et al. Complexity in quantitative food webs. *Ecology* **90**, 1470–1477 (2009).
54. Thébault, E. & Fontaine, C. Stability of ecological communities and the architecture of mutualistic and trophic networks. *Science* **329**, 853–856 (2010).
55. Bersier, L. F., Banasek-Richter, C. & Cattin, M. F. Quantitative descriptors of food-web matrices. *Ecology* **83**, 2934–2407 (2002).
56. Fortuna, M. A. et al. Nestedness versus modularity in ecological networks: two sides of the same coin? *J. Anim. Ecol.* **79**, 811–817 (2010).
57. Almeida-Neto, M. & Ulrich, W. A straightforward computational approach for measuring nestedness using quantitative matrices. *Environ. Model. Softw.* **26**, 173–178 (2011).
58. Blüthgen, N., Fründ, J., Vazquez, D. P. & Menzel, F. What do interaction network metrics tell us about specialization and biological traits? *Ecology* **89**, 3387–3399 (2008).
59. Poisot, T., Canard, E., Mouquet, N. & Hochberg, M. E. A comparative study of ecological specialization estimators. *Methods Ecol. Evol.* **3**, 537–544 (2012).
60. Beckett, S. J. Improved community detection in weighted bipartite networks. *R. Soc. Open Sci.* **3**, 140536 (2016).
61. Olesen, J. M., Bascompte, J., Dupont, Y. L. & Jordano, P. The modularity of pollination networks. *Proc. Natl. Acad. Sci. USA* **104**, 19891–19896 (2007).
62. Vizentin-Bugoni, J. et al. Influences of sampling effort on detected patterns and structuring processes of a Neotropical plant-hummingbird network. *J. Anim. Ecol.* **85**, 262–272 (2016).
63. Dormann, C. F., Frund, J., Bluthgen, N. & Gruber, B. Indices, graphs and null models: analyzing bipartite ecological networks. *Open Ecol. J.* **2**, 7–24 (2009).
64. Wood, S. N. Thin plate regression splines. *J. R. Stat. Soc. Ser. B Stat. Methodol.* **65**, 95–114 (2003).
65. Goslee, S. C. & Urban, D. L. The ecodist package for dissimilarity-based analysis of ecological data. *J. Stat. Softw.* **22**, 1–19 (2007).

66. Cirtwill, A. R., Stouffer, D. B. & Romanuk, T. N. Latitudinal gradients in biotic niche breadth vary across ecosystem types. *Proc. R. Soc. B Biol. Sci.* **282**, 20151589 (2015).
67. Vollstädt, M. G. R. et al. Seed-dispersal networks respond differently to resource effects in open and forest habitats. *Oikos* **127**, 847–854 (2017).
68. Fründ, J. Dissimilarity of species interaction networks: how to partition rewiring and species turnover components. *Ecosphere* **12**, e03653 (2021).
69. Wood S. N. & Scheipl, F. gamm4: generalized additive mixed models using "mgcv" and 'lme4'. R package version 0.2-6. https://cran.r-project.org/package=gamm4 (2020).
70. Martins, L. P. et al. Data and code: Global and regional ecological boundaries explain abrupt spatial discontinuities in avian frugivory interactions. Dryad Digital Repository, https://doi.org/10.5061/dryad.mcvdnck4d (2022).
71. Venter, O et al. Data from: Global terrestrial Human Footprint maps for 1993 and 2009. Dryad Digital Repository, https://doi.org/10.5061/dryad.052q5 (2016).
72. Boyle, B. et al. The taxonomic name resolution service: an online tool for automated standardization of plant names. *BMC Bioinform.* **14**, 16 (2013).

Acknowledgements

We thank all the researchers in Tylianakis and Stouffer lab groups for their insightful comments on this manuscript. The authors acknowledge the following funding: University of Canterbury Doctoral Scholarship (L.P.M.); The Marsden Fund grant UOC1705 (J.M.T., L.P.M.); The São Paulo Research Foundation - FAPESP 2014/01986-0 (M.G., C.E.), 2015/15172-7 and 2016/18355-8 (C.E.), 2004/00810-3 and 2008/10154-7 (C.I.D., M.G., M.A.P.); Earthwatch Institute and Conservation International for financial support (C.I.D., M.G., M.A.P.); Carlos Chagas Filho Foundation for Supporting Research in the Rio de Janeiro State – FAPERJ grant E-26/200.610/2022 (C.E.); Brazilian Research Council grants 540481/01-7 and 304742/2019-8 (M.A.P.) and 300970/2015-3 (M.G.); Rufford Small Grants for Nature Conservation No. 22426–1 (J.C.M., I.M.), No. 9163-1 (G.B.J.) and No. 11042-1 (MCM); Universidade Estadual de Santa Cruz (Propp-UESC; No. 00220.1100.1644/10-2018) (J.C.M., I.M.); Fundação de Amparo à Pesquisa do Estado da Bahia - FAPESB (No. 0525/2016) (J.C.M., I.M.); European Research Council under the European Union's Horizon 2020 research and innovation program (grant 787638) and The Swiss National Science Foundation (grant 173342), both awarded to C. Graham (D.M.D.); ARC SRIEAS grant SR200100005 Securing Antarctica's Environmental Future (D.M.D.); German Science Foundation —Deutsche Forschungsgemeinschaft PAK 825/1 and FOR 2730 (K.B.G., E.L.N., M.Q., V.S., M.S.), FOR 1246 (K.B.G., M.S., M.G.R.V.) and HE2041/20-1 (F.S., M.S.); Portuguese Foundation for Science and Technology - FCT/MCTES contract CEECIND/00135/2017 and grant UID/BIA/04004/2020 (S.T.) and contract CEECIND/02064/2017 (L.P.S.); National Scientific and Technical Research Council, PIP 592 (P.G.B.); Instituto Venezolano de Investigaciones Científicas - Project 898 (V.S.D.).

Author contributions

Conceptualization: L.P.M. and J.M.T.; Methodology: L.P.M., J.M.T., and D.B.S.; Collection of data: P.G.B., K.B.G., G.B.J., M.C., J.M.C., D.M.D., C.I.D., C.E., M.G., R.H., P.J., I.M., J.C.M., M.C.M., E.L.N., M.A.P., M.Q., R.A.R., F.S., V.S., V.S.D., M.S., L.P.S., F.R.S., S.T., A.T., M.G.R.V.; Writing of original draft: L.P.M. and J.M.T. All authors contributed to the final version of the manuscript.

Competing interests

The authors declare no competing interests.

Additional information

Supplementary information The online version contains supplementary material available at https://doi.org/10.1038/s41467-022-34355-w.

Correspondence and requests for materials should be addressed to Lucas P. Martins or Jason M. Tylianakis.

Peer review information *Nature Communications* thanks the anonymous reviewer(s) for their contribution to the peer review of this work. Peer review reports are available.

Reprints and permissions information is available at http://www.nature.com/reprints

Publisher's note Springer Nature remains neutral with regard to jurisdictional claims in published maps and institutional affiliations.

Lucas P. Martins[1] ✉, Daniel B. Stouffer[1], Pedro G. Blendinger[2,3], Katrin Böhning-Gaese[4,5], Galo Buitrón-Jurado[6,7], Marta Correia[8], José Miguel Costa[8], D. Matthias Dehling[9,10], Camila I. Donatti[11,12], Carine Emer[13,14], Mauro Galetti[14], Ruben Heleno[8], Pedro Jordano[15,16], Ícaro Menezes[17], José Carlos Morante-Filho[17], Marcia C. Muñoz[18], Eike Lena Neuschulz[4], Marco Aurélio Pizo[14], Marta Quitián[19,20], Roman A. Ruggera[21], Francisco Saavedra[22], Vinicio Santillán[23], Virginia Sanz D'Angelo[6], Matthias Schleuning[4], Luís Pascoal da Silva[24,25], Fernanda Ribeiro da Silva[26], Sérgio Timóteo[8], Anna Traveset[20], Maximilian G. R. Vollstädt[27] & Jason M. Tylianakis[1] ✉

[1]Centre for Integrative Ecology, School of Biological Sciences, University of Canterbury, Private bag 4800, Christchurch 8140, Aotearoa New Zealand. [2]Instituto de Ecología Regional, Universidad Nacional de Tucumán and CONICET; CC 34, 4107 Tucumán, Argentina. [3]Facultad de Ciencias Naturales e Instituto Miguel Lillo, Universidad Nacional de Tucumán, Miguel Lillo 2005, 4000 Tucumán, Argentina. [4]Senckenberg Biodiversity and Climate Research Centre (SBiK-F), Senckenberganlage 25, 60325 Frankfurt am Main, Germany. [5]Institute for Ecology, Evolution and Diversity, Goethe University Frankfurt, Max-

von-Laue-Straße 13, Frankfurt am Main 60439, Germany. [6]Laboratorio de Biología de Organismos, Centro de Ecología, Instituto Venezolano de Investigaciones Científicas (IVIC), Carretera Panamericana, km 11, Altos de Pipe, Edo, Miranda, Venezuela. [7]Universidad Estatal Amazónica-Sede Zamora Chinchipe; Calle Luis Imaicela entre Azuay y Rene Ulloa, El Pangui, Zamora Chinchipe, Ecuador. [8]Centre for Functional Ecology, Associate Laboratory TERRA, Department of Life Sciences, University of Coimbra, Calçada Martim de Freitas, 3000-456 Coimbra, Portugal. [9]Swiss Federal Research Institute WSL, Zürcherstrasse 111, 8903 Birmensdorf, Switzerland. [10]Securing Antarctica's Environmental Future, School of Biological Sciences, Monash University, Melbourne, Victoria 3800, Australia. [11]Conservation International, 2011 Crystal Dr. Suite 600, Arlington, VA 22202, USA. [12]Department of Biological Sciences, Northern Arizona University, 617S. Beaver St., Flagstaff, AZ 86011-5640, USA. [13]Rio de Janeiro Botanical Garden Research Institute, Rua Pacheco Leão 915, Jardim Botânico, Rio de Janeiro, RJ CEP 22460-030, Brazil. [14]Department of Biodiversity, São Paulo State University – UNESP, Rio Claro, SP, Brazil. [15]Estación Biológica de Doñana, CSIC, av. Americo Vespucio 26, 41092 Sevilla, Spain. [16]Departamento de Biología Vegetal y Ecología, Universidad de Sevilla, Sevilla, Spain. [17]Applied Conservation Ecology Lab, Santa Cruz State University, Rodovia Ilhéus- Itabuna, km 16, Salobrinho, Ilhéus, Bahia 45662-000, Brazil. [18]Programa de Biología, Universidad de La Salle, Carrera 2 # 10-70 Bogotá, Colombia. [19]Systematic Zoology Laboratory, Tokyo Metropolitan University, 1-1 Minami-Osawa, Hachioji-shi, Tokyo 192-0397, Japan. [20]Instituto Mediterráneo de Estudios Avanzados (CSIC-UIB), Miquel Marqués 21, Mallorca, Balearic Islands, 07190 Esporles, Spain. [21]Instituto de Ecorregiones Andinas (Consejo Nacional de Investigaciones Científicas y Técnicas - Universidad Nacional de Jujuy), Canónigo Gorriti 237, Y4600 San Salvador de Jujuy, Jujuy, Argentina. [22]Instituto de Ecología, Facultad de Ciencias Puras y Naturales, Universidad Mayor de San Andrés, La Paz, Bolivia. [23]Centro de Investigación, Innovación y Transferencia de Tecnología (CIITT), Unidad Académica de Posgrado, Universidad Católica de Cuenca, Av. de las Américas, Cuenca, Ecuador. [24]CIBIO, Centro de Investigação em Biodiversidade e Recursos Genéticos, InBIO Laboratório Associado, Campus de Vairão, Universidade do Porto, 4485-661 Vairão, Portugal. [25]BIOPOLIS Program in Genomics, Biodiversity and Land Planning, CIBIO, Campus de Vairão, 4485-661 Vairão, Portugal. [26]Laboratory of Human Ecology and Ethnobotany, Department of Ecology and Zoology, Federal University of Santa Catarina, UFSC, Campus Trindade, s/n, Florianópolis, SC 88010-970, Brazil. [27]Section for Molecular Ecology and Evolution, Globe Institute, University of Copenhagen, Oester Voldgade 5-7, 1350 Copenhagen K, Denmark.
✉e-mail: martinslucas.p@gmail.com; jason.tylianakis@canterbury.ac.nz

Supplementary Information

Global and regional ecological boundaries explain abrupt spatial discontinuities in avian frugivory interactions

Lucas P. Martins*, Daniel B. Stouffer, Pedro G. Blendinger, Katrin Böhning-Gaese, Galo Buitrón-Jurado, Marta Correia, José Miguel Costa, D. Matthias Dehling, Camila I. Donatti, Carine Emer, Mauro Galetti, Ruben Heleno, Pedro Jordano, Ícaro Menezes, José Carlos Morante-Filho, Marcia C. Muñoz, Eike Lena Neuschulz, Marco Aurélio Pizo, Marta Quitián, Roman A. Ruggera, Francisco Saavedra, Vinicio Santillán, Virginia Sanz D'Angelo, Matthias Schleuning, Luís Pascoal da Silva, Fernanda Ribeiro da Silva, Sérgio Timóteo, Anna Traveset, Maximilian G. R. Vollstädt, Jason M. Tylianakis*

*Corresponding authors. Email: martinslucas.p@gmail.com (L.P.M); jason.tylianakis@canterbury.ac.nz (J.M.T)

Supplementary Methods

Standardizing the taxonomy

Considering the variety of authors and studies in our dataset, which identified plants and birds with differing resolution, it was necessary to reduce the taxonomic uncertainty in a uniform way. For this, we extracted the frugivore and plant species lists from all networks and performed a series of filters in order to remove non-existent species names (e.g., morphospecies labels) and standardize synonymous names according to reference databases.

Frugivore species

To account for spelling errors, we checked the matching of frugivore species names in our database to those from several taxonomic sources using the Global Names Resolver (GNR)[1]. We accessed this database using the function *gnr_resolve* from the R package taxize[2] (Supplementary Fig. 3; step 1). This function provides a matching score and the name from any of GNR's sources that most closely matches each name in our species list. Matching is determined by a combination of checking for exact matches against the names in the data sources and fuzzy matching (of canonical forms or parts of the names) using the TaxaMatch algorithm[3]. Because we were only interested in birds, we used the function *classification* from the same package to retrieve the taxonomic hierarchy and remove non-avian species, using the National Center for Biotechnology Information (NCBI)[4] as the reference database (Supplementary Fig. 3; step 2). For those species classified as birds, we used the function *gnr_resolve* one more time using BirdLife International[5] as the reference database (Supplementary Fig. 3; step 3). We used data from the Integrated Taxonomic Information System (ITIS)[6] and the *synonyms* function from the taxize package[2] to obtain the synonyms of the species cross-checked with BirdLife International, as well as of those that were not found in the BirdLife database but were previously classified as birds (Supplementary Fig. 3; step 4). We did this because, while obsolete bird species names usually did not have a match in BirdLife, one of its synonyms could: e.g., the black-fronted piping-guan was not found in the BirdLife database when its former scientific name, *Penelope jacutinga*, was entered; however, its currently accepted scientific name, *Pipile jacutinga*, was found as being one of the synonyms of *Penelope jacutinga*, and this synonym was revealed during step 4.

We also downloaded the Handbook of the Birds of the World (HBW) and BirdLife International (version 4.0)[7] and automatically checked for matches of species names in our frugivore list with the names from the columns 'scientific name' and 'synonym' of the HBW-BirdLife spreadsheet (Supplementary Fig. 3; step 5). By doing this, we were able to retrieve all the scientific names associated with the matched name in HBW-Birdlife. We used a fuzzy matching algorithm based on the Levenshtein distance between two strings to search for other possible names on the HBW-BirdLife spreadsheet for the species without good matches in any of the GNR's sources or BirdLife International, as well as for those species that were not found in the ITIS database (Supplementary Fig. 3; step 6). On some occasions, even this fuzzy matching algorithm could not find matches for a species name, which usually occurred when the genus name was incorrect or obsolete (note that in the vast majority of cases obsolete scientific names were fixed during steps 4 and 5, but some obsolete names were not present in either the ITIS or HBW-BirdLife databases). For those species, we automatically searched for their epithet names

in the columns 'scientific name' and 'synonym' of HBW-BirdLife and retrieved only those that had one single match in each column (Supplementary Fig. 3; step 7). The reason for restraining our search for those with one single match is because some epithet names are common and do not necessarily represent the same species. However, even this restriction is not a guarantee that the species with a given epithet in our list is the same species with the epithet in HBW-Birdlife, since a misspelled epithet name may coincidentally match the epithet of other species. Thus, we checked manually the taxonomy of all species corrected using this method (N = 17 species). We did this by searching for both the original species name (before the data cleaning process) and the matched name in the Avibase[8] and BirdLife[5] databases. By applying this series of filters, we were able to correct and validate the names and synonyms of 1,019 bird species. For the remaining species, we checked the taxonomy manually by inspecting the same databases as in the previous step.

Finally, we generated a list object in R[9] in which element names correspond to scientific names accepted by either BirdLife International - obtained using the *gnr_resolve* function from the taxize package[2] in 28/07/2020 - or HBW-BirdLife[7], while strings within elements correspond to all their synonyms and original species names. We used this list to standardize the taxonomy of the bird species in our local networks, so that synonyms would not be treated as different species (i.e., if two species were synonyms, they were attributed the same name in the local networks). All species that were removed during the cleaning process (non-bird species and those without genus and/or species names, such as Undefined sp. and *Turdus* sp.) were removed from our local networks and further analyses (N = 82 species). Around 86% of frugivore species remained per network after the data cleaning. Supplementary Figure 3 shows a summary of the steps of the frugivore data cleaning.

Plant species

We checked the matching of plant species names with several taxonomic sources from the Global Names Resolver (GNR)[1] using the function *gnr_resolve* from the taxize package[2] (Supplementary Fig. 4; step 1), as with birds above. For those species without matches in any of GNR's sources, we applied a fuzzy matching algorithm based on the Levenshtein distance between two strings to compare these species' names with the matched names from GNR (Supplementary Fig. 4; step 2). We did this because some of the species' names without matches in our step 1 were misspelled names of plant species already included in our dataset but not found by the *gnr_resolve* function. After this process, we relied on the *gnr_resolve* function one more time to compare the list of matched names from GNR with the list from the International Plant Names Index (IPNI)[10] (Supplementary Fig. 4; step 3). The reason for using *gnr_resolve* twice is because we first wanted to make sure that the species had a match with at least one of the taxonomic sources from GNR (i.e., confirm that it is a scientific name) and then check whether the matched name represents a scientific name accepted by IPNI. By doing this, we were able to evaluate which species had high matching scores during our first step but not during the third, indicating that they are not internationally accepted scientific names.

We used data from the Tropicos database[11] to obtain the synonyms of the plant species that had been cross-checked with IPNI. We also relied on the iPlant Taxonomic Name Resolution Service[12] to complement the synonyms list and retrieve the most recent accepted names of the species (Supplementary Fig. 4; step 4). Using this series of filters, we were able to correct and validate the names and synonyms of 1,562 plant species. Finally, we generated a list

object in R[9] in which element names correspond to accepted scientific names of species (cross-checked with the IPNI database on 15/09/2020) and strings within elements correspond to all their synonyms and original species names (before the data cleaning process). We used this list to standardize the taxonomy of the plant species in our local networks, as we did for birds.

Because our plant list contained several cases in which two (or more) accepted species shared a synonym within their elements (N = 121), we had to deal with the standardization of these names. We did this by attributing the same name for all the occurrences of the species sharing a synonym only if the shared name was already present in our dataset. For example, *Cecropia digitata* is one of the synonyms of *C. angustifolia, C. obtusifolia* and *C. pachystachya* (and is therefore within the elements of these three species), but *C. digitata* was not present in any of the networks in our dataset, such that we could maintain the names C. *angustifolia, C. obtusifolia* and *C. pachystachya* in our local networks. We did this because shared synonyms that were not present in our dataset usually represented obsolete species that are no longer accepted. Alternatively, for the cases in which the shared synonym was present in our dataset (N = 37), we attributed the same name in the local networks for all the species that shared that given name. We adopted this conservative approach because, in this case, shared synonyms were usually species that were described multiple times by different authors, or species with several subspecies and varieties (note, however, that authors rarely include this level of taxonomic information on networks). Therefore, the shared name could potentially be any of the species that possess it as one of its synonyms.

Considering the high number of species (N = 184) with a valid genus name but without a valid epithet name (as indicated by the absence of matches in our steps 1 and 3, or by the low matching scores to any of the GNR's sources), as well as unresolved species names without good matches in the IPNI database (hereafter, *problematic species*) in our plant species list, we added two steps to evaluate whether such problematic species could be considered as a separate species from the other species in our dataset. For example, a species without an epithet (e.g., labelled in a study as '*Miconia* sp.') could still be treated as a distinct species in the analysis, provided we could be certain that it was not the same as another congeneric (*Miconia*) species, with or without epithet, in our dataset. Similarly, an unresolved species name that is not internationally accepted could only be considered as a distinct species in our analysis if we could disentangle it from its congeneric species in the dataset. Importantly, we did not perform these additional steps for birds because there were very few cases of birds with valid genus but invalid epithet names.

To determine whether problematic species could be treated as a distinct species for analysis, we evaluated whether the distribution of any of the congeners of problematic species in our dataset overlapped with the location of the problematic species, such that we cannot be confident that the problematic species is not simply another occurrence of one or more of its congeners already in the dataset. For this process, we used the coordinates of the networks in which each problematic species occurred and generated buffer zones (diameter = 500 km) around these network locations. Considering that the size of the buffer zones could potentially affect our results, we also conducted the analysis using buffer zone sizes of 100 km and 1000 km (note, however, that our results still hold independently of the buffer zone size used; see Supplementary Tables 9-32). We collected occurrence data for all other species in the same genus in our dataset to evaluate whether the occurrence points of any of these congeneric species overlapped with the buffer zone of the problematic species (Supplementary Fig. 4; step 5). For collecting occurrence points, we used data from the Global Biodiversity Information Facility (GBIF)[13] and applied a series of filters (for details, see the Occurrence data section below). If the

occurrence points of at least one of the congeneric species overlapped with the buffer zone of a given problematic species, we assumed that this problematic species could not be considered, with confidence, as a unique species in our dataset. Conversely, if none of the occurrence points of congeneric species overlapped with the buffer zone of the problematic species, we treated this problematic species as a separate species (Supplementary Fig. 5), provided that there were no other problematic species (without valid epithets) in the same genus from other studies in the dataset.

Alternatively, if a genus contained more than one problematic species in the same study (e.g., *Miconia* sp.1, *Miconia* sp.2), we assumed that the authors distinguished the congeners within the study. For the cases in which a problematic species occurred in a single study and was the only species belonging to that genus in our dataset, the original name of the species was maintained in the local network. However, if there were problematic species from the same genus in different studies, we needed to ascertain whether they could potentially be the same species. Our approach for dealing with this issue was to determine all the possible species that a problematic species could be in each location, and then compare the lists of possible species in each location to identify any overlap. To do this, we first generated buffer zones (as in step 5) for each network location in which these problematic species occurred and obtained occurrence data from GBIF for all known species belonging to that genus (see the Occurrence data section). We then checked whether there were congeneric species with occurrence points within the buffer zones of two (or more) problematic species belonging to the same genus (Supplementary Fig. 4; step 6). If yes, we could not consider that these problematic species were different from each other. Rather, in this case there was a chance that the problematic species were the same species whose occurrence points overlapped the buffer zones of both network locations (Supplementary Fig. 6). On the other hand, if there were no species whose distribution overlapped the buffer zones of both network locations, these problematic species could be considered as being distinct species in the dataset.

All species that were removed during the data cleaning process (i.e., the problematic species without a valid genus name, such as Rubiaceae sp. or Undefined sp.) were also removed from our local networks and further analyses (N = 166 species). Problematic species that could not be disentangled from resolved species or other problematic species in the dataset were named according to three distinct scenarios (for details, see the Alternative scenarios section). Around 89% percent of plant species remained per network after the data cleaning (note, however, that this percentage varies slightly depending on the scenario employed). Supplementary Figure 4 shows a summary of the steps of the plant data cleaning.

Occurrence data

We retrieved occurrence data from the Global Biodiversity Information Facility (GBIF)[13] using the function *occ_search* from the R package rgbif[14]. For each species, we only requested occurrence data for observations for which coordinate points were available and no geospatial issues were detected, as determined by GBIF's record interpretation. We also followed a previous study[15] and removed occurrence points with: (i) a coordinate uncertainty larger than 100 km (the size of our smallest buffer zone); (ii) those for which the collection date was before 1945, as older occurrence points are usually not properly geo-referenced[16]; (iii) those in which the number of counts associated with the occurrence point was zero; and (iv) those in which the 'basis of record' was not an observation or a preserved specimen.

In addition, we used the function *clean_coordinates* from the R package CoordinateCleaner[17] and land mass and country data (with a 1:10m scale) from Natural Earth[18] to remove occurrence points for which the coordinates: (v) fell within the ocean or outside the borders of the country where they were recorded, both of which indicate data-entry errors, (vi) were located around the country capital or the centroid of the country, indicating imprecise geo-referencing based on inadequate sampling site descriptions, (vii) both latitude and longitude were zero or had equal values, indicating failed geo-referencing, and (viii) were located around a biodiversity institution, suggesting that records might represent specimens that were erroneously geo-referenced to museums, herbaria or universities instead of their sampling localities[17]. After applying this series of filters, 456,582 occurrence points were retrieved for 610 plant species in our dataset. These occurrence points were used for disentangling 'problematic' species during step 5 of the plant species cleaning process (Supplementary Fig. 5).

Because the next step required us to retrieve occurrence data for all known species belonging to a given genus, we used the function *name_lookup* from the R package rgbif[14] to search for all accepted species names associated with the genus name. We used the same set of filters previously described to obtain the occurrence points for each species during the step 6 of the plant species cleaning process (Supplementary Fig. 6). In the end, 994,270 occurrence points were retrieved for 4,793 plant species.

Alternative scenarios

We used three distinct scenarios for attributing names for problematic plant species that could not be considered as unique species in our dataset. In the first scenario, we removed from the local network any problematic species whose buffer zone was overlapped by the distribution of 'resolved' congeneric species in the dataset (step 5 of the plant species cleaning process). For example, if the buffer zone of the problematic species '*Miconia* sp.' was overlapped by other resolved *Miconia* species in the dataset, we removed the species *Miconia* sp. (and all of its interactions) from its local network. We adopted this strategy rather than considering that the problematic species and the resolved species that overlap its buffer zone are the same because such problematic species could potentially be any of the resolved species that overlap its buffer zone. This, in turn, made it impractical to attribute the name of the resolved species to the problematic species in cases where the buffer zone of the problematic species was overlapped by several resolved species. In addition, our first scenario considers all problematic species that could not be disentangled from each other (step 6 of the plant species cleaning process) as being the same species. For example, if two problematic species labelled as '*Coussapoa* sp.' in two separate local networks could not be disentangled because there are congeneric species simultaneously overlapping the buffer zones of both network locations (Supplementary Fig. 6), we attributed the same name to these two problematic species.

Alternatively, our second scenario treats problematic species as being unique. Therefore, a unique name was given for the problematic species whose buffer zone was overlapped by 'resolved' congeneric species in the dataset. For instance, the problematic species '*Miconia* sp.' from the example above would receive a unique name in the second scenario instead of being removed from its local network. In this scenario, we also attributed unique names for problematic species that could not be disentangled from each other. For example, each of the two problematic *Coussapoa* species mentioned above would receive a unique name instead of sharing the same name.

Finally, the third scenario removes from the local networks all plant species that could not be considered as being unique species in the dataset and is therefore our most conservative scenario (which was used for obtaining the results presented in the main text). Because these three different scenarios could affect our response variables, we repeated the analyses using the sets of networks from all scenarios. Notably, results remained qualitatively the same independently of the scenario used in the analyses (Supplementary Tables 9-32).

Sensitivity analysis

Considering that the threshold of minimum network size used for analyses is arbitrary and has the potential to affect the reported patterns, we performed a sensitivity analysis to evaluate how sequentially removing local networks based on their size would affect the estimates (t and F values) and significance (obtained using a combination of Generalized Additive Models and Multiple Regression on distance Matrices) of our predictor variables. We did this by sequentially removing all networks below a specified threshold of size (i.e., class of network size) in our dataset, from smallest to largest (Supplementary Fig. 22). Note, however, that although we had 60 different classes of network sizes (minimum network size = 8 species; maximum network size = 238 species), we were only able to perform the analysis up to the removal of networks with 71 (or fewer) species (which represented 183 out of the 196 local networks in our dataset). We could not remove the local networks with larger sizes (N = 13 networks) because removing any of these remaining networks would lead to our Generalized Additive Models (GAMs) having more coefficients than data.

We found that removing small networks from our dataset did not strongly affect our results; for instance, removing networks with up to 10 species (which represent 17 out of 196 local networks in our dataset) would not affect any of the reported patterns (Supplementary Figs. 23 and 24). We also highlight that even though all estimates tend to approach zero with the removal of larger networks, this is partially because beyond a certain number of network removals there are too few data points and insufficient range of the predictor value for the model to be able to detect an effect.

Importantly, of the significant effects in the full model using interaction dissimilarity as response, only biome boundaries seem to be sensitive to the sequential removal of small networks from the dataset (Supplementary Fig. 23). However, biome boundaries explained a relatively low unique proportion of the variation in interaction dissimilarity in our full model. In fact, most of the deviance explained by biomes was shared with ecoregions (Supplementary Fig. 12), which is likely because biomes share boundaries with ecoregions and the latter explain finer-resolution environmental differences[19]. This strong effect of ecoregion borders on interaction dissimilarity is corroborated in our sensitivity analysis: the effect of ecoregions remained significant even after the removal of networks with up to 57 species (which represented around 88% of the local networks in our dataset; Supplementary Fig. 22).

In addition, the two significant effects in our full model using network dissimilarity as response variable were very robust to the removal of small networks from the dataset (Supplementary Fig. 24). More specifically, the effect of spatial distance remained significant even after the removal of networks with up to 22 species (which represented around 50% of our local networks), while the effect of sampling intensity was still significant after the removal of networks with up to 32 species (~ 68% of the local networks in the dataset).

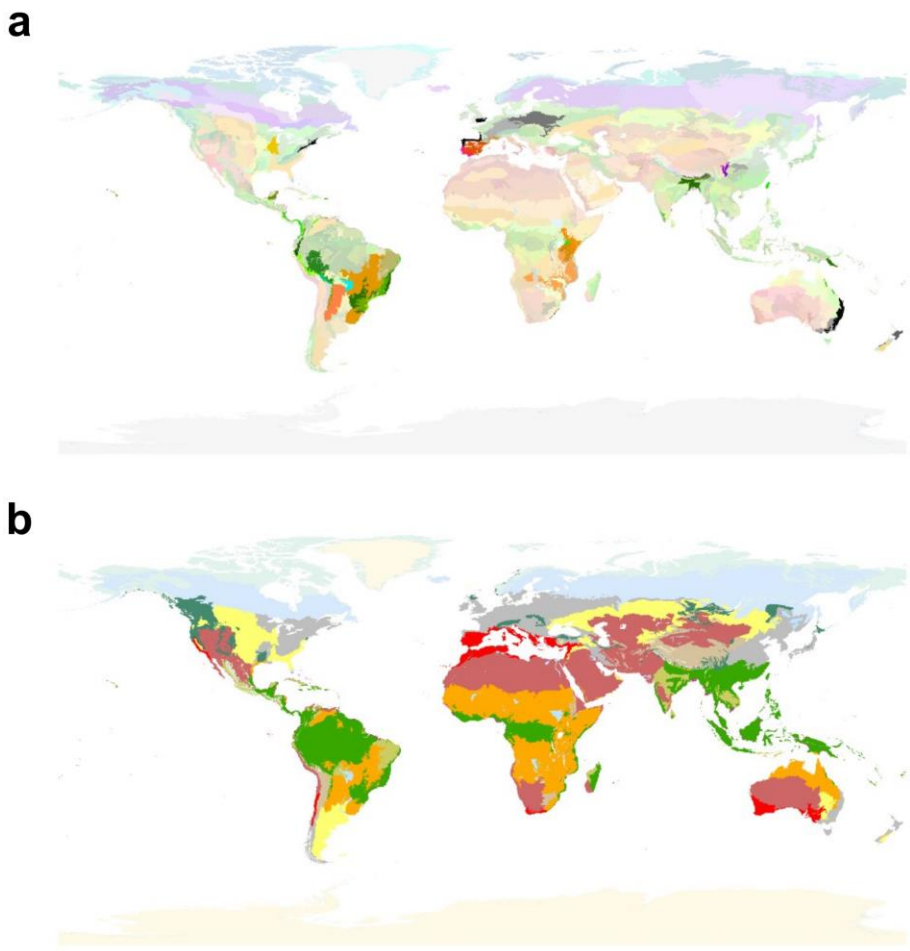

Supplementary Fig 1. Maps of ecoregions and biomes of the world. a Terrestrial ecoregions, with stronger color tones indicating the 67 ecoregions (out of 846) represented in our dataset. **b** Global biomes, with stronger color tones indicating the 11 biomes (out of 14) represented in our dataset. Ecoregions and biomes were defined based on the map developed by Dinerstein et al.[19] (available at https://ecoregions.appspot.com/ under a CC-BY 4.0 license).

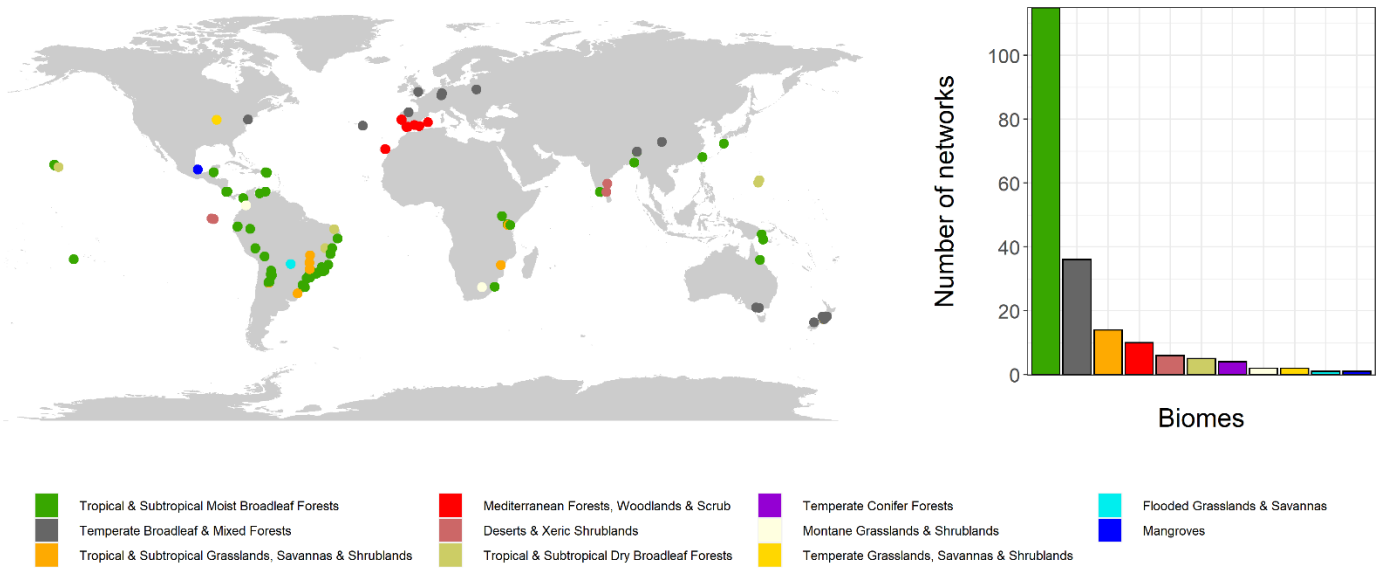

Supplementary Fig. 2. Geographic distribution of the 196 avian frugivory networks in our dataset. Local networks were distributed across 11 biomes, with most of these being located within a single biome, the Tropical & Subtropical Moist Broadleaf Forests, which covers around 11% of the world's ice-free land surface. Biomes were defined based on the map developed by Dinerstein et al.[19] (available at https://ecoregions.appspot.com/ under a CC-BY 4.0 license).

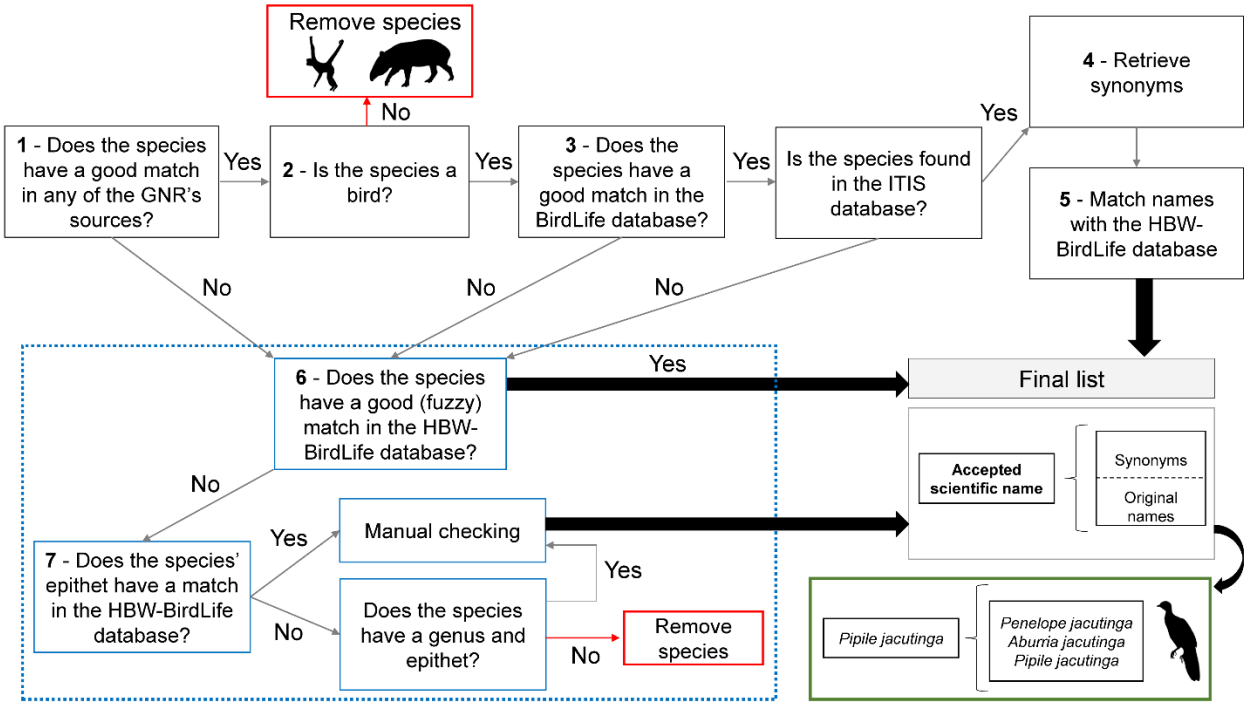

Supplementary Fig. 3. An overview of the steps for cleaning and standardizing the frugivore species data. Red boxes represent species that were removed from the analyses (non-avian species and species without epithet or genus names). The dashed box comprises the steps performed for the species without good matches in any of the Global Names Resolver (GNR) sources and in the BirdLife International database, or that were not found in the Integrated Taxonomic Information System (ITIS). The final list comprises elements whose names represent scientific names accepted either by the BirdLife International or by the Handbook of the Birds of the World and BirdLife International, and strings within elements comprise their synonymous and original names (before the cleaning process). For example, *Pipile jacutinga* (Cracidae) is the current accepted name of the black-fronted piping-guan, while its synonymous names include *Penelope jacutinga* and *Aburria jacutinga* (green box). All names (strings of synonyms) within elements (accepted names) were replaced by the element name in the local networks, such that a given species had the same name for all its occurrences in the entire database. Numbers inside boxes correspond to the steps of the frugivore data cleaning process. Silhouettes were obtained from http://phylopic.org under a Public Domain license.

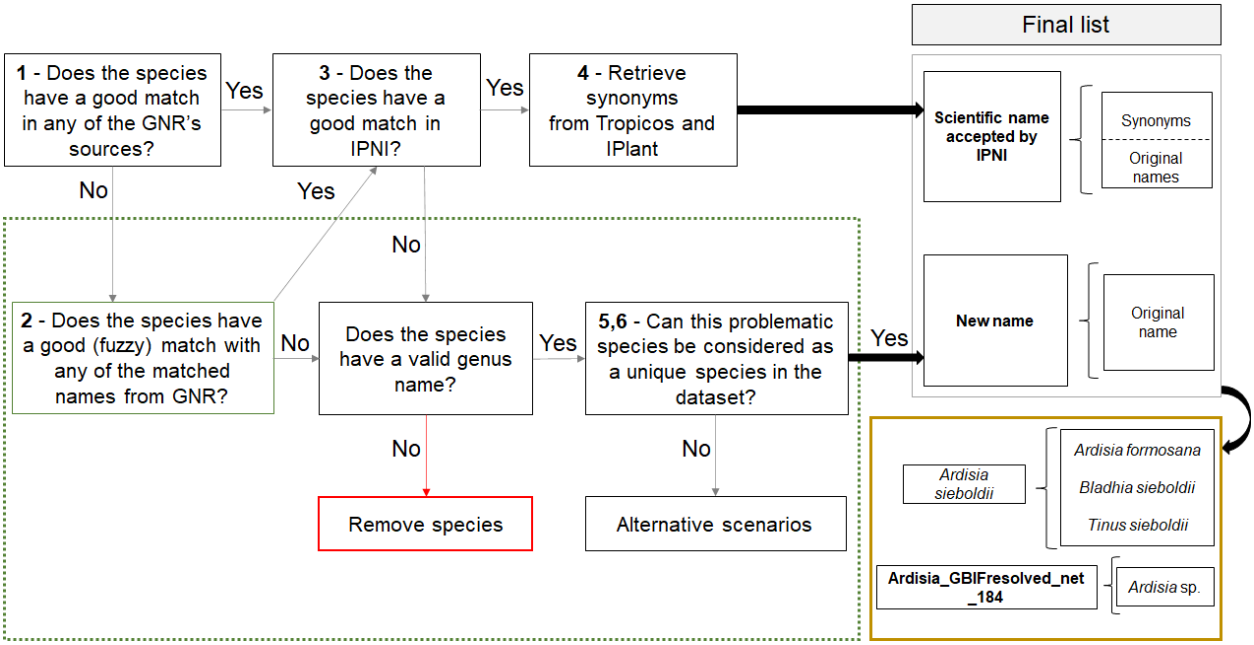

Supplementary Fig. 4. **Overview of the steps for cleaning and standardizing the plant species data.** The red box represents species that were removed from the analyses (species without valid genus names). The dashed box comprises the steps performed for the species without good matches in any of the Global Names Resolver (GNR) sources and in the International Plant Names Index (IPNI) database (i.e., 'problematic species'). We performed two steps to determine if problematic species could be considered as being unique species in our dataset (see steps 5 and 6 of the plant species data cleaning process described in the text and visualized in Supplementary Figs. 5 and 6). The final list comprises elements whose names represent scientific names cross-checked with the IPNI database and strings within elements comprise their synonymous and original names (before the cleaning process), or elements whose names represent new names given for problematic species that can be considered as unique species in our dataset, and the strings within elements comprise their original name. For example (yellow box), *Ardisia sieboldii* (Primulaceae) is a scientific name accepted by IPNI, while *A. formosana, Bladhia sieboldii* and *Tinus sieboldii* represent some of its synonymous names. Meanwhile, Ardisia_GBIFresolved_net_184 is the new name given for the problematic (but unique) species *Ardisia* sp., as revealed by the step 5 of the plant species data cleaning process. Note that, in the former case, all names (strings) within elements were replaced by the element name in the local networks, while in the latter case strings within elements were replaced by the element name only in the network where the problematic species was observed (in this example, network 184). Numbers inside boxes correspond to the steps of the plant data cleaning process. See the Alternative scenarios section for details on how we attributed names for plant species that could not be considered as unique species in our dataset.

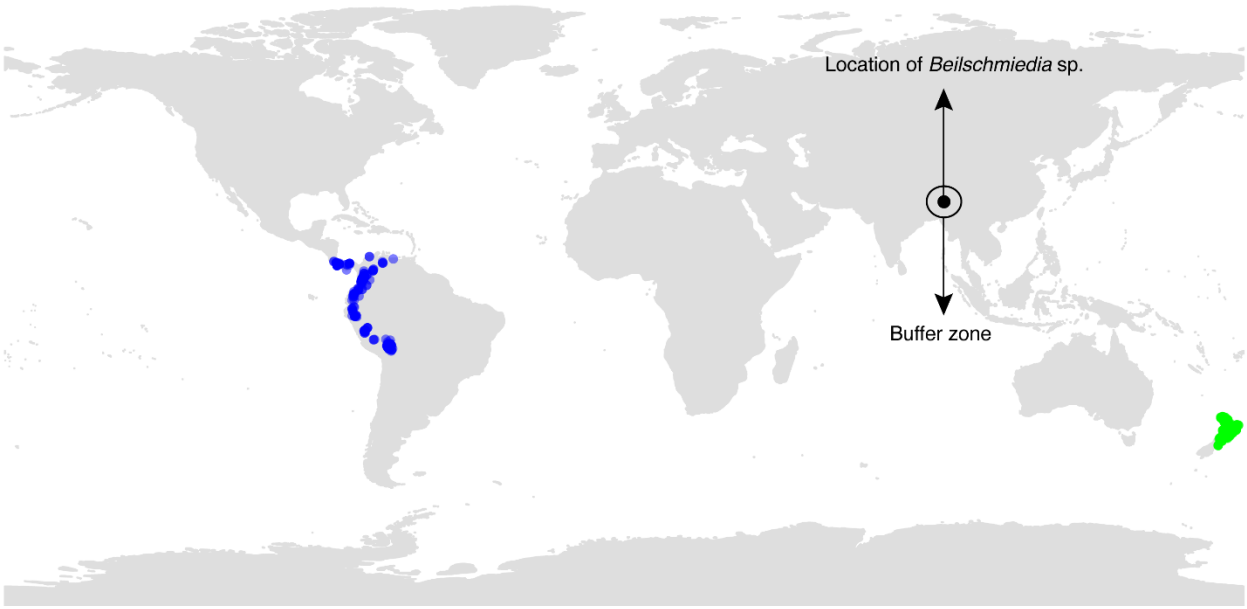

Supplementary Fig. 5. Graphical example (for an unresolved *Beilschmiedia* species) of step 5 of the plant species cleaning process. Coloured points indicate the distribution of *Beilschmiedia* species already contained within our dataset, and these are compared with the occurrence location of a 'problematic species' (a species with genus name only). The distributions of both *Beilschmiedia tawa* (green dots) and *Beilschmiedia tovarensis* (blue dots) do not overlap with the buffer zone of the problematic species *Beilschmiedia* sp., such that *Beilschmiedia* sp. can be considered as a separate species in our dataset.

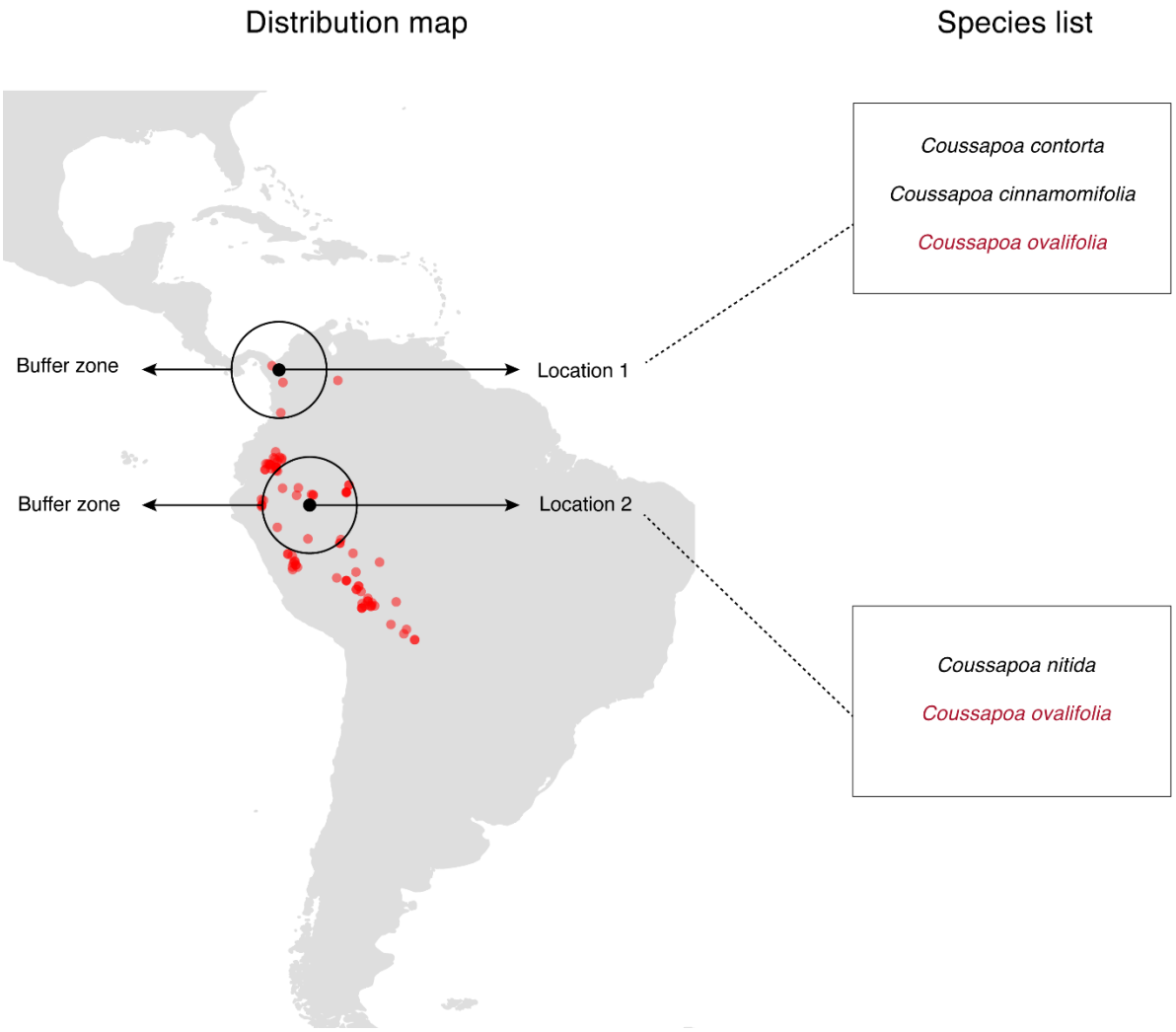

Supplementary Fig. 6. Graphical example of step 6 of the plant species cleaning process. In this example, there are two occurrences of species labelled '*Coussapoa* sp.' in separate studies (locations 1 and 2). The distribution of *Coussapoa ovalifolia* (red dots) simultaneously overlaps the buffer zones of two 'problematic species' (i.e., species with genus name only) belonging to the same genus, such that these problematic species could not confidently be considered as being separate species. A distribution map like this was created for all congeneric species with occurrence data in either buffer zone. Note that *C. ovalifolia* is present in the potential list of *Coussapoa* species in both network sites (other *Coussapoa* species were omitted in the species lists for clarity).

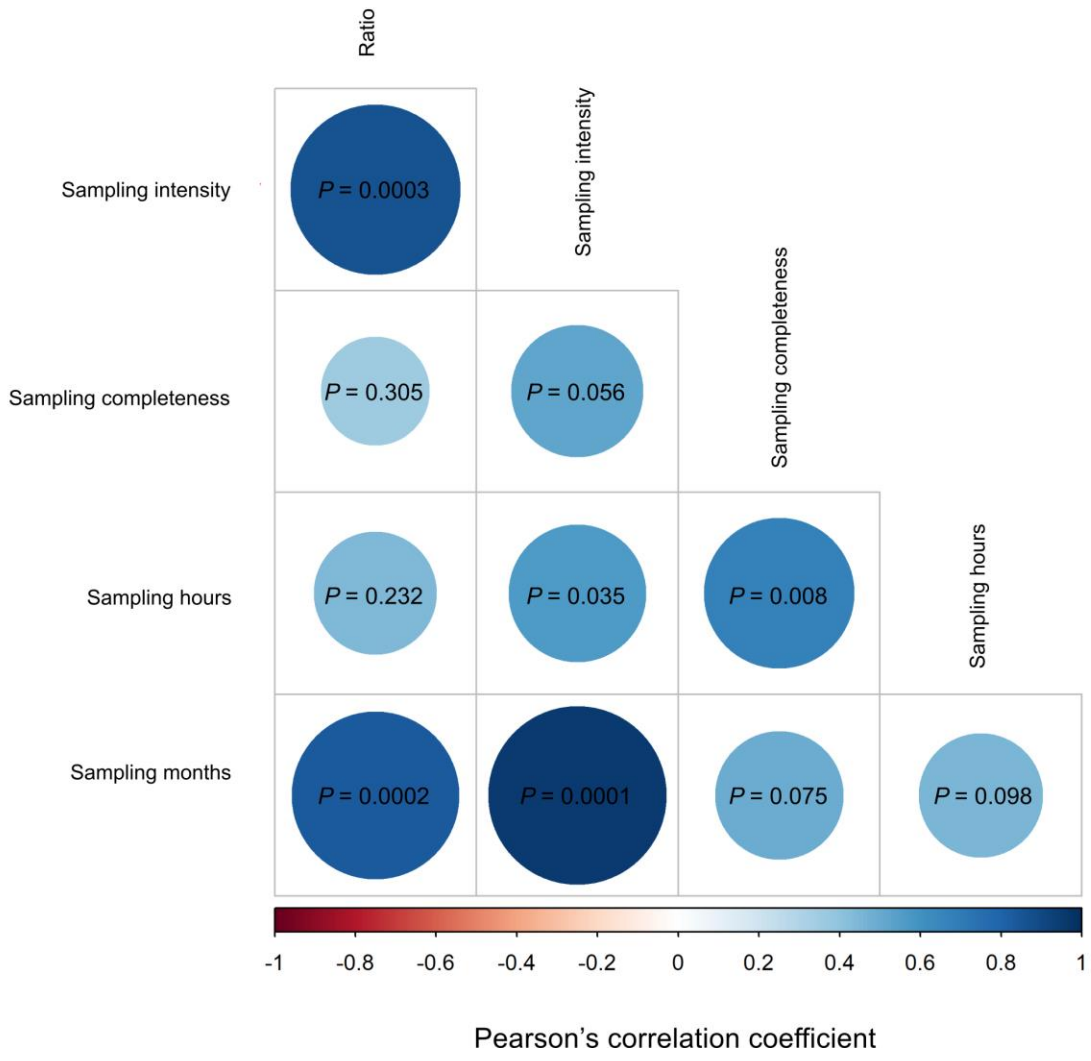

Supplementary Fig. 7. Results from Pearson's correlation tests between sampling metrics. For this analysis, we used the subset of networks sampled in Aotearoa New Zealand (N = 14). Numbers inside circles indicate P values obtained using a two-tailed Pearson correlation test. Sizes of the circles and colors are proportional to the correlation coefficient.

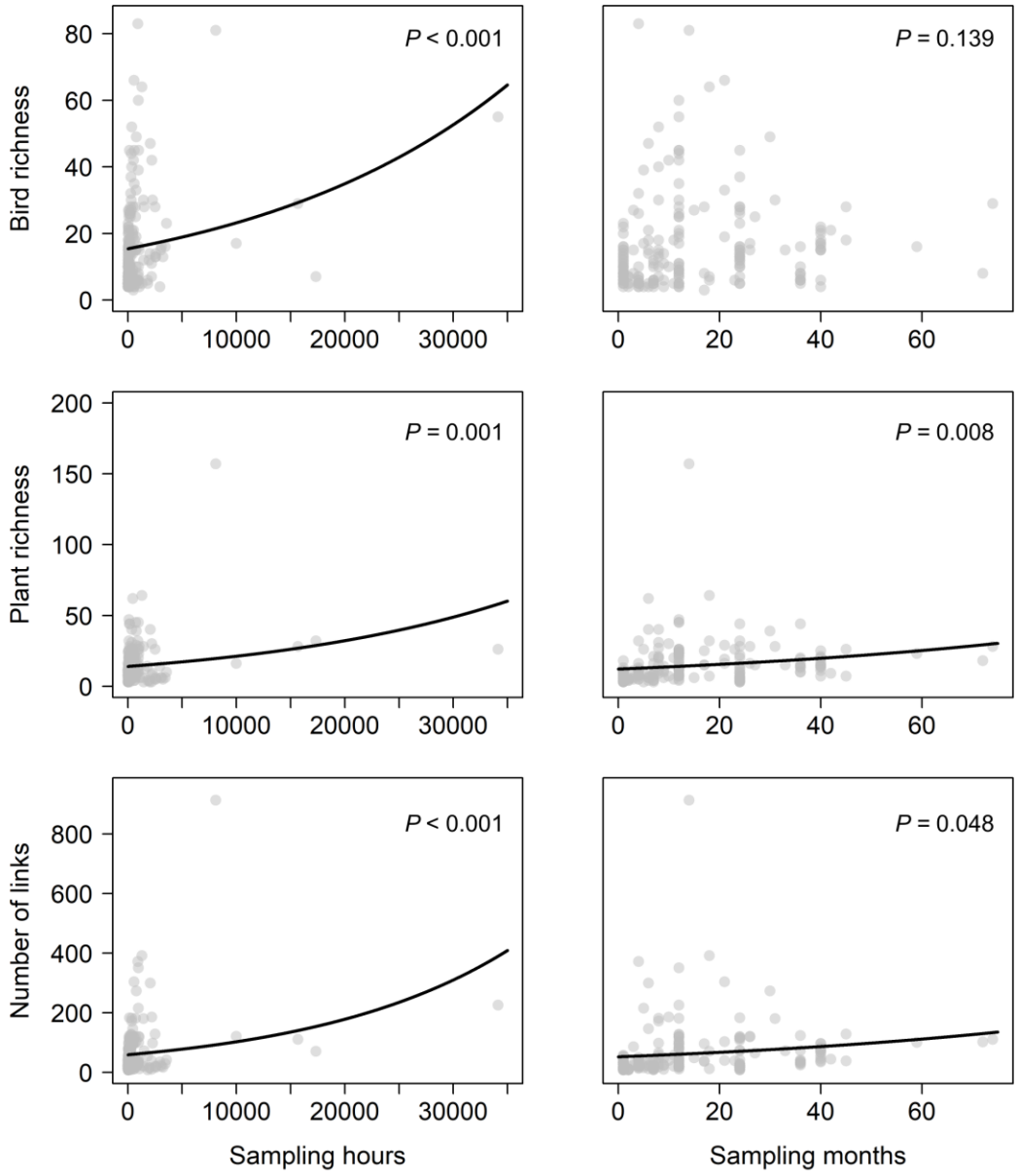

Supplementary Fig. 8. Relationships between network metrics and sampling hours and months. We used Generalized Linear Models (with Poisson errors, fitted with quasi-likelihood to deal with overdispersion) to obtain significance values. Points represent the 196 local frugivory networks in our dataset. Solid lines represent significant relationships.

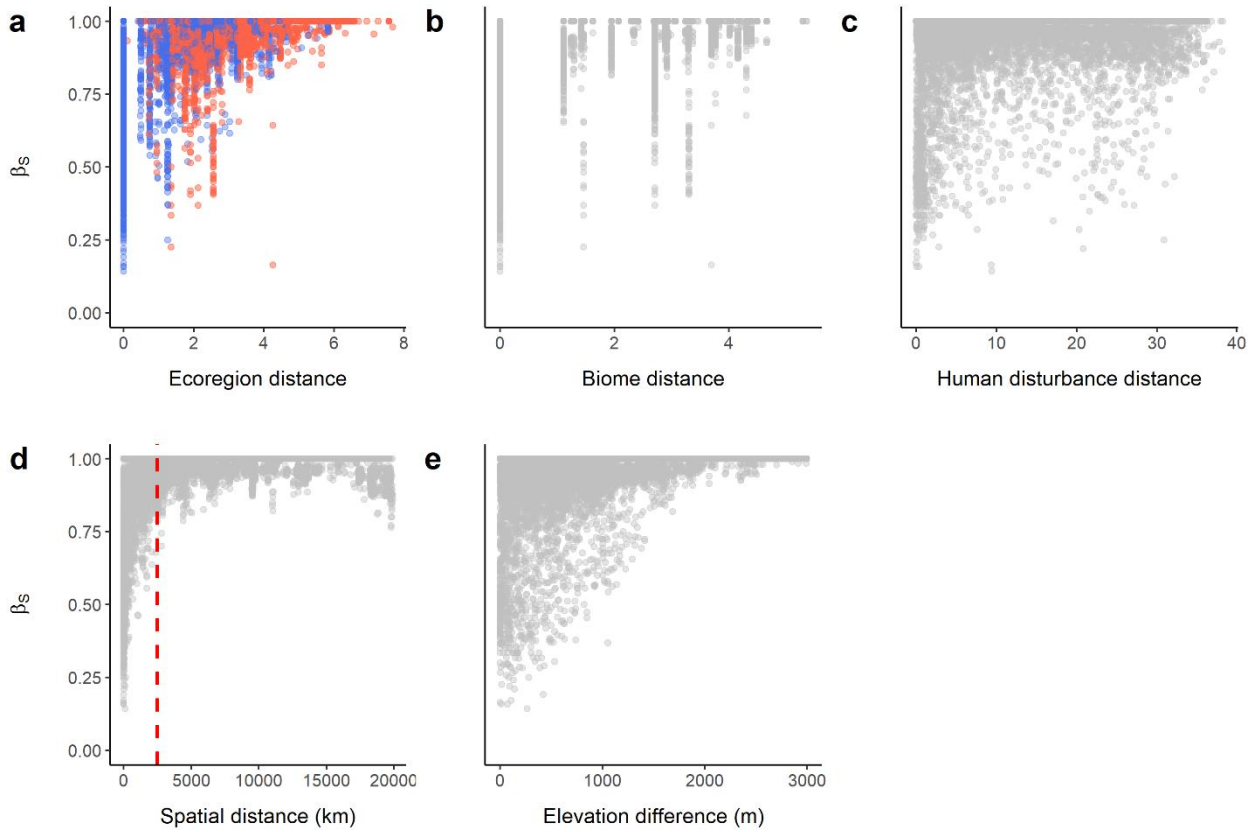

Supplementary Fig. 9. Scatterplots of the relationships between our predictor variables of interest (not those used for controlling sampling effects) and species turnover (βs). a The relationship between the quantitative version (environmental dissimilarity) of ecoregion distance and species turnover; point colors indicate whether the pair of local networks belong to the same (blue) or distinct (red) biomes. **b** The relationship between the quantitative version (environmental dissimilarity) of biome distance and species turnover. **c** The relationship between local human disturbance distance and species turnover. **d** The relationship between spatial distance and species turnover. Note that, contrary to species interactions (Fig. 6 in the main text and Supplementary Fig. 14c), several networks still shared species beyond the threshold distance of 2,500 km (dotted red line). **e** The relationship between elevation difference and species turnover.

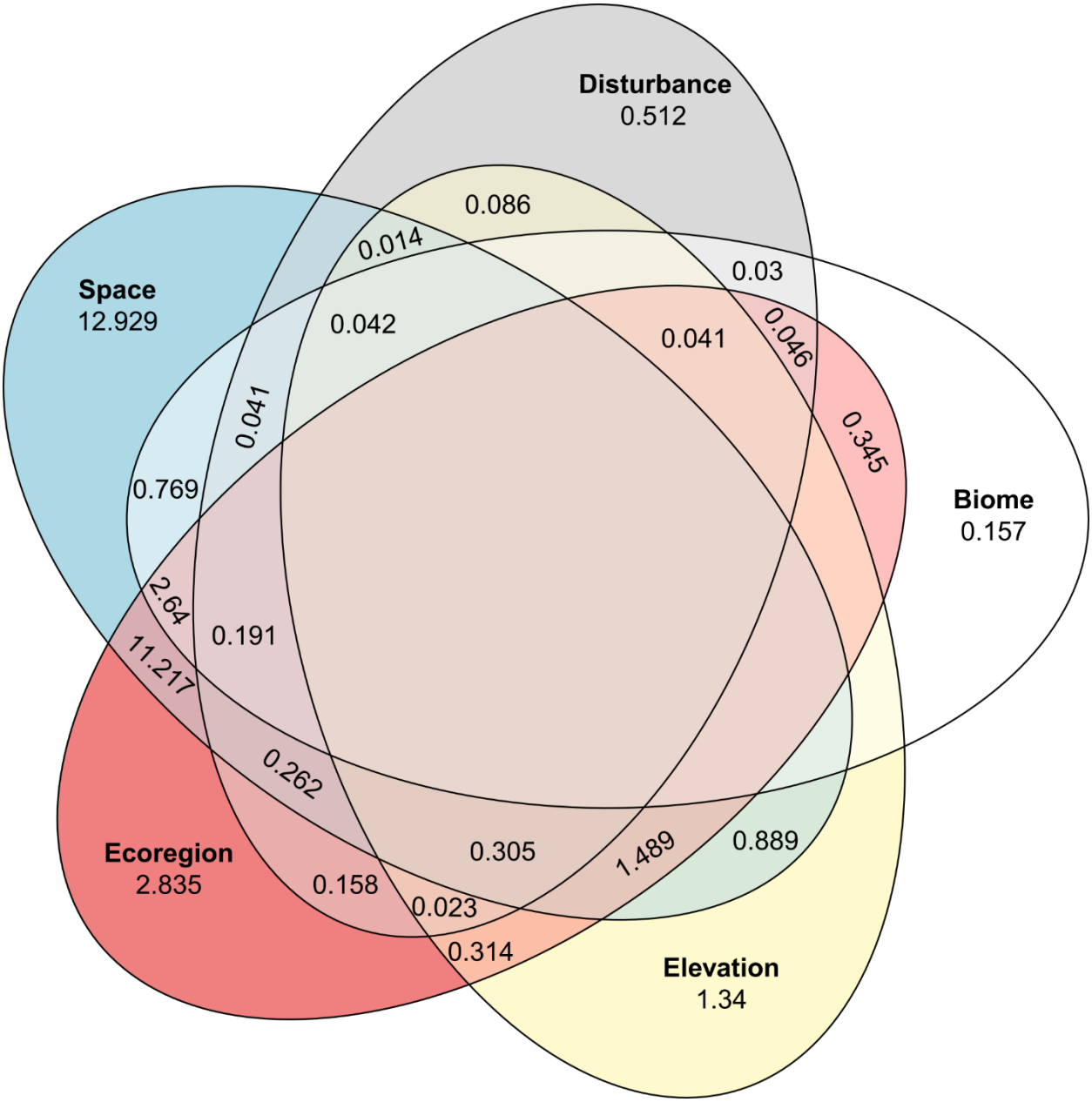

Supplementary Fig. 10. Venn diagram showing the relative contributions (%) of our main predictor variables to explaining the variation in species turnover (βS) across networks, calculated using deviance partitioning. Spatial distance alone explained the greatest proportion (12.9%) of the variation in species turnover, followed by the shared effect of spatial distance and ecoregion boundaries. Note that, to aid visualization, we only included our predictor variables of interest (i.e., not those used for controlling sampling effects). Terms that reduce explanatory power are not shown.

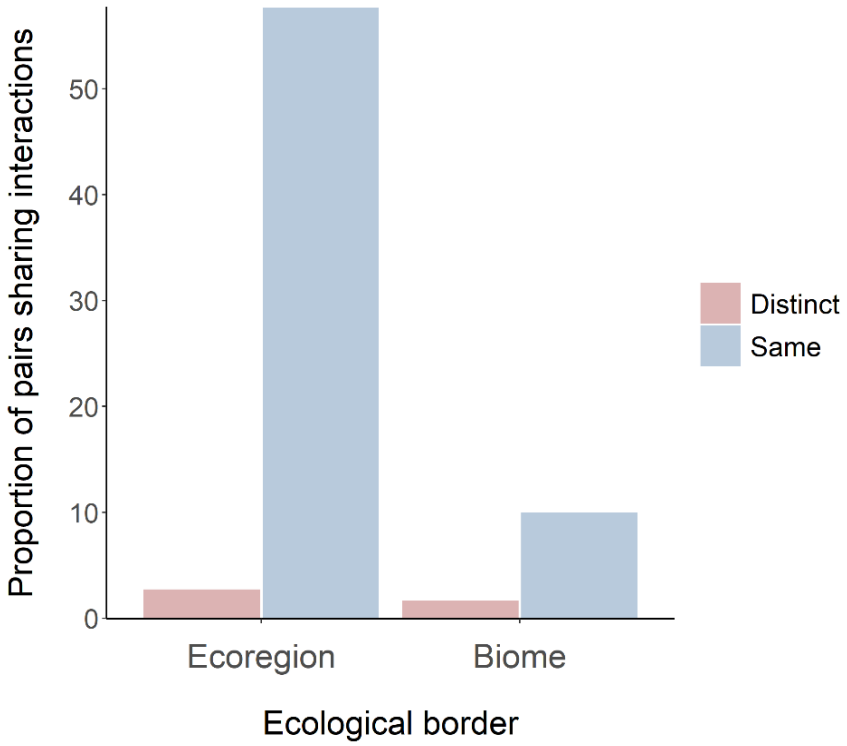

Supplementary Fig. 11. The effect of large-scale ecological boundaries on the proportion of pairs of local networks sharing interactions. Avian frugivory networks located within the same ecoregion/biome were more likely to share interactions than those located across distinct ecoregions/biomes. Note that over 50% of the pairs of networks located within the same ecoregion shared interactions.

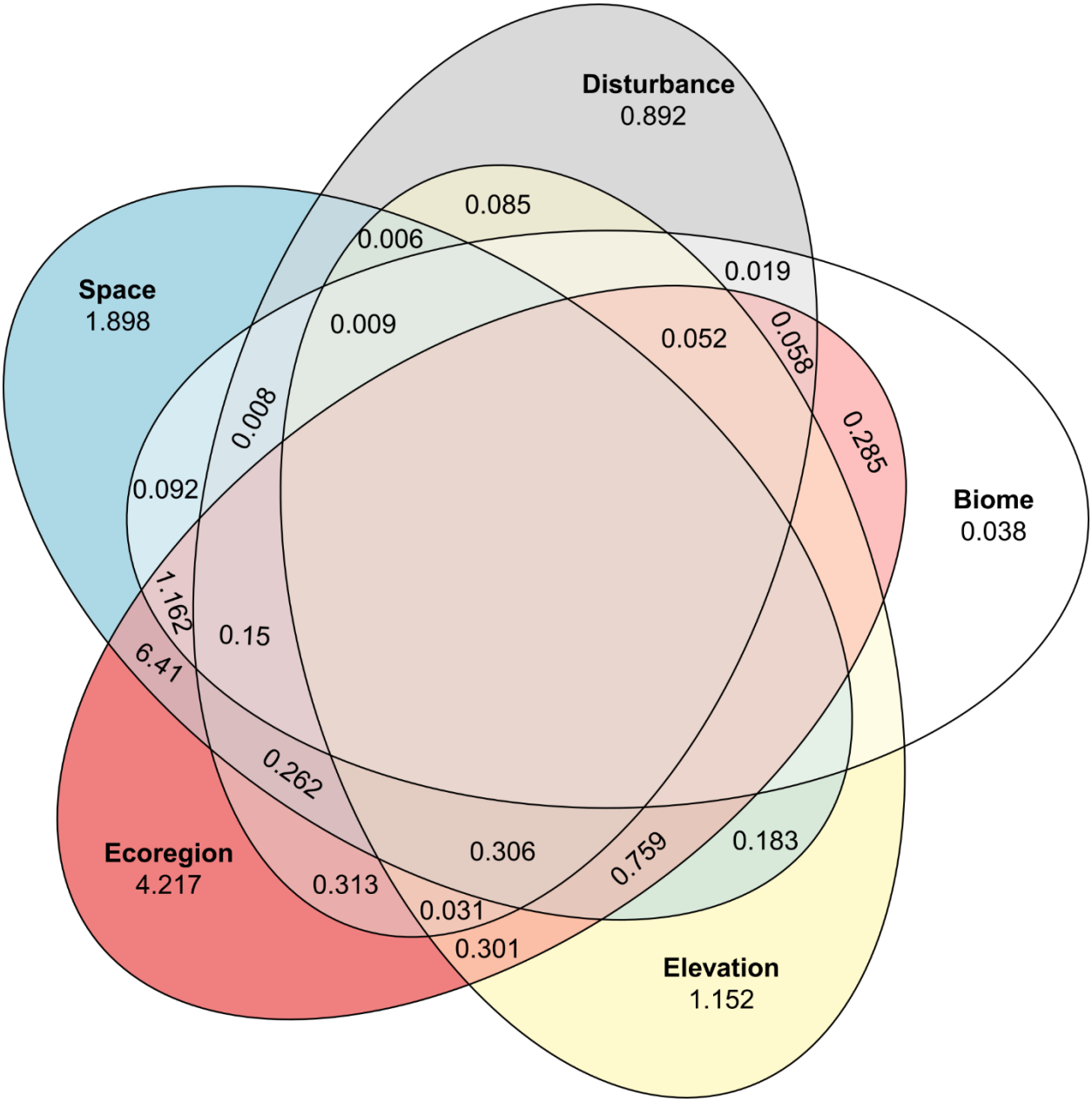

Supplementary Fig. 12. Venn diagram showing the relative contributions (%) of our main predictor variables to explaining the variation in plant-frugivore interaction dissimilarity (β_{WN}), calculated using deviance partitioning. The shared effect of ecoregions and spatial distance explained the greatest proportion (6.41%) of the variation in interaction dissimilarity, followed by the unique contributions of these two variables. Note that, to aid visualization, we only included our predictor variables of interest (i.e., not those used for controlling sampling effects). Terms that reduce explanatory power are not shown.

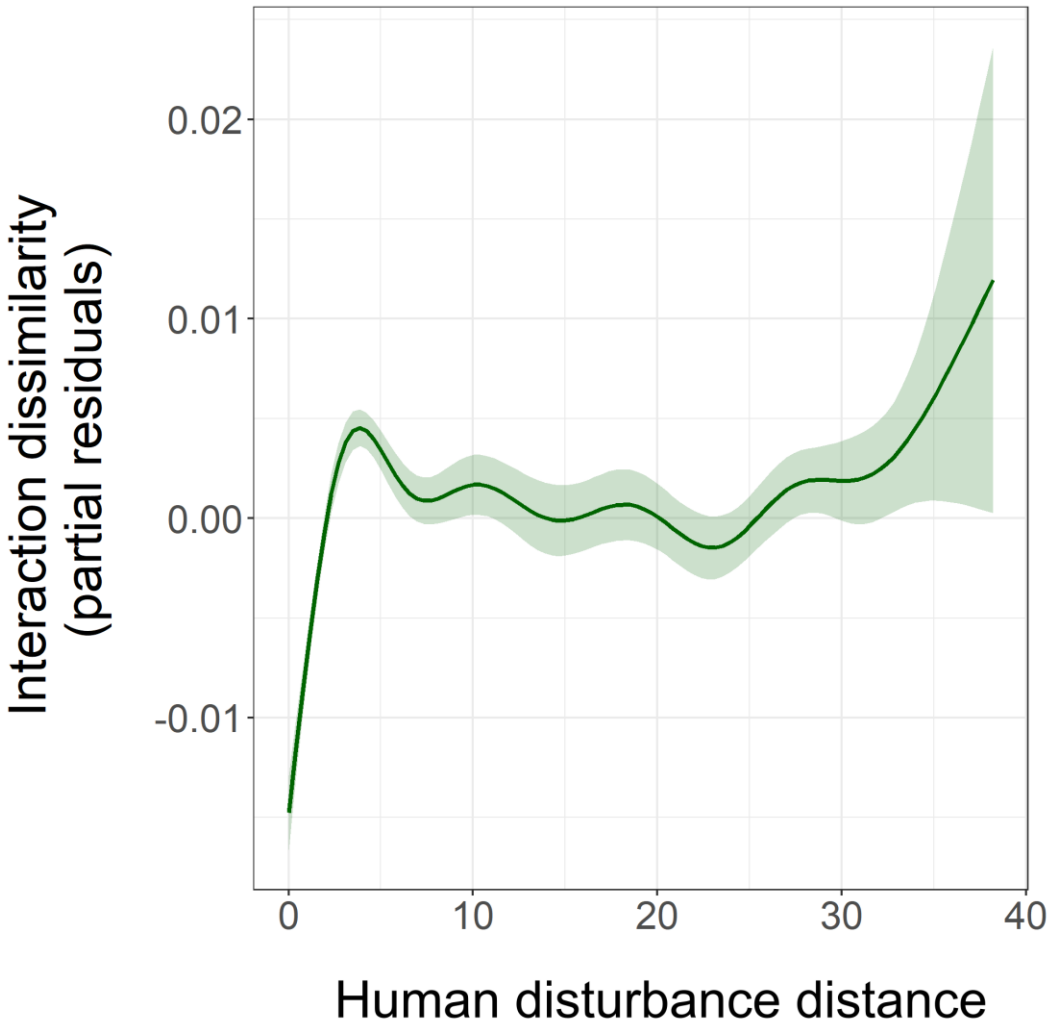

Supplementary Fig. 13. Partial effects plot of the relationship between human disturbance distance and interaction dissimilarity (β_{WN}). The smoothed line was fitted using a Generalized Additive Model (GAM) with interaction dissimilarity as response variable and all of our predictor variables included (see Table 1 in the main text). The lighter green area represents 2 standard errors above and below the estimate of the smooth being plotted.

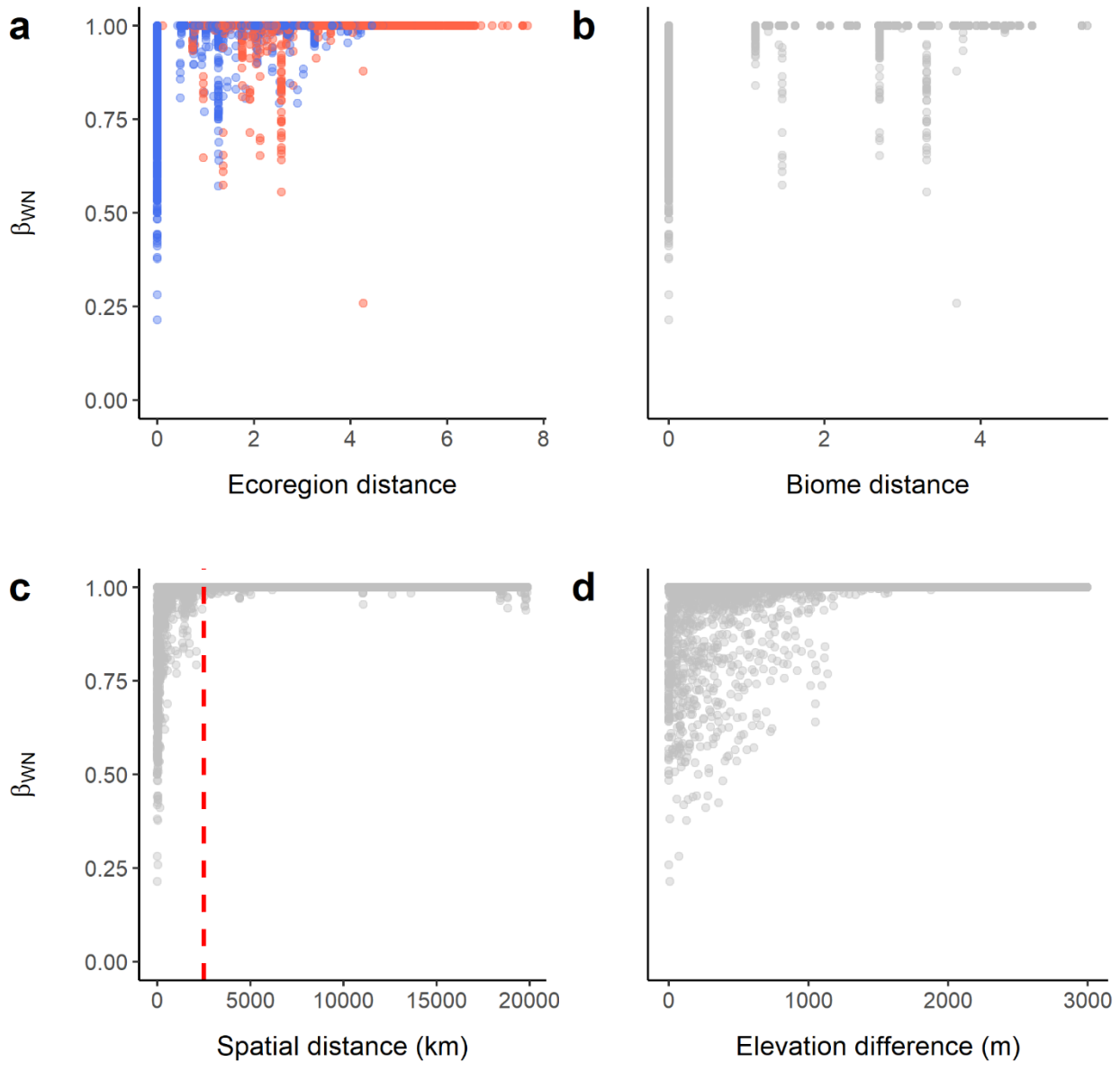

Supplementary Fig. 14. Scatterplots of the relationships between our predictor variables of interest (except human disturbance distance, which is presented in the main text) and interaction dissimilarity (β_{WN}). a The relationship between the quantitative version (environmental dissimilarity) of ecoregion distance and interaction dissimilarity; point colors indicate whether the pair of networks belong to the same (blue) or distinct (red) biomes. **b** The relationship between the quantitative version (environmental dissimilarity) of biome distance and interaction dissimilarity. **c** The relationship between spatial distance and interaction dissimilarity. Note that interaction dissimilarity increases sharply until a threshold distance of 2,500 km (dotted red line), beyond which few networks shared interactions (a similar pattern can be seen in Fig. 6 in the main text). **d** The relationship between elevation difference and interaction dissimilarity.

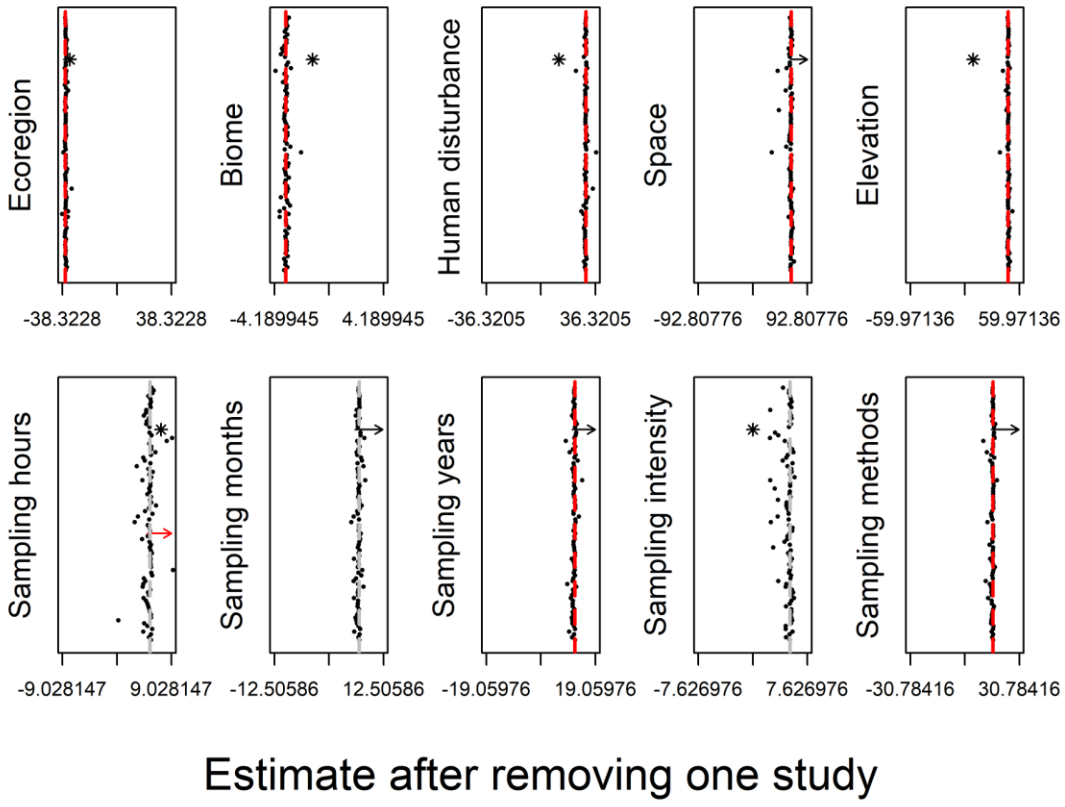

Supplementary Fig. 15. Effect of individual studies on estimates of t (for ecoregion and biome) and F values (for the remaining predictor variables) of Generalized Additive Models with interaction dissimilarity (β_{WN}) as response variable. Points represent estimate values after removing one study from the data, while asterisks indicate the estimates when the study with the greatest number of networks (N = 35) in our dataset (study ID 76)[20] is removed from the data. The estimates of the full model (with all studies included) are represented by the vertical lines. Red lines indicate a significant effect ($P < 0.05$), while gray lines indicate a non-significant effect. P values were calculated using a two-tailed statistical test that combines Generalized Additive Models (GAM) and Multiple Regression on distance Matrices (MRM). In this approach, the non-independence of distances from each local network is accounted for in the hypothesis testing by performing 1,000 permutations of the response matrix (see Methods). The range of the x-axis was defined as ± 3 times the standard deviation of the estimates. Arrows indicate outliers beyond this range (black: when study 76 is removed; red: when other studies are removed).

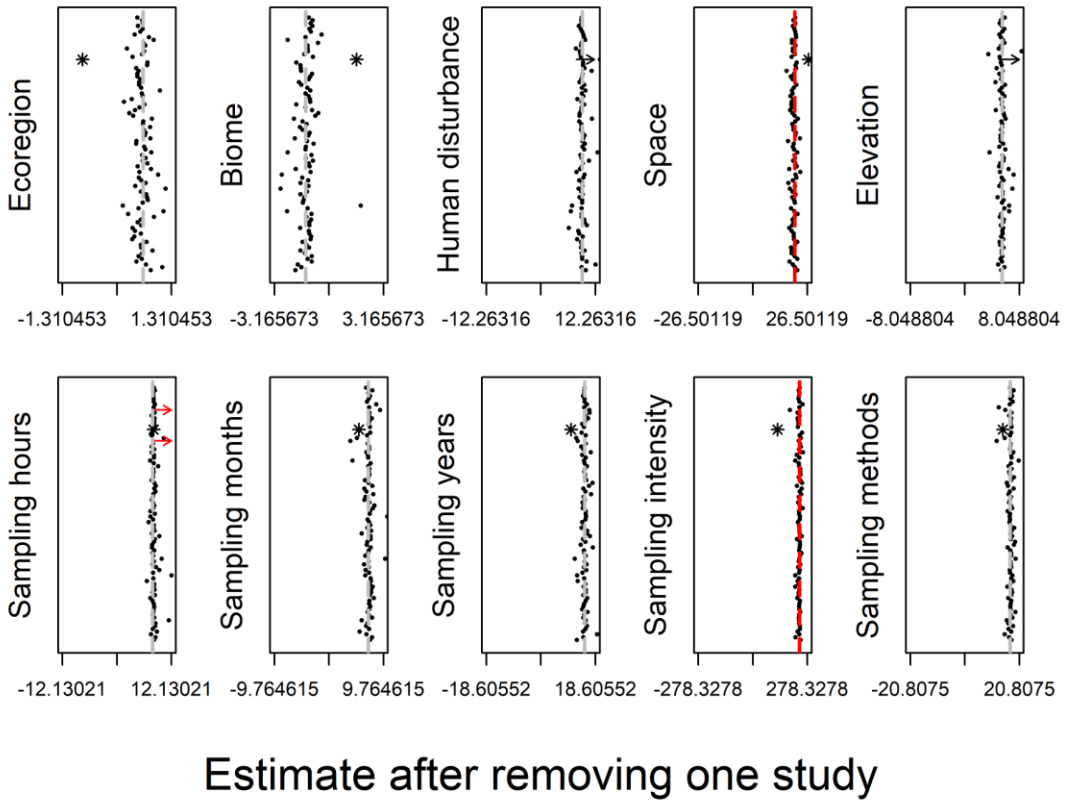

Supplementary Fig. 16. Effect of individual studies on estimates of t (for ecoregion and biome) and F values (for the remaining predictor variables) of Generalized Additive Models with network structural dissimilarity as response variable. Points represent estimate values after removing one study from the data, while asterisks indicate the estimates when the study with the greatest number of networks (N = 35) in our dataset (study ID 76)[20], is removed from the data. The estimates of the full model (with all studies included) are represented by the vertical lines. Red lines indicate a significant effect ($P < 0.05$), while gray lines indicate a non-significant effect. P values were calculated using a two-tailed statistical test that combines Generalized Additive Models (GAM) and Multiple Regression on distance Matrices (MRM). In this approach, the non-independence of distances from each local network is accounted for in the hypothesis testing by performing 1,000 permutations of the response matrix (see Methods). The range of the x-axis was defined as ± 3 times the standard deviation of the estimates. Arrows indicate outliers beyond this range (black: when study 76 is removed; red: when other studies are removed).

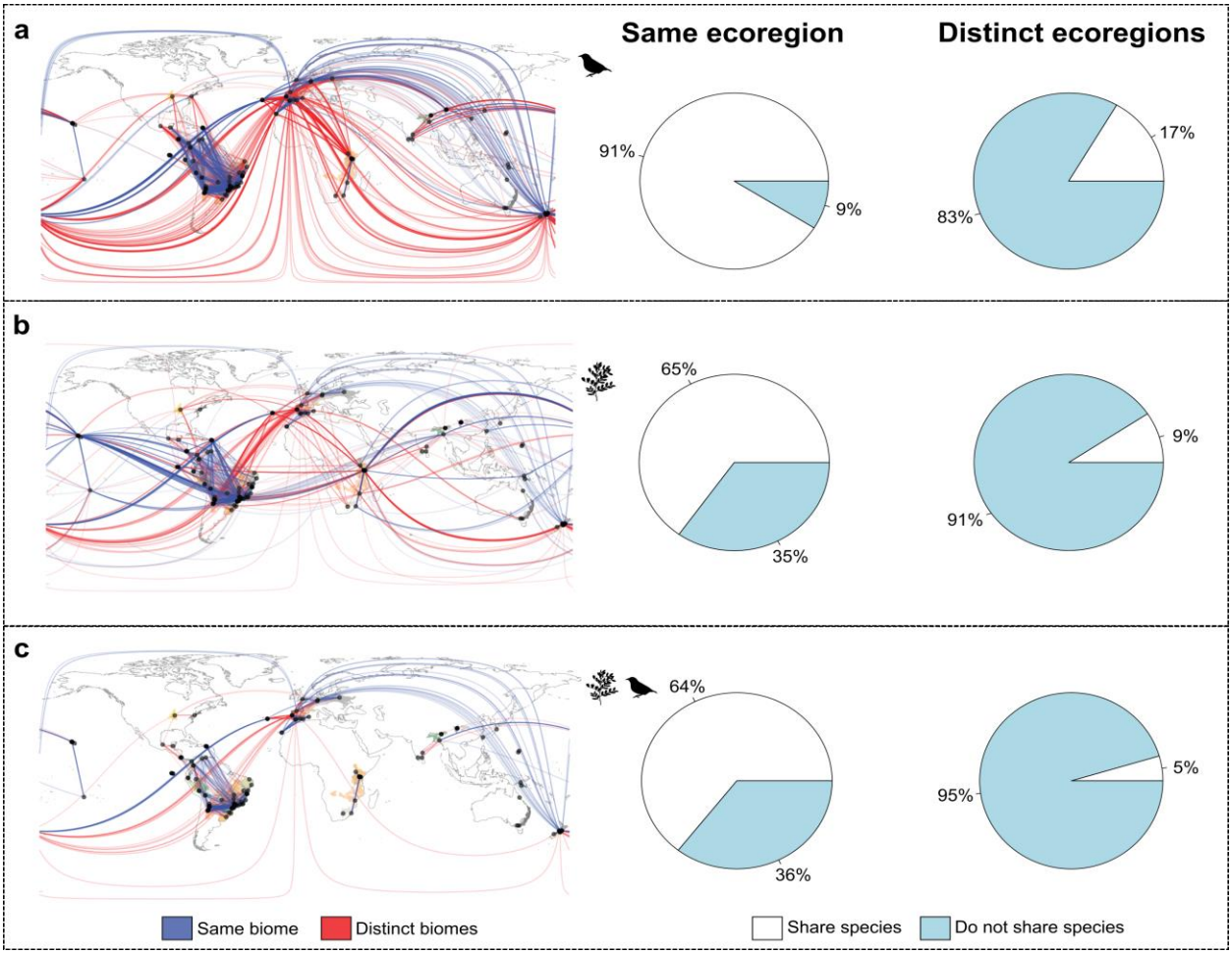

Supplementary Fig. 17. Plant and bird species connecting local networks, ecoregions and biomes. World map with points representing the 196 local avian frugivory networks in our dataset. As in Fig. 2 in the main text, colors of shaded areas represent the 67 ecoregions where networks were located, with similar colors indicating ecoregions that belong to the same biome. Lines represent the connections (shared species) plotted along the great circle distance between networks. Blue lines represent connections within biomes, while red lines represent connections across biomes. Stronger color tones of lines indicate higher similarity of species ($1-\beta_S$) between networks. **a** Lines represent connections between networks sharing bird species. Pie charts depict the proportion of pairs of local networks sharing bird species across vs. within ecoregions. **b** Lines represent connections between networks sharing plant species. Pie charts depict the proportion of pairs of local networks sharing plant species across vs. within ecoregions. **c** Lines represent connections between networks sharing both plant and bird species. Pie charts depict the proportion of pairs of local networks sharing both plant and bird species across vs. within ecoregions (see Fig. 2 for the world map of shared plant-frugivore interactions). Ecoregions and biomes were defined based on the map developed by Dinerstein et al.[19] (available at https://ecoregions.appspot.com/ under a CC-BY 4.0 license). Silhouettes were obtained from http://phylopic.org under a Public Domain license.

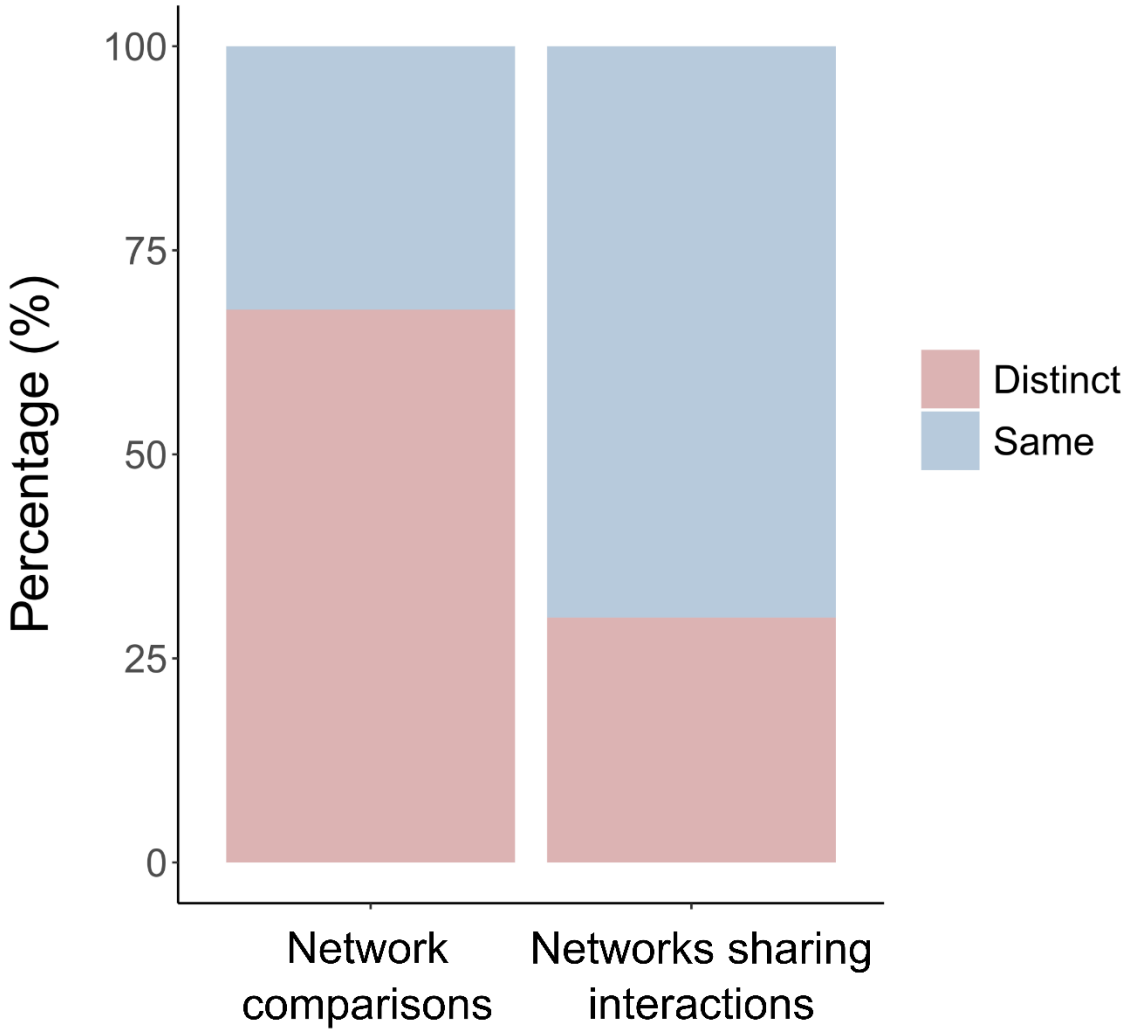

Supplementary Fig. 18. Percentage of long-distance network comparisons and connections (shared interactions) across ('distinct') and within ('same') biomes. Around 67% of the pairs of networks located >10,000 km of distance from each other (i.e., long-distance network comparisons) involved networks from distinct biomes. On the other hand, 70% of the long-distance connections (i.e., 70% of the pairs of networks that are located > 10,000 km from each other *and* share interactions) involved networks from the same biome.

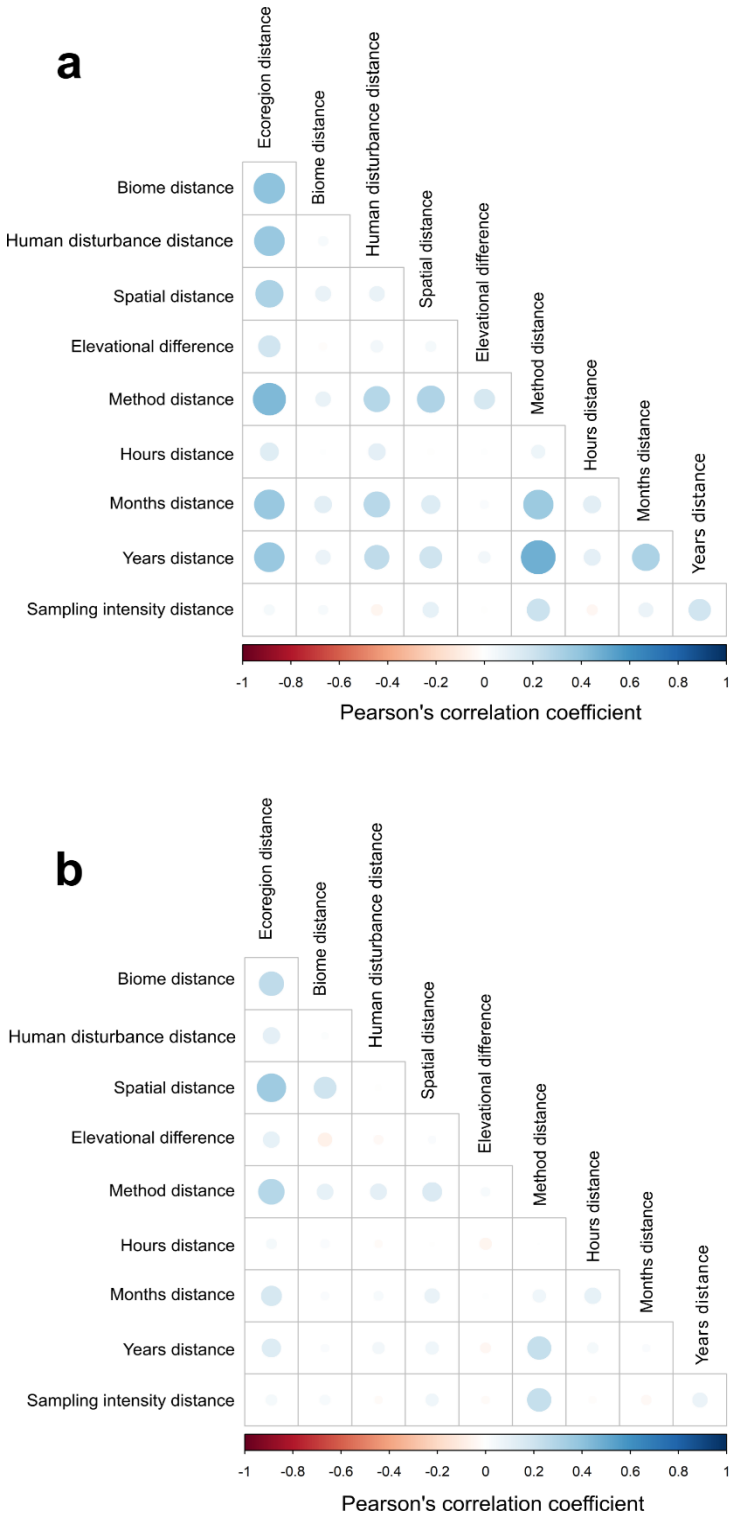

Supplementary Fig. 19. Correlations between the predictor variables used in our models. a Correlations between predictors used in our interaction rewiring analysis. **b** Correlations between predictors used in our model with interaction dissimilarity as the response variable (see Table 1 in the main text). Sizes of the circles and colors are proportional to the correlation coefficient.

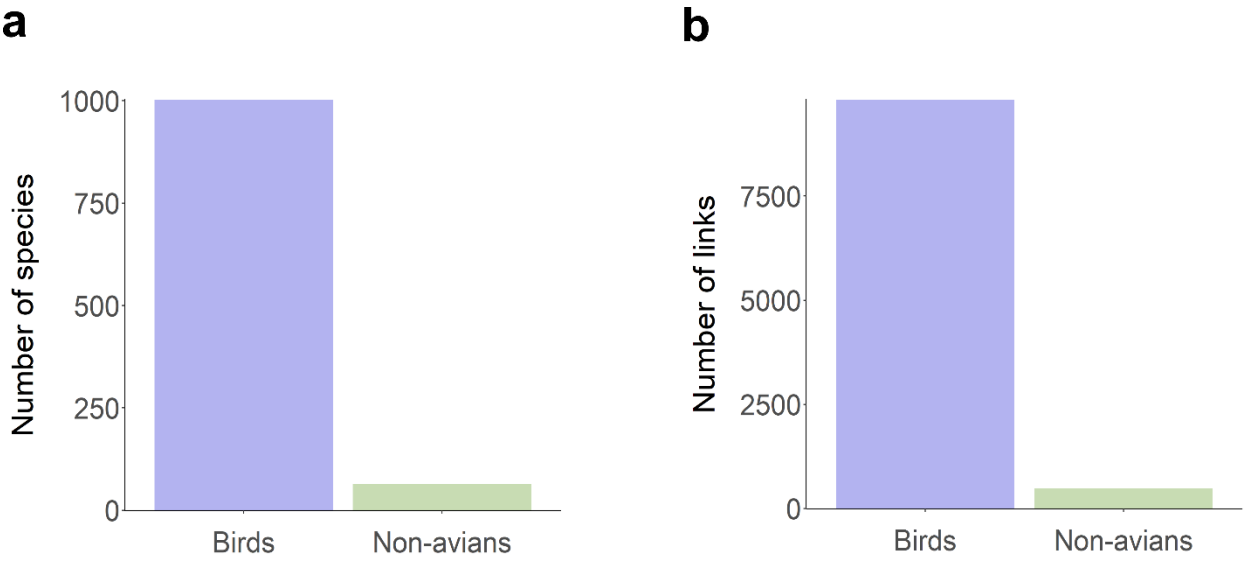

Supplementary Fig. 20. The number of bird and non-avian frugivore species and links (i.e., the frugivore fed on a plant species) in our dataset. The removal of non-avian frugivores from our local networks did not strongly decrease **a** the total number of frugivore species in our dataset, and **b** the number of links in the global network of frugivory.

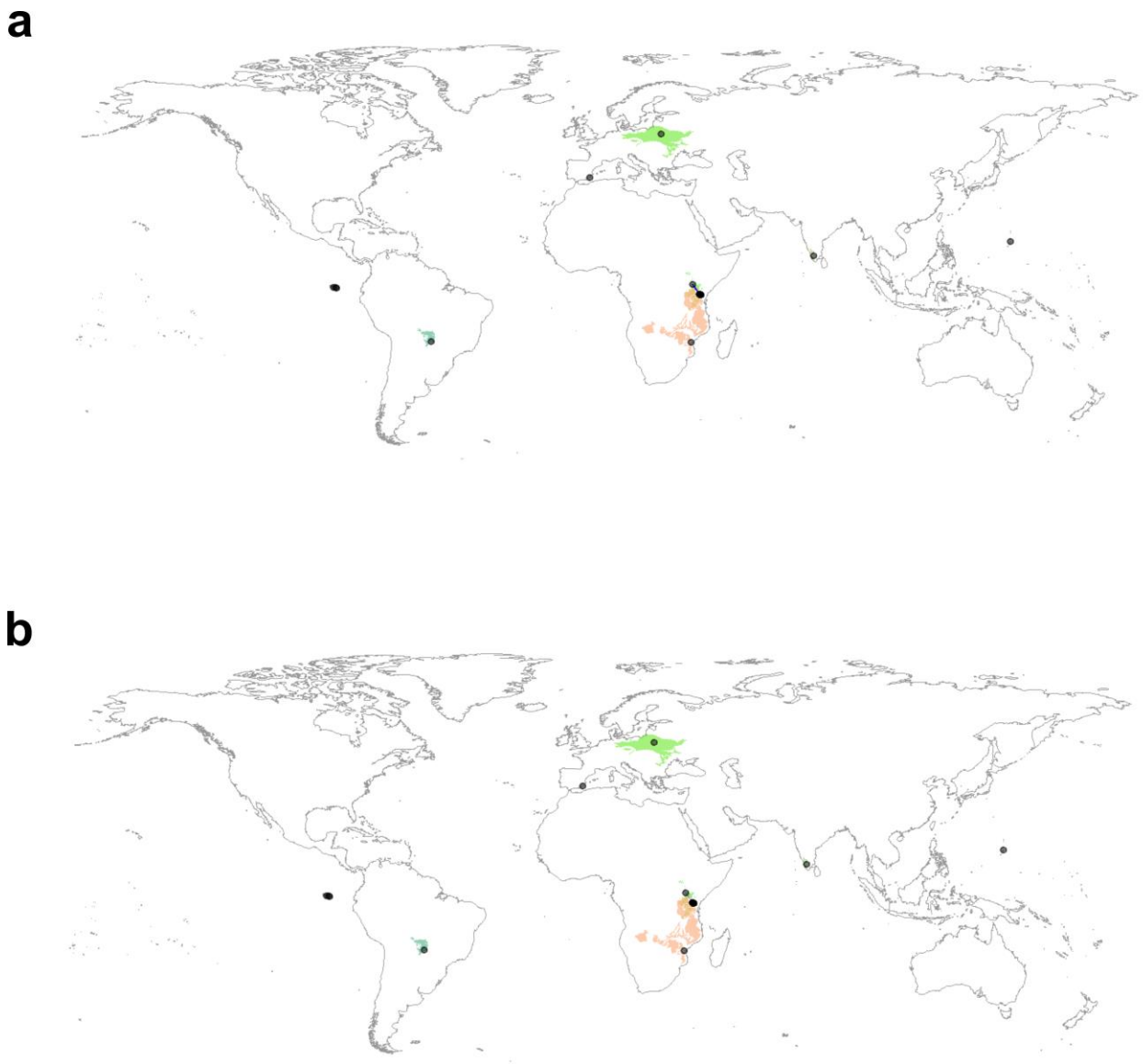

Supplementary Fig. 21. World map with points representing the 28 local networks containing non-avian frugivores in our dataset. Colors of shaded areas represent the nine ecoregions where networks were located. Note the lack of lines representing connections (shared non-avian frugivore species in **a** and shared interactions in **b**, as shown for avian frugivores in Fig. 2 in the main text) between networks located at distinct ecoregions and biomes. Ecoregions and biomes were defined based on the map developed by Dinerstein et al.[19] (available at https://ecoregions.appspot.com/ under a CC-BY 4.0 license).

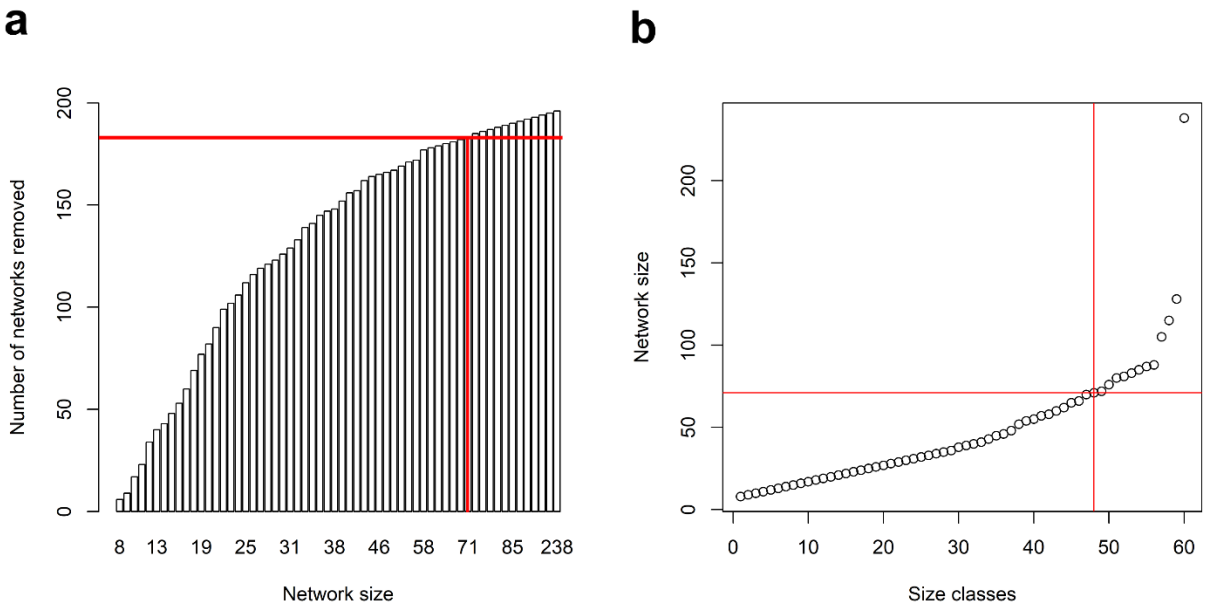

Supplementary Fig. 22. Thresholds used for sequentially removing networks in our sensitivity analysis. a Bars represent the 60 classes of network sizes in our dataset. Numbers below bars indicate the maximum size of the networks within each class. The vertical red line indicates the class of network size up until which analysis could be performed (i.e., after removing all networks up to and including this class; maximum network size = 71 species). The horizontal red line indicates the number of networks removed (*N* networks = 183) in the final round of our sensitivity analysis (i.e., when the maximum network size = 71). **b** Plot showing the number of size classes and network sizes in our dataset. The vertical red line indicates the size class up until which removal could occur and analysis could still be performed (size class rank = 48). The horizontal red line indicates the maximum size (71 species) of networks within this class.

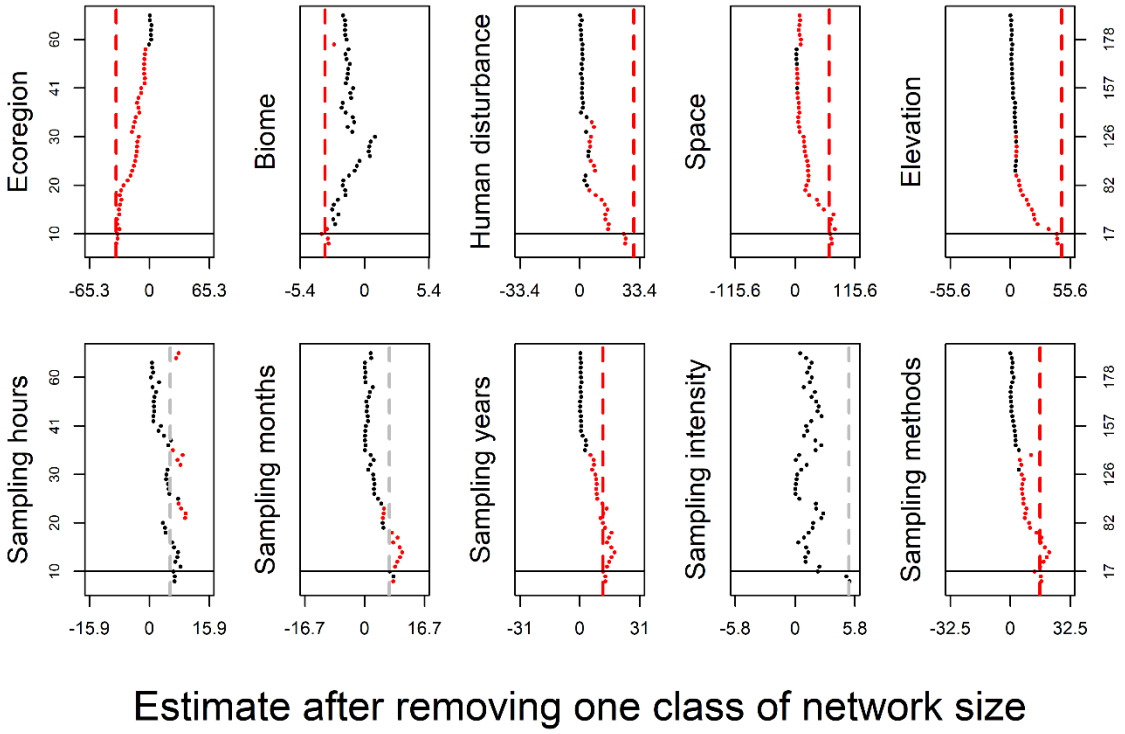

Supplementary Fig. 23. Sensitivity analysis showing the effect of sequentially removing classes of network size on estimates of t (for ecoregion and biome) and F values (for the remaining predictor variables) of Generalized Additive Models with interaction dissimilarity as the response variable. Points represent estimate values after removing all networks below a specified threshold of size [from smallest (bottom) to largest (top) network size; see Supplementary Fig. 22]. Red points indicate a significant effect ($P < 0.05$), while black points indicate a non-significant effect. *P* values were calculated using a combination of Generalized Additive Models and Multiple Regression on distance Matrices (see Methods). The left y-axis represents the threshold network size class below which networks were removed, while the right axis represents the number of networks removed at this threshold. For reference, horizontal black lines indicate the point where networks with up to 10 species (which represented 17 networks) were removed from the dataset. The estimates of the full model (with all networks included) are represented by the vertical lines, with red lines indicating a significant effect and gray lines indicating a non-significant effect. The range of the x-axis was defined as ± 4 times the standard deviation of the estimates (to allow visualization of all estimates). Note that the significant effects in the full model are robust to the removal of small networks (up to 10 species) from the dataset, even though their estimates progressively tend towards zero as larger networks are removed (similarly, *P* values tend to increase and fluctuate around the significance threshold as estimates approach zero). Notably, the effect that seems to be most sensitive to the removal of small networks (i.e., biome distance) explained a low unique proportion of the variation in interaction dissimilarity in our full model, as most of the deviance explained by biome boundaries was shared with ecoregions (Supplementary Fig. 12).

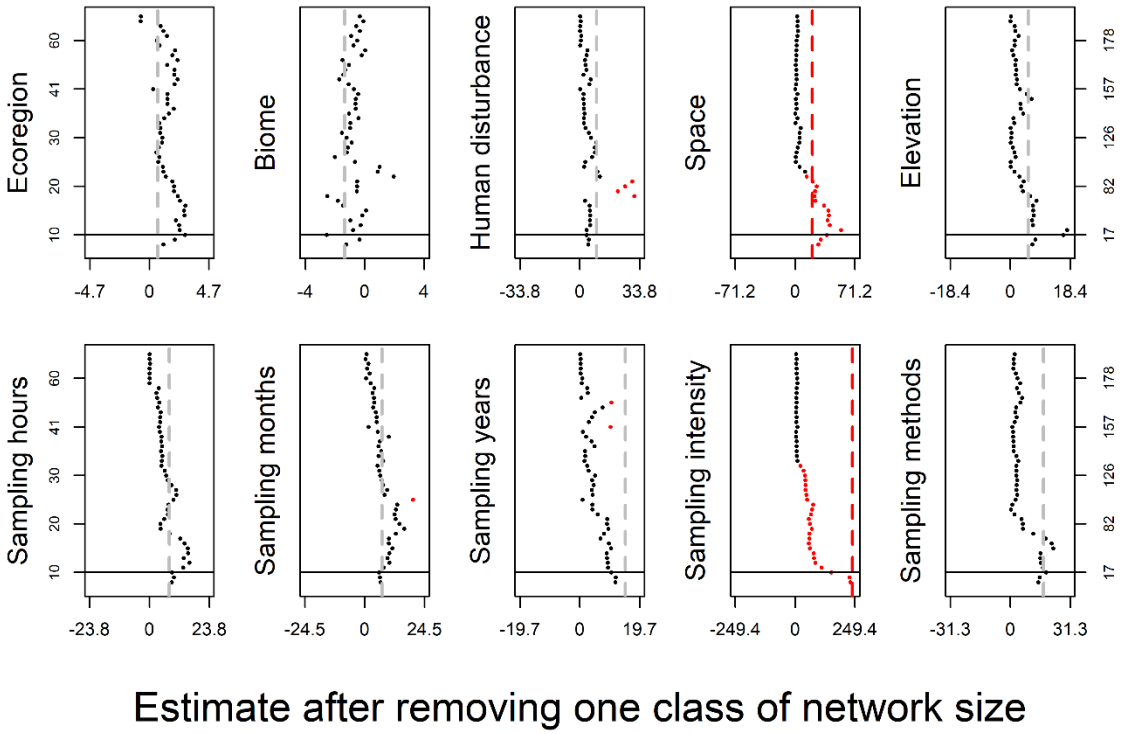

Supplementary Fig. 24. Sensitivity analysis showing the effect of sequentially removing classes of network size on estimates of t (for ecoregion and biome) and F values (for the remaining predictor variables) of Generalized Additive Models with network structural dissimilarity as response variable. Points represent estimate values after removing all networks below a specified threshold of size [from smallest (bottom) to largest (top) network size; see Supplementary Fig. 22]. Red points indicate a significant effect ($P < 0.05$), while black points indicate a non-significant effect. *P* values were calculated using a combination of Generalized Additive Models and Multiple Regression on distance Matrices (see Methods). The left y-axis represents the threshold network size class below which networks were removed, while the right axis represents the number of networks removed at this threshold. For reference, horizontal black lines indicate the point where networks with up to 10 species (which represented 17 networks) were removed from the dataset. The estimates of the full model (with all networks included) are represented by the vertical lines, with red lines indicating a significant effect and gray lines indicating a non-significant effect. The range of the x-axis was defined as ± 4 times the standard deviation of the estimates (to allow visualization of all estimates). Note that the significant effects in the full model (spatial and sampling intensity distances) are very robust to the removal of small networks from the dataset, even though their estimates progressively tend towards zero as larger networks are removed.

Supplementary Table 1. Description of the 196 avian frugivory networks in our dataset. Geographic coordinates were rounded to two decimal places. The metadata of local networks (e.g., original coordinates, sampling methods) are available as Supplementary Data.

Network ID	Latitude	Longitude	Location	Reference
1*	40.33	-74.67	New Jersey, USA	21
2*	18.30	-66.78	Caguana, Puerto Rico	22
3*	18.26	-66.53	Cialitos, Puerto Rico	22
4*	18.17	-66.59	Cordillera, Puerto Rico	22
5*	18.31	-66.56	Fronton, Puerto Rico	22
6*	-28.95	31.75	Mtunzini, South Africa	23
7*	-22.82	-47.11	Mata Santa Genebra, São Paulo, Brazil	24
8*	-22.82	-47.11	Mata Santa Genebra, São Paulo, Brazil	24
9*	18.51	-89.49	Campeche state, Mexico	25
10*	51.77	-1.33	Oxford, United Kingdom	26
11*	-24.32	-48.39	Intervales, São Paulo, Brazil	27
12	-24.13	-47.95	Carlos Botelho, São Paulo, Brazil	28
13	-25.13	-47.96	Ilha do Cardoso, São Paulo, Brazil	29
14	-22.55	-42.28	Poço das Antas, Rio de Janeiro, Brazil	30
15	-23.55	-45.06	Ilha Anchieta, São Paulo, Brazil	31
16	-20.80	-42.86	Viçosa, Minas Gerais, Brazil	32
17	-28.22	-51.17	Estação Aracuri, Rio Grande do Sul, Brazil	33
18	-22.94	-46.75	Itatiba, São Paulo, Brazil	34
19	-22.48	-47.59	Rio Claro, São Paulo, Brazil	35
20	-22.82	-47.43	Santa Barbara do Oeste, São Paulo, Brazil	36
21	-22.67	-47.20	Cosmópolis, São Paulo, Brazil	36
22	-22.57	-47.50	Iracemápolis, São Paulo, Brazil	36
23	-23.55	-46.72	São Paulo, Brazil	37
24	-22.71	-47.61	Piracicaba, São Paulo, Brazil	38
25	-22.77	-43.69	Rio de Janeiro, Brazil	39
26	37.79	-25.18	Azores, Portugal	40
27*	0.30	34.79	Kakamega Forest, Kenya	41
28	-25.49	-49.26	Curitiba, Paraná, Brazil	42
29	-25.44	-49.24	Curitiba, Paraná, Brazil	42
30	-25.44	-49.22	Curitiba, Paraná, Brazil	42
31	-25.42	-49.37	Curitiba, Paraná, Brazil	42
32	-25.41	-49.27	Curitiba, Paraná, Brazil	42
33	-25.36	-49.26	Curitiba, Paraná, Brazil	42
34	-25.38	-49.32	Curitiba, Paraná, Brazil	42
35	-25.17	-48.41	Paraná, Brazil	43
36	28.03	-15.46	Bandama, Gran Canaria, Spain	44
37	28.07	-15.46	El Palomar, Gran Canaria, Spain	44
38	-12.99	-41.34	Chapada Diamantina, Bahia, Brazil	45
39	37.18	-6.32	Hato Ratón, Sevilla, Spain	46
40	-16.40	-67.50	Chulumani, Bolivia	47
41	30.33	130.50	Yakushima Island, Japan	48

Network ID	Latitude	Longitude	Location	Reference
42	-18.95	-48.20	Uberlândia, Minas Gerais, Brazil	[49]
43	21.44	-158.08	Ēkahanui, Hawai'i, USA	[50]
44	21.54	-158.19	Kahanahāiki, Hawai'i, USA	[50]
45	21.38	-157.87	Moanalua, Hawai'i, USA	[50]
46	21.51	-158.14	Mount Ka'ala, Hawai'i, USA	[50]
47	21.54	-158.18	Pahole, Hawai'i, USA	[50]
48	21.34	-157.81	Tantalus, Hawai'i, USA	[50]
49	21.63	-158.04	Waimea Valley, Hawai'i, USA	[50]
50	37.57	-0.91	Sierra de la Fausilla, Murcia, Spain	[51]
51	26.99	92.94	Pakke Tiger Reserve, India	[52]
52	7.77	-76.67	Tulenapa, Antioquia, Colombia	[53]
53	43.28	-5.50	Cantabrian Range, Spain	[54]
54	-29.06	-50.07	Rio Grande do Sul, Brazil	[55]
55	-31.67	-53.25	Rio Grande do Sul, Brazil	[55]
56	15.17	145.77	Saipan, Mariana Islands	[56]
57	14.14	145.21	Rota, Mariana Islands	[56]
58	-0.75	-90.32	Santa Cruz, Galapagos Islands	[57]
59	52.74	23.78	Białowieża Forest, Poland	[58]
60	-4.92	-73.75	Jenaro Herrera, Peru	[59]
61	18.47	-67.11	Finca Montaña, Aguadilla, Puerto Rico	[60]
62	19.59	-96.38	Veracruz, Mexico	[61]
63	-8.97	-36.05	Coimbra Forest, Alagoas, Brazil	[62]
64	-41.29	174.73	Wellington, Aotearoa New Zealand	[63]
65	-41.29	174.75	Wellington, Aotearoa New Zealand	[63]
66	-41.30	174.75	George Denton Park, Aotearoa New Zealand	[63]
67	-41.29	174.80	Charles Plimmer Park, Aotearoa New Zealand	[63]
68	-41.28	174.77	Wellington, Aotearoa New Zealand	[63]
69	-42.35	173.57	Hinau Reserve, Aotearoa New Zealand	[63]
70	-42.33	173.63	Mount Fyffe Reserve, Aotearoa New Zealand	[63]
71	-42.28	173.74	Puhi-Puhi, Aotearoa New Zealand	[63]
72	-42.24	173.78	Blue Duck Reserve, Aotearoa New Zealand	[63]
73	40.22	-8.46	Choupal, Coimbra, Portugal	[64]
74	-41.30	174.75	Wellington, Aotearoa New Zealand	[65]
75	-12.93	-38.40	Salvador, Bahia, Brazil	[66]
76	26.93	92.97	Pakke Tiger Reserve, India	[67]
77	27.02	92.95	Papum Reserve Forest, India	[67]
78	-43.75	169.40	Windbag Valley, Aotearoa New Zealand	[68]
79	37.78	-25.15	Azores, Portugal	[40]
80	37.80	-25.16	Azores, Portugal	[40]
81	37.79	-25.16	Azores, Portugal	[40]
82	40.31	-8.40	Coimbra, Portugal	[69]
83	40.26	-8.48	Coimbra, Portugal	Unpublished[1]
84	-0.66	-90.32	Santa Cruz, Galapagos Islands	[57]
85	-0.91	-89.43	San Cristóbal, Galapagos Islands	[57]
86	-0.89	-89.49	San Cristóbal, Galapagos Islands	[57]

Network ID	Latitude	Longitude	Location	Reference
87	-19.95	34.37	Gorongosa National Park, Mozambique	[70]
88	13.70	80.19	Sriharikota Island, India	[71]
89	-5.05	-37.52	Furna Feia, Rio Grande do Norte, Brazil	[72]
90	-7.22	146.81	Mount Missim, New Guinea	[73]
91	-9.45	147.35	Varirata National Park, New Guinea	[74]
92	-29.12	26.17	Bloemfontein, South Africa	[75]
93	-37.62	144.42	Lerderderg Park, Australia	[76]
94	-37.72	145.57	Mt Healesville and Donna Buang, Australia	[77]
95	-41.33	173.05	Brightwater, Aotearoa New Zealand	[78]
96	-41.32	173.26	Nelson, Aotearoa New Zealand	[78]
97	-41.41	173.04	Faulkners, Wakefield, Aotearoa New Zealand	[78]
98	-22.28	-41.68	Restinga de Jurubatiba, Rio de Janeiro, Brazil	[79]
99	-15.95	-47.97	Brasília, Brazil	[80]
100	-19.77	-40.04	Comboios, Espírito Santo, Brazil	[81]
101	-23.37	-46.60	Cantareira, São Paulo, Brazil	[82]
102	-19.57	-56.20	Pantanal, Brazil	[83]
103	-22.39	-47.54	Rio Claro, São Paulo, Brazil	Unpublished[2]
104	-21.73	-48.02	Araraquara, São Paulo, Brazil	[84]
105	-24.73	-64.67	El Rey National Park, Argentina	[85]
106	-27.25	-65.88	Campo de Los Alisos, Argentina	[85]
107	-27.23	-65.62	La Florida Provincial Park, Argentina	[85]
108	-26.80	-65.30	San Javier y Yerba Huasi, Argentina	[86]
109	-24.76	-64.69	Pozo Verde, El Rey National Park, Argentina	[87]
110	-27.03	-65.77	Quebrada del Portugues, Argentina	[85]
111	-24.10	-64.45	EcoPortal de Piedra, Argentina	[85]
112	-23.69	-64.88	Calilegua National Park, Argentina	[85]
113	-23.69	-64.87	Calilegua National Park, Argentina	[85]
114	-22.28	-64.71	El Nogalar de los Toldos, Argentina	[85]
115	-26.75	-65.33	Parque Sierra de San Javier, Argentina	[87]
116	-26.80	-65.33	Parque Sierra de San Javier, Argentina	Unpublished[3]
117	-15.35	-39.20	Bahia, Brazil	[88]
118	-15.21	-39.14	Bahia, Brazil	[88]
119	-15.13	-39.12	Bahia, Brazil	[88]
120	-15.25	-39.08	Bahia, Brazil	[88]
121	-15.26	-39.09	Bahia, Brazil	[88]
122	10.28	-84.05	Rara Avis Reserve, Costa Rica	[89]
123	-17.85	146.08	Mission Beach, Queensland, Australia	[90]
124	10.35	77.04	Valparai and Anamalai Reserve, India	[91]
125	31.07	103.71	Dujiangyan, Sichuan Province, China	[92]
126	31.05	103.74	Dujiangyan, Sichuan Province, China	[92]
127	31.05	103.73	Dujiangyan, Sichuan Province, China	[92]
128	31.06	103.72	Dujiangyan, Sichuan Province, China	[92]
129	31.05	103.72	Dujiangyan, Sichuan Province, China	[92]
130	31.08	103.70	Dujiangyan, Sichuan Province, China	[92]
131	31.09	103.72	Dujiangyan, Sichuan Province, China	[92]

Network ID	Latitude	Longitude	Location	Reference
132	31.09	103.73	Dujiangyan, Sichuan Province, China	92
133	31.08	103.72	Dujiangyan, Sichuan Province, China	92
134	31.06	103.73	Dujiangyan, Sichuan Province, China	92
135	31.06	103.72	Dujiangyan, Sichuan Province, China	92
136	31.05	103.73	Dujiangyan, Sichuan Province, China	92
137	31.05	103.73	Dujiangyan, Sichuan Province, China	92
138	37.98	-2.90	Serranía de Cazorla, Spain	93
139	37.38	-5.71	El Viso del Alcor, Sevilla, Spain	93
140	50.30	8.66	Friedberg, Hesse, Germany	94
141	51.15	9.00	Kellerwald-Edersee, Germany	95
142	-3.23	37.27	Mt Kilimanjaro, Tanzania	20
143	-3.25	37.32	Mt Kilimanjaro, Tanzania	20
144	-3.27	37.47	Mt Kilimanjaro, Tanzania	20
145	-3.17	37.24	Mt Kilimanjaro, Tanzania	20
146	-3.21	37.34	Mt Kilimanjaro, Tanzania	20
147	-3.26	37.42	Mt Kilimanjaro, Tanzania	20
148	-3.26	37.42	Mt Kilimanjaro, Tanzania	20
149	-3.23	37.52	Mt Kilimanjaro, Tanzania	20
150	-3.14	37.24	Mt Kilimanjaro, Tanzania	20
151	-3.13	37.24	Mt Kilimanjaro, Tanzania	20
152	-3.14	37.30	Mt Kilimanjaro, Tanzania	20
153	-3.14	37.31	Mt Kilimanjaro, Tanzania	20
154	-3.17	37.36	Mt Kilimanjaro, Tanzania	20
155	-3.15	37.29	Mt Kilimanjaro, Tanzania	20
156	-3.18	37.36	Mt Kilimanjaro, Tanzania	20
157	-3.19	37.51	Mt Kilimanjaro, Tanzania	20
158	-3.20	37.52	Mt Kilimanjaro, Tanzania	20
159	-3.19	37.44	Mt Kilimanjaro, Tanzania	20
160	-3.10	37.26	Mt Kilimanjaro, Tanzania	20
161	-3.17	37.36	Mt Kilimanjaro, Tanzania	20
162	-3.16	37.36	Mt Kilimanjaro, Tanzania	20
163	-3.19	37.44	Mt Kilimanjaro, Tanzania	20
164	-3.18	37.51	Mt Kilimanjaro, Tanzania	20
165	-3.18	37.25	Mt Kilimanjaro, Tanzania	20
166	-3.30	37.50	Mt Kilimanjaro, Tanzania	20
167	-3.33	37.50	Mt Kilimanjaro, Tanzania	20
168	-3.30	37.62	Mt Kilimanjaro, Tanzania	20
169	-3.19	37.25	Mt Kilimanjaro, Tanzania	20
170	-3.27	37.60	Mt Kilimanjaro, Tanzania	20
171	-3.32	37.67	Mt Kilimanjaro, Tanzania	20
172	-3.37	37.45	Mt Kilimanjaro, Tanzania	20
173	-3.38	37.50	Mt Kilimanjaro, Tanzania	20
174	-3.33	37.64	Mt Kilimanjaro, Tanzania	20
175	-3.32	37.68	Mt Kilimanjaro, Tanzania	20
176	-3.31	37.68	Mt Kilimanjaro, Tanzania	20

Network ID	Latitude	Longitude	Location	Reference
177	-16.40	-67.50	Chulumani, Bolivia	[47]
178	4.72	-75.57	Otún Quimbaya, Colombia	[96]
179	4.70	-75.48	Ucumarí, Colombia	[96]
180	-3.96	-79.06	Podocarpus National Park, Ecuador	[97]
181	-4.10	-79.17	Podocarpus National Park, Ecuador	[97]
182	-13.05	-71.54	San Pedro, Peru	[98]
183	-13.17	-71.58	Wayqecha, Peru	[98]
184	9.71	-69.58	Yacambú National Park, Venezuela	[99]
185	10.39	-67.02	Altos de Pipe, Coastal Cordillera, Venezuela	[99]
186	10.30	79.85	Point Calimere Wildlife Sanctuary, India	[100]
187	20.60	-156.33	Kanaio Natural Area Reserve, Hawai'i	[101]
188	-3.37	38.33	Taita Hills, Kenya	[102]
189	40.13	-88.17	Champaign County, Illinois, USA	[103]
190	-17.53	-149.83	Moorea, French Polynesia	[104]
191	10.47	-83.51	Tortuguero, Costa Rica	[105]
192	24.80	121.25	Fushan Experimental Forest, Taiwan	[106]
193	22.46	91.77	Chittagong, Bangladesh	[107]
194	10.42	-84.01	La Selva Biological Station, Costa Rica	[108]
195	10.42	-84.02	La Selva Biological Station, Costa Rica	[109]
196	39.14	2.94	Cabrera Island, Spain	[110]

*Obtained through the Web of Life database[111].
Unpublished[1]: Data provided by Ruben Heleno.
Unpublished[2]: Data provided by Marco Aurélio Pizo.
Unpublished[3]: Data provided by Pedro G. Blendinger.

Supplementary Table 2. Quantitative metrics of network sampling. Sampling intensity and completeness aim to account for how complete network sampling was in terms of species interactions, while sampling hours and months account for the time-span of the study.

Sampling metric	Rationale
Sampling intensity	Sampling intensity was calculated as the square-root of the number of interaction events divided by the square-root of the product of the number of plant and animal species in the local network[112]. Sampling intensity was included in our models because it presented a strong and positive relationship with the ratio between the number of interactions sampled in the local network and the number of known possible interactions (among that same set of species) in the region (for the subset of networks within the Aotearoa New Zealand meta-network) (Supplementary Fig. 7).
Sampling completeness	Sampling completeness was calculated as the observed richness of links divided by the estimated richness of links in the local network[113]. We used the Chao 1 richness estimator[114] to obtain the estimated number of links in our networks. Sampling completeness was not included in our models because it did not present a significant relationship with the ratio between the number of interactions in the local network and the number of known possible interactions (among that same set of species) in the region (Supplementary Fig. 7). Thus, we considered that this metric did not provide a good representation of how complete network sampling was in terms of species interactions.
Sampling hours	Number of sampling hours was included in our statistical models because it presented strong and positive relationships with bird richness, plant richness and number of links in the local networks (Supplementary Fig. 8).
Sampling months	Number of sampling months was included in our statistical models because it presented a strong and positive relationship with the ratio between the number of interactions in the local network and the number of known possible interactions (among that same set of species) in the region (Supplementary Fig. 7), as well as with plant richness and number of links in the local networks (for the entire dataset) (Supplementary Fig. 8).

Supplementary Table 3. Description of variables used to generate the method's dissimilarity matrix.

Variable	Description
Sampling design	Whether the sampling design was 'transect', 'plot', 'mist-net', 'focal observation', 'camera-trap', or any combination of these.
Sampling focus	Whether the focal organisms were birds, plants, or both. As such, this variable determines if authors used a zoocentric or a phytocentric sampling method (or a combination of the two).
Sampling coverage	Whether there were focal species ('partial coverage') or not ('total coverage').
Interaction frequency type	Whether interaction frequency was estimated by counting the number of bird visits, number of fruits consumed by the bird, number of seeds in bird droppings, or number of bird droppings with seeds.

Supplementary Table 4. Multiple predictors of species turnover (βs) on plant-frugivore networks. Here, we used the binary version of ecoregion and biome distance matrices. *P* values were calculated using a two-tailed statistical test that combines Generalized Additive Models (GAM) and Multiple Regression on distance Matrices (MRM). In this approach, the non-independence of distances from each local network is accounted for in the hypothesis testing by performing 1,000 permutations of the response matrix (see Methods). EDF represents the estimated degrees of freedom for each smooth term in the model. *N* pairs of networks = 19,110.

Parametric coefficients	**Estimate**	**t**	**P**
Intercept	0.976	1734.300	**0.001**
Ecoregion (same)	-0.122	-38.093	**0.001**
Biome (same)	-0.008	-8.799	**0.001**
Smooth Terms	**EDF**	**F**	**P**
s (human disturbance distance)	8.312	28.504	**0.001**
s (spatial distance)	8.866	725.571	**0.001**
s (elevational difference)	5.589	99.954	**0.001**
s (hours distance)	6.917	4.004	0.619
s (months distance)	6.755	6.525	0.089
s (years distance)	6.402	7.422	0.068
s (sampling intensity distance)	1.007	26.580	**0.005**
s (methods distance)	8.039	10.911	**0.015**

Bold values indicate statistically significant results ($P < 0.05$).

Supplementary Table 5. Multiple predictors of species turnover (βS) on plant-frugivore networks. Here, we used the quantitative version (environmental dissimilarity) of ecoregion and biome distance matrices. *P* values were calculated using a two-tailed statistical test that combines Generalized Additive Models (GAM) and Multiple Regression on distance Matrices (MRM). In this approach, the non-independence of distances from each local network is accounted for in the hypothesis testing by performing 1,000 permutations of the response matrix (see Methods). EDF represents the estimated degrees of freedom for each smooth term in the model. *N* pairs of networks = 19,110.

Smooth Terms	EDF	F	P
s (ecoregion distance)	8.570	137.969	**0.001**
s (biome distance)	8.202	37.937	**0.001**
s (human disturbance distance)	8.339	29.465	**0.001**
s (spatial distance)	8.890	698.382	**0.001**
s (elevational difference)	5.517	98.173	**0.001**
s (hours distance)	7.330	4.876	0.448
s (months distance)	5.371	5.811	0.109
s (years distance)	6.152	7.741	0.063
s (sampling intensity distance)	4.365	6.108	0.315
s (methods distance)	7.996	11.474	**0.017**

Bold values indicate statistically significant results ($P < 0.05$).

Supplementary Table 6. Multiple predictors of plant-frugivore interaction dissimilarity (β_{WN}). Here, we used the quantitative version (environmental dissimilarity) of ecoregion and biome distance matrices. *P* values were calculated using a two-tailed statistical test that combines Generalized Additive Models (GAM) and Multiple Regression on distance Matrices (MRM). In this approach, the non-independence of distances from each local network is accounted for in the hypothesis testing by performing 1,000 permutations of the response matrix (see Methods). EDF represents the estimated degrees of freedom for each smooth term in the model. ($P < 0.05$). *N* pairs of networks = 19,110.

Smooth Terms	EDF	F	P
s (ecoregion distance)	8.595	110.122	**0.001**
s (biome distance)	7.827	10.492	**0.022**
s (human disturbance distance)	8.570	32.573	**0.001**
s (spatial distance)	8.855	81.843	**0.001**
s (elevational difference)	6.024	48.426	**0.001**
s (hours distance)	1.353	10.637	**0.043**
s (months distance)	5.800	7.876	**0.045**
s (years distance)	7.135	13.007	**0.020**
s (sampling intensity distance)	1.010	5.437	0.267
s (methods distance)	7.878	17.094	**0.003**

Bold values indicate statistically significant results ($P < 0.05$).

Supplementary Table 7. Multiple predictors of plant-frugivore network structural dissimilarity. Here, we used the binary version of ecoregion and biome distance matrices. *P* values were calculated using a two-tailed statistical test that combines Generalized Additive Models (GAM) and Multiple Regression on distance Matrices (MRM). In this approach, the non-independence of distances from each local network is accounted for in the hypothesis testing by performing 1,000 permutations of the response matrix (see Methods). EDF represents the estimated degrees of freedom for each smooth term in the model. *N* pairs of networks = 19,110.

Parametric coefficients	**Estimate**	**t**	**P**
Intercept	2.689	222.572	**0.002**
Ecoregion (same)	0.043	0.632	0.788
Biome (same)	-0.028	-1.345	0.770
Smooth Terms	**EDF**	**F**	**P**
s (human disturbance distance)	5.923	9.346	0.429
s (spatial distance)	8.474	20.408	**0.021**
s (elevational difference)	8.220	5.510	0.749
s (hours distance)	8.006	7.944	0.969
s (months distance)	5.961	7.078	0.693
s (years distance)	6.868	14.999	0.461
s (sampling intensity distance)	8.762	238.987	**0.002**
s (methods distance)	8.586	17.372	0.231

Bold values indicate statistically significant results ($P < 0.05$).

Supplementary Table 8. Multiple predictors of plant-frugivore network structural dissimilarity. Here, we used the quantitative version (environmental dissimilarity) of ecoregion and biome distance matrices. *P* values were calculated using a two-tailed statistical test that combines Generalized Additive Models (GAM) and Multiple Regression on distance Matrices (MRM). In this approach, the non-independence of distances from each local network is accounted for in the hypothesis testing by performing 1,000 permutations of the response matrix (see Methods). EDF represents the estimated degrees of freedom for each smooth term in the model. *N* pairs of networks = 19,110.

Smooth Terms	EDF	F	P
s (ecoregion distance)	4.272	15.275	0.193
s (biome distance)	7.697	12.115	0.568
s (human disturbance distance)	5.993	9.264	0.438
s (spatial distance)	8.465	18.465	**0.018**
s (elevational difference)	8.290	5.679	0.713
s (hours distance)	7.857	8.913	0.955
s (months distance)	6.173	8.239	0.606
s (years distance)	6.751	12.872	0.545
s (sampling intensity distance)	8.760	239.475	**0.002**
s (methods distance)	8.501	15.584	0.257

Bold values indicate statistically significant results ($P < 0.05$).

Supplementary Table 9. **Multiple predictors of species turnover (βS) on plant-frugivore networks.** Here, we used a buffer zone of 500 km and the alternative scenario 1 (see Alternative scenarios section) during the data cleaning process. The binary versions of ecoregion and biome distance matrices were used for estimating the effects of ecoregion and biome borders on the response variable. *P* values were calculated using a two-tailed statistical test that combines Generalized Additive Models (GAM) and Multiple Regression on distance Matrices (MRM). In this approach, the non-independence of distances from each local network is accounted for in the hypothesis testing by performing 1,000 permutations of the response matrix (see Methods). EDF represents the estimated degrees of freedom for each smooth term in the model. *N* pairs of networks = 19,110.

Parametric coefficients	**Estimate**	**t**	**P**
Intercept	0.976	1735.328	**0.001**
Ecoregion (same)	-0.122	-38.147	**0.001**
Biome (same)	-0.008	-8.809	**0.001**
Smooth Terms	**EDF**	**F**	**P**
s (human disturbance distance)	8.312	28.538	**0.001**
s (spatial distance)	8.867	725.453	**0.001**
s (elevational difference)	5.600	99.711	**0.001**
s (hours distance)	6.928	4.042	0.580
s (months distance)	6.761	6.566	0.083
s (years distance)	6.412	7.472	0.059
s (sampling intensity distance)	1.001	26.885	**0.005**
s (methods distance)	8.032	10.833	**0.023**

Bold values indicate statistically significant results ($P < 0.05$).

Supplementary Table 10. **Multiple predictors of species turnover (βs) on plant-frugivore networks.** Here, we used a buffer zone of 500 km and the alternative scenario 2 (see Alternative scenarios section) during the data cleaning process. The binary versions of ecoregion and biome distance matrices were used for estimating the effects of ecoregion and biome borders on the response variable. *P* values were calculated using a two-tailed statistical test that combines Generalized Additive Models (GAM) and Multiple Regression on distance Matrices (MRM). In this approach, the non-independence of distances from each local network is accounted for in the hypothesis testing by performing 1,000 permutations of the response matrix (see Methods). EDF represents the estimated degrees of freedom for each smooth term in the model. *N* pairs of networks = 19,110.

Parametric coefficients	**Estimate**	**t**	**P**
Intercept	0.976	1752.859	**0.001**
Ecoregion (same)	-0.123	-38.615	**0.001**
Biome (same)	-0.008	-8.084	**0.001**
Smooth Terms	**EDF**	**F**	**P**
s (human disturbance distance)	8.437	28.851	**0.001**
s (spatial distance)	8.865	719.288	**0.001**
s (elevational difference)	5.600	99.486	**0.001**
s (hours distance)	7.126	4.330	0.559
s (months distance)	4.001	6.532	0.091
s (years distance)	6.548	8.206	0.069
s (sampling intensity distance)	3.464	8.113	0.166
s (methods distance)	8.114	11.641	**0.013**

Bold values indicate statistically significant results ($P < 0.05$).

Supplementary Table 11. **Multiple predictors of species turnover (βs) on plant-frugivore networks.** Here, we used a buffer zone of 100 km and the alternative scenario 1 (see Alternative scenarios section) during the data cleaning process. The binary versions of ecoregion and biome distance matrices were used for estimating the effects of ecoregion and biome borders on the response variable. *P* values were calculated using a two-tailed statistical test that combines Generalized Additive Models (GAM) and Multiple Regression on distance Matrices (MRM). In this approach, the non-independence of distances from each local network is accounted for in the hypothesis testing by performing 1,000 permutations of the response matrix (see Methods). EDF represents the estimated degrees of freedom for each smooth term in the model. *N* pairs of networks = 19,110.

Parametric coefficients	**Estimate**	**t**	**P**
Intercept	0.976	1736.530	**0.001**
Ecoregion (same)	-0.122	-38.181	**0.001**
Biome (same)	-0.009	-8.781	**0.001**
Smooth Terms	**EDF**	**F**	**P**
s (human disturbance distance)	8.317	28.664	**0.002**
s (spatial distance)	8.866	725.286	**0.001**
s (elevational difference)	5.606	99.783	**0.001**
s (hours distance)	6.888	3.931	0.606
s (months distance)	6.827	6.601	0.091
s (years distance)	6.406	7.500	0.073
s (sampling intensity distance)	1.002	26.760	**0.008**
s (methods distance)	8.029	10.895	**0.016**

Bold values indicate statistically significant results ($P < 0.05$).

Supplementary Table 12. **Multiple predictors of species turnover (βs) on plant-frugivore networks.** Here, we used a buffer zone of 100 km and the alternative scenario 2 (see Alternative scenarios section) during the data cleaning process. The binary versions of ecoregion and biome distance matrices were used for estimating the effects of ecoregion and biome borders on the response variable. *P* values were calculated using a two-tailed statistical test that combines Generalized Additive Models (GAM) and Multiple Regression on distance Matrices (MRM). In this approach, the non-independence of distances from each local network is accounted for in the hypothesis testing by performing 1,000 permutations of the response matrix (see Methods). EDF represents the estimated degrees of freedom for each smooth term in the model. *N* pairs of networks = 19,110.

Parametric coefficients	**Estimate**	**t**	**P**
Intercept	0.976	1755.726	**0.001**
Ecoregion (same)	-0.122	-38.561	**0.001**
Biome (same)	-0.008	-8.354	**0.001**
Smooth Terms	**EDF**	**F**	**P**
s (human disturbance distance)	8.341	29.073	**0.002**
s (spatial distance)	8.863	716.735	**0.001**
s (elevational difference)	5.578	100.041	**0.001**
s (hours distance)	6.987	3.990	0.592
s (months distance)	6.819	6.693	0.107
s (years distance)	6.484	7.966	0.063
s (sampling intensity distance)	1.000	24.580	**0.005**
s (methods distance)	8.013	11.066	**0.018**

Bold values indicate statistically significant results ($P < 0.05$).

Supplementary Table 13. Multiple predictors of species turnover (βs) on plant-frugivore networks. Here, we used a buffer zone of 100 km and the alternative scenario 3 (see Alternative scenarios section) during the data cleaning process. The binary versions of ecoregion and biome distance matrices were used for estimating the effects of ecoregion and biome borders on the response variable. *P* values were calculated using a two-tailed statistical test that combines Generalized Additive Models (GAM) and Multiple Regression on distance Matrices (MRM). In this approach, the non-independence of distances from each local network is accounted for in the hypothesis testing by performing 1,000 permutations of the response matrix (see Methods). EDF represents the estimated degrees of freedom for each smooth term in the model. *N* pairs of networks = 19,110.

Parametric coefficients	**Estimate**	**t**	**P**
Intercept	0.976	1735.345	**0.001**
Ecoregion (same)	-0.122	-38.157	**0.001**
Biome (same)	-0.009	-8.775	**0.001**
Smooth Terms	**EDF**	**F**	**P**
s (human disturbance distance)	8.317	28.665	**0.002**
s (spatial distance)	8.866	723.914	**0.001**
s (elevational difference)	5.587	99.935	**0.001**
s (hours distance)	6.918	4.014	0.605
s (months distance)	6.783	6.589	0.100
s (years distance)	6.406	7.492	0.078
s (sampling intensity distance)	1.000	26.866	**0.004**
s (methods distance)	8.033	10.910	**0.011**

Bold values indicate statistically significant results ($P < 0.05$).

Supplementary Table 14. **Multiple predictors of species turnover (βs) on plant-frugivore networks.** Here, we used a buffer zone of 1000 km and the alternative scenario 1 (see Alternative scenarios section) during the data cleaning process. The binary versions of ecoregion and biome distance matrices were used for estimating the effects of ecoregion and biome borders on the response variable. *P* values were calculated using a two-tailed statistical test that combines Generalized Additive Models (GAM) and Multiple Regression on distance Matrices (MRM). In this approach, the non-independence of distances from each local network is accounted for in the hypothesis testing by performing 1,000 permutations of the response matrix (see Methods). EDF represents the estimated degrees of freedom for each smooth term in the model. *N* pairs of networks = 19,110.

Parametric coefficients	**Estimate**	**t**	**P**
Intercept	0.976	1734.871	**0.001**
Ecoregion (same)	-0.122	-38.147	**0.001**
Biome (same)	-0.009	-8.789	**0.001**
Smooth Terms	**EDF**	**F**	**P**
s (human disturbance distance)	8.309	28.531	**0.001**
s (spatial distance)	8.866	725.141	**0.001**
s (elevational difference)	5.605	99.321	**0.001**
s (hours distance)	6.911	4.049	0.602
s (months distance)	6.761	6.579	0.099
s (years distance)	6.414	7.440	0.067
s (sampling intensity distance)	1.002	26.590	**0.005**
s (methods distance)	8.030	10.869	**0.019**

Bold values indicate statistically significant results ($P < 0.05$).

Supplementary Table 15. **Multiple predictors of species turnover (βS) on plant-frugivore networks.** Here, we used a buffer zone of 1000 km and the alternative scenario 2 (see Alternative scenarios section) during the data cleaning process. The binary versions of ecoregion and biome distance matrices were used for estimating the effects of ecoregion and biome borders on the response variable. *P* values were calculated using a two-tailed statistical test that combines Generalized Additive Models (GAM) and Multiple Regression on distance Matrices (MRM). In this approach, the non-independence of distances from each local network is accounted for in the hypothesis testing by performing 1,000 permutations of the response matrix (see Methods). EDF represents the estimated degrees of freedom for each smooth term in the model. *N* pairs of networks = 19,110.

Parametric coefficients	**Estimate**	**t**	**P**
Intercept	0.976	1755.726	**0.001**
Ecoregion (same)	-0.122	-38.561	**0.001**
Biome (same)	-0.008	-8.354	**0.001**
Smooth Terms	**EDF**	**F**	**P**
s (human disturbance distance)	8.341	29.073	**0.001**
s (spatial distance)	8.863	716.735	**0.001**
s (elevational difference)	5.578	100.041	**0.001**
s (hours distance)	6.987	3.990	0.608
s (months distance)	6.819	6.693	0.087
s (years distance)	6.484	7.966	0.061
s (sampling intensity distance)	1.000	24.580	**0.008**
s (methods distance)	8.013	11.066	**0.016**

Bold values indicate statistically significant results ($P < 0.05$).

Supplementary Table 16. **Multiple predictors of species turnover (βS) on plant-frugivore networks.** Here, we used a buffer zone of 1000 km and the alternative scenario 3 (see Alternative scenarios section) during the data cleaning process. The binary versions of ecoregion and biome distance matrices were used for estimating the effects of ecoregion and biome borders on the response variable. *P* values were calculated using a two-tailed statistical test that combines Generalized Additive Models (GAM) and Multiple Regression on distance Matrices (MRM). In this approach, the non-independence of distances from each local network is accounted for in the hypothesis testing by performing 1,000 permutations of the response matrix (see Methods). EDF represents the estimated degrees of freedom for each smooth term in the model. *N* pairs of networks = 19,110.

Parametric coefficients	**Estimate**	**t**	**P**
Intercept	0.976	1733.860	**0.001**
Ecoregion (same)	-0.122	-38.095	**0.001**
Biome (same)	-0.009	-8.778	**0.001**
Smooth Terms	**EDF**	**F**	**P**
s (human disturbance distance)	8.308	28.497	**0.001**
s (spatial distance)	8.866	725.333	**0.001**
s (elevational difference)	5.594	99.561	**0.001**
s (hours distance)	6.899	4.011	0.608
s (months distance)	6.744	6.537	0.109
s (years distance)	6.404	7.389	0.063
s (sampling intensity distance)	1.004	26.506	**0.006**
s (methods distance)	8.037	10.951	**0.021**

Bold values indicate statistically significant results ($P < 0.05$).

Supplementary Table 17. **Multiple predictors of plant-frugivore interaction dissimilarity (β_{WN}).** Here, we used a buffer zone of 500 km and the alternative scenario 1 (see Alternative scenarios section) during the data cleaning process. The binary versions of ecoregion and biome distance matrices were used for estimating the effects of ecoregion and biome borders on the response variable. *P* values were calculated using a two-tailed statistical test that combines Generalized Additive Models (GAM) and Multiple Regression on distance Matrices (MRM). In this approach, the non-independence of distances from each local network is accounted for in the hypothesis testing by performing 1,000 permutations of the response matrix (see Methods). EDF represents the estimated degrees of freedom for each smooth term in the model. *N* pairs of networks = 19,110.

Parametric coefficients	**Estimate**	**t**	**P**
Intercept	0.997	2966.347	**0.001**
Ecoregion (same)	-0.070	-36.417	**0.001**
Biome (same)	-0.002	-3.317	**0.039**
Smooth Terms	**EDF**	**F**	**P**
s (human disturbance distance)	8.536	30.035	**0.001**
s (spatial distance)	8.785	65.220	**0.001**
s (elevational difference)	6.185	47.606	**0.001**
s (hours distance)	1.545	5.545	0.294
s (months distance)	5.502	6.966	0.074
s (years distance)	7.216	11.880	**0.013**
s (sampling intensity distance)	1.062	4.686	0.331
s (methods distance)	7.848	15.987	**0.004**

Bold values indicate statistically significant results ($P < 0.05$).

Supplementary Table 18. **Multiple predictors of plant-frugivore interaction dissimilarity (β_{WN}).** Here, we used a buffer zone of 500 km and the alternative scenario 2 (see Alternative scenarios section) during the data cleaning process. The binary versions of ecoregion and biome distance matrices were used for estimating the effects of ecoregion and biome borders on the response variable. *P* values were calculated using a two-tailed statistical test that combines Generalized Additive Models (GAM) and Multiple Regression on distance Matrices (MRM). In this approach, the non-independence of distances from each local network is accounted for in the hypothesis testing by performing 1,000 permutations of the response matrix (see Methods). EDF represents the estimated degrees of freedom for each smooth term in the model. *N* pairs of networks = 19,110.

Parametric coefficients	**Estimate**	**t**	**P**
Intercept	0.997	3002.392	**0.001**
Ecoregion (same)	-0.069	-36.473	**0.001**
Biome (same)	-0.002	-3.313	**0.034**
Smooth Terms	**EDF**	**F**	**P**
s (human disturbance distance)	8.551	30.504	**0.001**
s (spatial distance)	8.783	64.233	**0.001**
s (elevational difference)	6.107	47.553	**0.001**
s (hours distance)	1.590	5.325	0.307
s (months distance)	5.475	7.030	0.092
s (years distance)	7.216	11.941	**0.022**
s (sampling intensity distance)	1.003	5.041	0.319
s (methods distance)	7.867	16.082	**0.003**

Bold values indicate statistically significant results ($P < 0.05$).

Supplementary Table 19. **Multiple predictors of plant-frugivore interaction dissimilarity (β_{WN}).** Here, we used a buffer zone of 100 km and the alternative scenario 1 (see Alternative scenarios section) during the data cleaning process. The binary versions of ecoregion and biome distance matrices were used for estimating the effects of ecoregion and biome borders on the response variable. *P* values were calculated using a two-tailed statistical test that combines Generalized Additive Models (GAM) and Multiple Regression on distance Matrices (MRM). In this approach, the non-independence of distances from each local network is accounted for in the hypothesis testing by performing 1,000 permutations of the response matrix (see Methods). EDF represents the estimated degrees of freedom for each smooth term in the model. *N* pairs of networks = 19,110.

Parametric coefficients	**Estimate**	**t**	**P**
Intercept	0.997	2966.503	**0.001**
Ecoregion (same)	-0.070	-36.418	**0.001**
Biome (same)	-0.002	-3.321	**0.047**
Smooth Terms	**EDF**	**F**	**P**
s (human disturbance distance)	8.536	30.011	**0.001**
s (spatial distance)	8.785	65.161	**0.001**
s (elevational difference)	6.190	47.625	**0.001**
s (hours distance)	1.546	5.546	0.272
s (months distance)	5.504	6.965	0.074
s (years distance)	7.215	11.883	**0.021**
s (sampling intensity distance)	1.056	4.744	0.330
s (methods distance)	7.851	16.023	**0.005**

Bold values indicate statistically significant results ($P < 0.05$).

Supplementary Table 20. **Multiple predictors of plant-frugivore interaction dissimilarity (β_{WN}).** Here, we used a buffer zone of 100 km and the alternative scenario 2 (see Alternative scenarios section) during the data cleaning process. The binary versions of ecoregion and biome distance matrices were used for estimating the effects of ecoregion and biome borders on the response variable. *P* values were calculated using a two-tailed statistical test that combines Generalized Additive Models (GAM) and Multiple Regression on distance Matrices (MRM). In this approach, the non-independence of distances from each local network is accounted for in the hypothesis testing by performing 1,000 permutations of the response matrix (see Methods). EDF represents the estimated degrees of freedom for each smooth term in the model. *N* pairs of networks = 19,110.

Parametric coefficients	**Estimate**	**t**	**P**
Intercept	0.997	3002.382	**0.001**
Ecoregion (same)	-0.069	-36.474	**0.001**
Biome (same)	-0.002	-3.312	**0.049**
Smooth Terms	**EDF**	**F**	**P**
s (human disturbance distance)	8.551	30.506	**0.002**
s (spatial distance)	8.782	64.153	**0.001**
s (elevational difference)	6.109	47.538	**0.001**
s (hours distance)	1.579	5.376	0.298
s (months distance)	5.483	7.037	0.075
s (years distance)	7.217	11.954	**0.019**
s (sampling intensity distance)	1.003	5.036	0.311
s (methods distance)	7.867	16.089	**0.004**

Bold values indicate statistically significant results ($P < 0.05$).

Supplementary Table 21. Multiple predictors of plant-frugivore interaction dissimilarity (β_{WN}). Here, we used a buffer zone of 100 km and the alternative scenario 3 (see Alternative scenarios section) during the data cleaning process. The binary versions of ecoregion and biome distance matrices were used for estimating the effects of ecoregion and biome borders on the response variable. *P* values were calculated using a two-tailed statistical test that combines Generalized Additive Models (GAM) and Multiple Regression on distance Matrices (MRM). In this approach, the non-independence of distances from each local network is accounted for in the hypothesis testing by performing 1,000 permutations of the response matrix (see Methods). EDF represents the estimated degrees of freedom for each smooth term in the model. *N* pairs of networks = 19,110.

Parametric coefficients	**Estimate**	**t**	**P**
Intercept	0.997	2964.236	**0.001**
Ecoregion (same)	-0.070	-36.405	**0.001**
Biome (same)	-0.002	-3.324	**0.046**
Smooth Terms	**EDF**	**F**	**P**
s (human disturbance distance)	8.534	29.980	**0.001**
s (spatial distance)	8.785	65.228	**0.001**
s (elevational difference)	6.171	47.691	**0.001**
s (hours distance)	1.559	5.453	0.301
s (months distance)	5.490	6.908	0.076
s (years distance)	7.210	11.881	**0.020**
s (sampling intensity distance)	1.022	5.148	0.281
s (methods distance)	7.850	16.024	**0.004**

Bold values indicate statistically significant results ($P < 0.05$).

Supplementary Table 22. Multiple predictors of plant-frugivore interaction dissimilarity (β_{WN}). Here, we used a buffer zone of 1000 km and the alternative scenario 1 (see Alternative scenarios section) during the data cleaning process. The binary versions of ecoregion and biome distance matrices were used for estimating the effects of ecoregion and biome borders on the response variable. *P* values were calculated using a two-tailed statistical test that combines Generalized Additive Models (GAM) and Multiple Regression on distance Matrices (MRM). In this approach, the non-independence of distances from each local network is accounted for in the hypothesis testing by performing 1,000 permutations of the response matrix (see Methods). EDF represents the estimated degrees of freedom for each smooth term in the model. *N* pairs of networks = 19,110.

Parametric coefficients	**Estimate**	**t**	**P**
Intercept	0.997	2966.167	**0.001**
Ecoregion (same)	-0.070	-36.419	**0.001**
Biome (same)	-0.002	-3.311	**0.032**
Smooth Terms	**EDF**	**F**	**P**
s (human disturbance distance)	8.536	30.036	**0.001**
s (spatial distance)	8.785	65.100	**0.001**
s (elevational difference)	6.187	47.586	**0.001**
s (hours distance)	1.532	5.585	0.299
s (months distance)	5.511	6.974	0.076
s (years distance)	7.217	11.890	**0.019**
s (sampling intensity distance)	1.085	4.382	0.377
s (methods distance)	7.849	15.996	**0.004**

Bold values indicate statistically significant results ($P < 0.05$).

Supplementary Table 23. Multiple predictors of plant-frugivore interaction dissimilarity (β_{WN}). Here, we used a buffer zone of 1000 km and the alternative scenario 2 (see Alternative scenarios section) during the data cleaning process. The binary versions of ecoregion and biome distance matrices were used for estimating the effects of ecoregion and biome borders on the response variable. *P* values were calculated using a two-tailed statistical test that combines Generalized Additive Models (GAM) and Multiple Regression on distance Matrices (MRM). In this approach, the non-independence of distances from each local network is accounted for in the hypothesis testing by performing 1,000 permutations of the response matrix (see Methods). EDF represents the estimated degrees of freedom for each smooth term in the model. *N* pairs of networks = 19,110.

Parametric coefficients	**Estimate**	**t**	**P**
Intercept	0.997	3002.382	**0.001**
Ecoregion (same)	-0.069	-36.474	**0.001**
Biome (same)	-0.002	-3.312	**0.048**
Smooth Terms	**EDF**	**F**	**P**
s (human disturbance distance)	8.551	30.506	**0.002**
s (spatial distance)	8.782	64.153	**0.001**
s (elevational difference)	6.109	47.538	**0.001**
s (hours distance)	1.579	5.376	0.311
s (months distance)	5.483	7.037	0.054
s (years distance)	7.217	11.954	**0.017**
s (sampling intensity distance)	1.003	5.036	0.320
s (methods distance)	7.867	16.089	**0.004**

Bold values indicate statistically significant results ($P < 0.05$).

Supplementary Table 24. **Multiple predictors of plant-frugivore interaction dissimilarity (β_{WN}).** Here, we used a buffer zone of 1000 km and the alternative scenario 3 (see Alternative scenarios section) during the data cleaning process. The binary versions of ecoregion and biome distance matrices were used for estimating the effects of ecoregion and biome borders on the response variable. *P* values were calculated using a two-tailed statistical test that combines Generalized Additive Models (GAM) and Multiple Regression on distance Matrices (MRM). In this approach, the non-independence of distances from each local network is accounted for in the hypothesis testing by performing 1,000 permutations of the response matrix (see Methods). EDF represents the estimated degrees of freedom for each smooth term in the model. *N* pairs of networks = 19,110.

Parametric coefficients	**Estimate**	**t**	**P**
Intercept	0.997	2964.095	**0.001**
Ecoregion (same)	-0.070	-36.404	**0.001**
Biome (same)	-0.002	-3.318	**0.042**
Smooth Terms	**EDF**	**F**	**P**
s (human disturbance distance)	8.534	29.989	**0.002**
s (spatial distance)	8.785	65.276	**0.001**
s (elevational difference)	6.170	47.687	**0.001**
s (hours distance)	1.547	5.482	0.300
s (months distance)	5.491	6.909	0.073
s (years distance)	7.210	11.857	**0.020**
s (sampling intensity distance)	1.026	4.983	0.287
s (methods distance)	7.849	16.010	**0.003**

Bold values indicate statistically significant results ($P < 0.05$).

Supplementary Table 25. **Multiple predictors of plant-frugivore network structural dissimilarity.** Here, we used a buffer zone of 500 km and the alternative scenario 1 (see Alternative scenarios section) during the data cleaning process. The binary versions of ecoregion and biome distance matrices were used for estimating the effects of ecoregion and biome borders on the response variable. *P* values were calculated using a two-tailed statistical test that combines Generalized Additive Models (GAM) and Multiple Regression on distance Matrices (MRM). In this approach, the non-independence of distances from each local network is accounted for in the hypothesis testing by performing 1,000 permutations of the response matrix (see Methods). EDF represents the estimated degrees of freedom for each smooth term in the model. *N* pairs of networks = 19,110.

Parametric coefficients	**Estimate**	**t**	**P**
Intercept	2.686	221.962	**0.004**
Ecoregion (same)	0.044	0.646	0.775
Biome (same)	-0.024	-1.115	0.826
Smooth Terms	**EDF**	**F**	**P**
s (human disturbance distance)	5.948	9.481	0.439
s (spatial distance)	8.473	20.322	**0.015**
s (elevational difference)	8.233	5.501	0.724
s (hours distance)	8.051	7.960	0.968
s (months distance)	6.239	7.217	0.667
s (years distance)	6.830	13.941	0.497
s (sampling intensity distance)	8.759	240.837	**0.001**
s (methods distance)	8.595	17.496	0.233

Bold values indicate statistically significant results ($P < 0.05$).

Supplementary Table 26. Multiple predictors of plant-frugivore network structural dissimilarity. Here, we used a buffer zone of 500 km and the alternative scenario 2 (see Alternative scenarios section) during the data cleaning process. The binary versions of ecoregion and biome distance matrices were used for estimating the effects of ecoregion and biome borders on the response variable. *P* values were calculated using a two-tailed statistical test that combines Generalized Additive Models (GAM) and Multiple Regression on distance Matrices (MRM). In this approach, the non-independence of distances from each local network is accounted for in the hypothesis testing by performing 1,000 permutations of the response matrix (see Methods). EDF represents the estimated degrees of freedom for each smooth term in the model. *N* pairs of networks = 19,110.

Parametric coefficients	**Estimate**	**t**	**P**
Intercept	2.685	222.539	**0.002**
Ecoregion (same)	0.084	1.229	0.561
Biome (same)	-0.024	-1.157	0.801
Smooth Terms	**EDF**	**F**	**P**
s (human disturbance distance)	5.417	9.472	0.460
s (spatial distance)	8.587	28.061	**0.002**
s (elevational difference)	7.800	3.418	0.904
s (hours distance)	8.088	7.568	0.973
s (months distance)	7.129	7.330	0.682
s (years distance)	6.823	12.437	0.555
s (sampling intensity distance)	8.758	275.291	**0.001**
s (methods distance)	8.550	18.139	0.191

Bold values indicate statistically significant results ($P < 0.05$).

Supplementary Table 27. Multiple predictors of plant-frugivore network structural dissimilarity. Here, we used a buffer zone of 100 km and the alternative scenario 1 (see Alternative scenarios section) during the data cleaning process. The binary versions of ecoregion and biome distance matrices were used for estimating the effects of ecoregion and biome borders on the response variable. *P* values were calculated using a two-tailed statistical test that combines Generalized Additive Models (GAM) and Multiple Regression on distance Matrices (MRM). In this approach, the non-independence of distances from each local network is accounted for in the hypothesis testing by performing 1,000 permutations of the response matrix (see Methods). EDF represents the estimated degrees of freedom for each smooth term in the model. *N* pairs of networks = 19,110.

Parametric coefficients	**Estimate**	**t**	**P**
Intercept	2.691	222.709	**0.007**
Ecoregion (same)	0.052	0.757	0.743
Biome (same)	-0.028	-1.364	0.762
Smooth Terms	**EDF**	**F**	**P**
s (human disturbance distance)	5.834	9.562	0.428
s (spatial distance)	8.470	20.654	**0.018**
s (elevational difference)	8.080	4.412	0.817
s (hours distance)	8.130	8.456	0.965
s (months distance)	6.321	7.283	0.647
s (years distance)	6.827	13.789	0.501
s (sampling intensity distance)	8.745	241.194	**0.003**
s (methods distance)	8.590	17.524	0.209

Bold values indicate statistically significant results ($P < 0.05$).

Supplementary Table 28. **Multiple predictors of plant-frugivore network structural dissimilarity.** Here, we used a buffer zone of 100 km and the alternative scenario 2 (see Alternative scenarios section) during the data cleaning process. The binary versions of ecoregion and biome distance matrices were used for estimating the effects of ecoregion and biome borders on the response variable. *P* values were calculated using a two-tailed statistical test that combines Generalized Additive Models (GAM) and Multiple Regression on distance Matrices (MRM). In this approach, the non-independence of distances from each local network is accounted for in the hypothesis testing by performing 1,000 permutations of the response matrix (see Methods). EDF represents the estimated degrees of freedom for each smooth term in the model. *N* pairs of networks = 19,110.

Parametric coefficients	**Estimate**	**t**	**P**
Intercept	2.684	222.432	**0.004**
Ecoregion (same)	0.089	1.311	0.549
Biome (same)	-0.023	-1.085	0.812
Smooth Terms	**EDF**	**F**	**P**
s (human disturbance distance)	5.330	9.475	0.436
s (spatial distance)	8.590	28.764	**0.003**
s (elevational difference)	1.026	4.544	0.803
s (hours distance)	8.122	7.758	0.981
s (months distance)	7.189	7.442	0.677
s (years distance)	6.821	12.365	0.583
s (sampling intensity distance)	8.761	275.772	**0.001**
s (methods distance)	8.540	17.893	0.205

Bold values indicate statistically significant results ($P < 0.05$).

Supplementary Table 29. **Multiple predictors of plant-frugivore network structural dissimilarity.** Here, we used a buffer zone of 100 km and the alternative scenario 3 (see Alternative scenarios section) during the data cleaning process. The binary versions of ecoregion and biome distance matrices were used for estimating the effects of ecoregion and biome borders on the response variable. *P* values were calculated using a two-tailed statistical test that combines Generalized Additive Models (GAM) and Multiple Regression on distance Matrices (MRM). In this approach, the non-independence of distances from each local network is accounted for in the hypothesis testing by performing 1,000 permutations of the response matrix (see Methods). EDF represents the estimated degrees of freedom for each smooth term in the model. *N* pairs of networks = 19,110.

Parametric coefficients	**Estimate**	**t**	**P**
Intercept	2.689	222.557	**0.008**
Ecoregion (same)	0.044	0.639	0.754
Biome (same)	-0.031	-1.443	0.741
Smooth Terms	**EDF**	**F**	**P**
s (human disturbance distance)	5.869	9.131	0.446
s (spatial distance)	8.479	20.589	**0.021**
s (elevational difference)	8.217	5.476	0.755
s (hours distance)	8.052	7.939	0.966
s (months distance)	6.005	7.020	0.675
s (years distance)	6.834	14.956	0.411
s (sampling intensity distance)	8.746	238.220	**0.003**
s (methods distance)	8.583	17.496	0.206

Bold values indicate statistically significant results ($P < 0.05$).

Supplementary Table 30. **Multiple predictors of plant-frugivore network structural dissimilarity.** Here, we used a buffer zone of 1000 km and the alternative scenario 1 (see Alternative scenarios section) during the data cleaning process. The binary versions of ecoregion and biome distance matrices were used for estimating the effects of ecoregion and biome borders on the response variable. *P* values were calculated using a two-tailed statistical test that combines Generalized Additive Models (GAM) and Multiple Regression on distance Matrices (MRM). In this approach, the non-independence of distances from each local network is accounted for in the hypothesis testing by performing 1,000 permutations of the response matrix (see Methods). EDF represents the estimated degrees of freedom for each smooth term in the model. *N* pairs of networks = 19,110.

Parametric coefficients	**Estimate**	**t**	**P**
Intercept	2.687	222.335	**0.001**
Ecoregion (same)	0.047	0.681	0.776
Biome (same)	-0.026	-1.251	0.802
Smooth Terms	**EDF**	**F**	**P**
s (human disturbance distance)	5.954	9.761	0.432
s (spatial distance)	8.483	20.514	**0.010**
s (elevational difference)	8.243	5.492	0.736
s (hours distance)	8.009	7.896	0.970
s (months distance)	6.128	6.943	0.699
s (years distance)	6.852	13.832	0.496
s (sampling intensity distance)	8.789	245.694	**0.002**
s (methods distance)	8.593	17.437	0.229

Bold values indicate statistically significant results ($P < 0.05$).

Supplementary Table 31. **Multiple predictors of plant-frugivore network structural dissimilarity.** Here, we used a buffer zone of 1000 km and the alternative scenario 2 (see Alternative scenarios section) during the data cleaning process. The binary versions of ecoregion and biome distance matrices were used for estimating the effects of ecoregion and biome borders on the response variable. *P* values were calculated using a two-tailed statistical test that combines Generalized Additive Models (GAM) and Multiple Regression on distance Matrices (MRM). In this approach, the non-independence of distances from each local network is accounted for in the hypothesis testing by performing 1,000 permutations of the response matrix (see Methods). EDF represents the estimated degrees of freedom for each smooth term in the model. *N* pairs of networks = 19,110.

Parametric coefficients	**Estimate**	**t**	**P**
Intercept	2.685	222.527	**0.004**
Ecoregion (same)	0.084	1.225	0.562
Biome (same)	-0.022	-1.058	0.844
Smooth Terms	**EDF**	**F**	**P**
s (human disturbance distance)	5.417	9.454	0.427
s (spatial distance)	8.588	28.139	**0.008**
s (elevational difference)	7.796	3.409	0.893
s (hours distance)	8.098	7.547	0.977
s (months distance)	7.123	7.341	0.669
s (years distance)	6.851	12.533	0.570
s (sampling intensity distance)	8.757	275.296	**0.001**
s (methods distance)	8.551	18.041	0.182

Bold values indicate statistically significant results ($P < 0.05$).

Supplementary Table 32. Multiple predictors of plant-frugivore network structural dissimilarity. Here, we used a buffer zone of 1000 km and the alternative scenario 3 (see Alternative scenarios section) during the data cleaning process. The binary versions of ecoregion and biome distance matrices were used for estimating the effects of ecoregion and biome borders on the response variable. *P* values were calculated using a two-tailed statistical test that combines Generalized Additive Models (GAM) and Multiple Regression on distance Matrices (MRM). In this approach, the non-independence of distances from each local network is accounted for in the hypothesis testing by performing 1,000 permutations of the response matrix (see Methods). EDF represents the estimated degrees of freedom for each smooth term in the model. *N* pairs of networks = 19,110.

Parametric coefficients	**Estimate**	**t**	**P**
Intercept	2.692	223.088	**0.008**
Ecoregion (same)	0.045	0.663	0.766
Biome (same)	-0.033	-1.581	0.748
Smooth Terms	**EDF**	**F**	**P**
s (human disturbance distance)	5.943	9.649	0.423
s (spatial distance)	8.491	20.649	**0.013**
s (elevational difference)	8.230	5.556	0.727
s (hours distance)	8.063	8.161	0.956
s (months distance)	5.980	6.955	0.711
s (years distance)	6.778	14.670	0.479
s (sampling intensity distance)	8.792	243.787	**0.001**
s (methods distance)	8.578	17.155	0.237

Bold values indicate statistically significant results ($P < 0.05$).

Supplementary Table 33. Multiple predictors of plant-frugivore interaction dissimilarity (β_{WN}). Here, we used the binary versions of ecoregion and biome distance matrices and removed the study with the greatest number of networks in our dataset (study ID 76)[20] from the data. *P* values were calculated using a two-tailed statistical test that combines Generalized Additive Models (GAM) and Multiple Regression on distance Matrices (MRM). In this approach, the non-independence of distances from each local network is accounted for in the hypothesis testing by performing 1,000 permutations of the response matrix (see Methods). EDF represents the estimated degrees of freedom for each smooth term in the model. *N* pairs of networks = 12,880.

Parametric coefficients	**Estimate**	**t**	**P**
Intercept	0.995	2816.925	**0.001**
Ecoregion (same)	-0.077	-33.132	**0.001**
Biome (same)	-0.0008	-1.254	0.380
Smooth Terms	**EDF**	**F**	**P**
s (human disturbance distance)	6.871	11.919	**0.005**
s (spatial distance)	8.917	139.693	**0.001**
s (elevational difference)	5.502	9.025	**0.035**
s (hours distance)	2.007	7.295	0.106
s (months distance)	7.806	23.758	**0.001**
s (years distance)	8.500	33.731	**0.001**
s (sampling intensity distance)	1.002	0.015	0.992
s (methods distance)	8.571	61.413	**0.001**

Bold values indicate statistically significant results ($P < 0.05$).

Supplementary Table 34. Multiple predictors of plant-frugivore network structural dissimilarity. Here, we used the binary versions of ecoregion and biome distance matrices and removed the study with the greatest number of networks in our dataset (study ID 76)[20] from the data. *P* values were calculated using a two-tailed statistical test that combines Generalized Additive Models (GAM) and Multiple Regression on distance Matrices (MRM). In this approach, the non-independence of distances from each local network is accounted for in the hypothesis testing by performing 1,000 permutations of the response matrix (see Methods). EDF represents the estimated degrees of freedom for each smooth term in the model. *N* pairs of networks = 12,880.

Parametric coefficients	**Estimate**	**t**	**P**
Intercept	2.568	184.419	**0.022**
Ecoregion (same)	-0.075	-0.826	0.544
Biome (same)	0.041	1.595	0.679
Smooth Terms	**EDF**	**F**	**P**
s (human disturbance distance)	4.419	13.240	0.121
s (spatial distance)	8.540	27.067	**0.005**
s (elevational difference)	7.486	11.064	0.364
s (hours distance)	7.717	8.123	0.923
s (months distance)	6.900	5.378	0.714
s (years distance)	5.505	10.312	0.424
s (sampling intensity distance)	8.534	126.502	**0.008**
s (methods distance)	8.489	14.492	0.190

Bold values indicate statistically significant results ($P < 0.05$).

Supplementary Table 35. Multiple predictors of interaction rewiring (βos) on plant-frugivore networks. Here, we show the results from a Generalized Additive Mixed-effects Model (GAMM) using network IDs as random effects (one random factor for each of the pairs across which distance is compared) to account for the non-independence of distances (see Rewiring analysis section). *P* values of smooth terms are associated with Wald-type tests of smooth components' equality to zero. Linear terms are used for the categorical variables (ecoregions and biomes). EDF represents the estimated degrees of freedom for each smooth term in the model. *N* pairs of networks = 1,314.

Parametric coefficients	**Estimate**	**t**	**P**
Intercept	0.576	25.267	**$2x10^{-16}$**
Ecoregion (same)	-0.017	-0.643	0.521
Biome (same)	-0.033	-1.354	0.176
Smooth Terms	**EDF**	**F**	**P**
s (human disturbance distance)	1.864	5.039	**0.005**
s (spatial distance)	2.861	17.983	**$2x10^{-16}$**
s (elevational difference)	3.114	13.422	**$2x10^{-16}$**
s (hours distance)	1.000	5.634	**0.018**
s (months distance)	3.434	1.441	0.139
s (years distance)	1.000	0.906	0.341
s (sampling intensity distance)	2.026	3.767	**0.023**
s (methods distance)	1.000	5.129	**0.024**

Bold values indicate statistically significant results ($P < 0.05$).

Supplementary Table 36. The effect of large-scale ecological boundaries on interaction rewiring (β_{OS}). Here, we show the results from a Generalized Additive Mixed-effects Model (GAMM) using ecoregion and biome distance metrics as predictors and network IDs as random effects (one random factor for each of the pairs across which distance is compared) to account for the non-independence of distances (see Rewiring analysis section). Note that, contrary to the full model (Supplementary Table 35), only categorical variables are included in this model (with a fixed effect for each level of the category). The effect of ecoregion boundaries is significant, likely because of their collinearity with our other predictor variables. *N* pairs of networks = 1,314.

Parametric coefficients	**Estimate**	**t**	**P**
Intercept	0.579	22.975	**$2x10^{-16}$**
Ecoregion (same)	-0.155	-6.756	**$2.13x10^{-11}$**
Biome (same)	0.005	0.202	0.84

Bold values indicate statistically significant results ($P < 0.05$).

Supplementary Note

Prisma flowchart

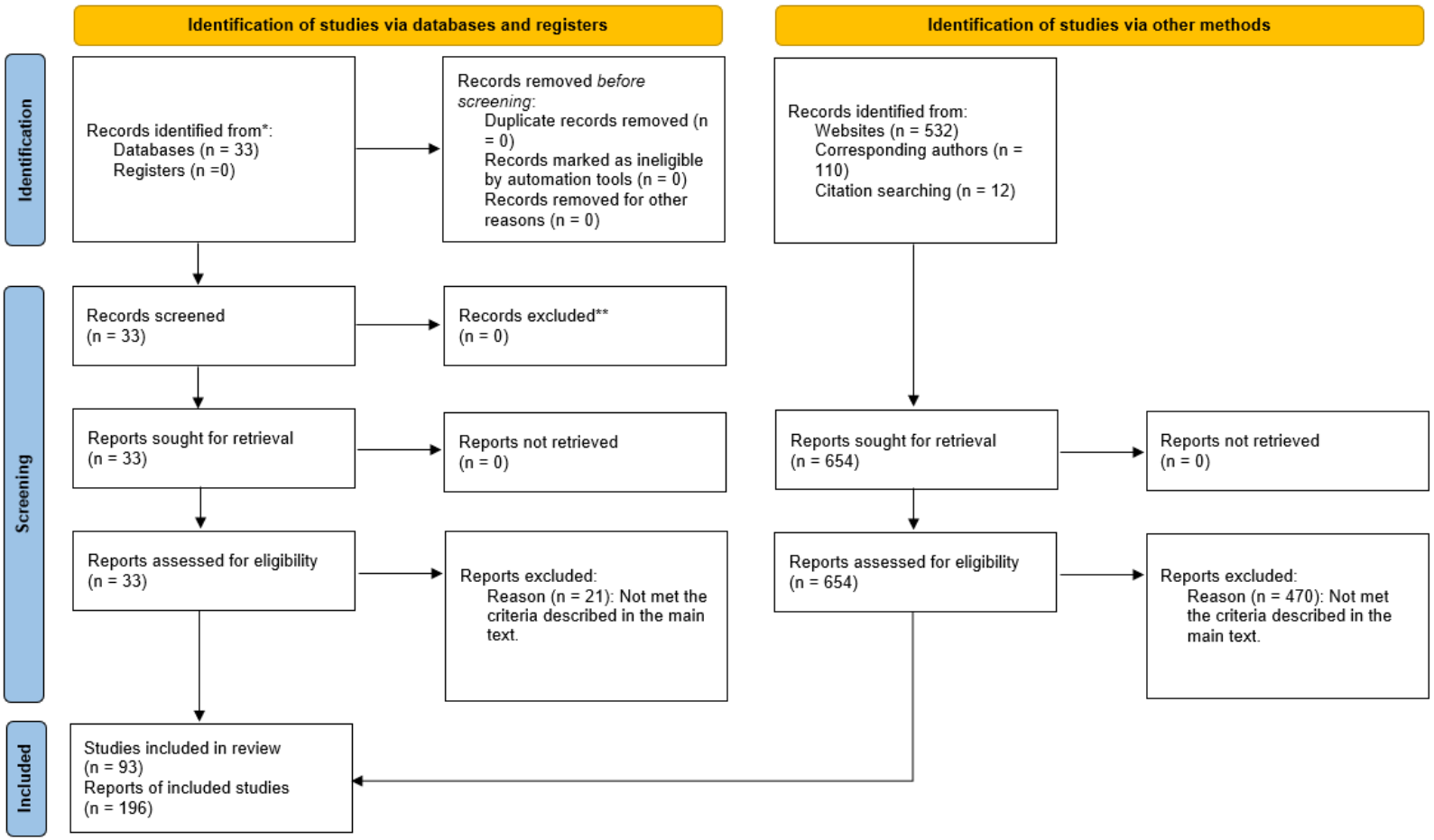

Supplementary References

1. Global Names Resolver: Global Names resolution tools and services. https://resolver.globalnames.org. (2020).
2. Chamberlain, S. A. & Szöcs, E. taxize: taxonomic search and retrieval in R. *F1000Research* **2**, 191 (2013).
3. Rees, T. Taxamatch, an algorithm for near ('Fuzzy') matching of scientific names in taxonomic databases. *PLoS One* **9**, e107510 (2014).
4. National Center for Biotechnology Information. https://www.ncbi.nlm.nih.gov./ (2020).
5. BirdLife International. https://www.birdlife.org/ (2020).
6. Integrated Taxonomic Information System. https://itis.gov/ (2020).
7. Handbook of the birds of the world and BirdLife International digital checklist of the birds of the world. Version 4.0. http://datazone.birdlife.org/species/taxonomy (2019).
8. Avibase, The world bird database. https://avibase.bsc-eoc.org/ (2020).
9. R Core Team. R: A language and environment for statistical computing (R Foundation for Statistical Computing, Vienna, Austria, 2020).
10. International Plant Name Index. https://www.ipni.org/ (2020).
11. Tropicos: connecting the world to botanical data since 1982. http://www.tropicos.org/ (2020).
12. Boyle, B. *et al*. The taxonomic name resolution service: an online tool for automated standardization of plant names. *BMC Bioinformatics* **14**, 16 (2013).
13. GBIF: The Global Biodiversity Information Facility. What is GBIF? https://www.gbif.org/what-is-gbif (2020).
14. Chamberlain *et al*. rgbif: interface to the Global Biodiversity Information Facility API. R

package version 1.4.0 https://cran.r-project.org/package=rgbif (2021).

15. Cagua, E. F., Lustig, A. & Tylianakis, J. M. Environment affects specialisation of plants and pollinators. Preprint at https://www.biorxiv.org/content/10.1101/866772v1 (2019).
16. Gaiji, S. *et al*. Content assessment of the primary biodiversity data published through GBIF network: status, challenges and potentials. *Biodivers. Informatics* **8**, 94–172 (2013).
17. Zizka, A. *et al*. CoordinateCleaner: standardized cleaning of occurrence records from biological collection databases. *Methods Ecol. Evol.* **10**, 744–751 (2019).
18. Natural Earth. http://www.naturalearthdata.com/ (2020)
19. Dinerstein, E. *et al.* An ecoregion-based approach to protecting half the terrestrial realm. *Bioscience* **67**, 534–545 (2017).
20. Vollstädt, M. G. R. *et al*. Seed-dispersal networks respond differently to resource effects in open and forest habitats. *Oikos* **127**, 847–854 (2017).
21. Baird, J. W. The selection and use of fruit by birds in an eastern forest. *Wilson Bull.* **92**, 63–73 (1980).
22. Carlo, T. A., Collazo, J. A. & Groom, M. J. Avian fruit preferences across a Puerto Rican forested landscape: pattern consistency and implications for seed removal. *Oecologia* **134**, 119–131 (2003).
23. Frost, P. G. H. Fruit-frugivore interactions in a South African coastal dune forest. *Acta XVII Congressus Internationalis Ornithologici* **2**, 1179–1184 (1980).
24. Galetti, M. & Pizo, M. A. Fruit eating by birds in a forest fragment in southeastern Brazil. Ararajuba **4**, 71–79 (1996).
25. Kantak, G. E. Observations on some fruit-eating birds in Mexico. *Auk* **96**, 183–186 (1979).

26. Sorensen, A. E. Interactions between birds and fruit in a temperate woodland. *Oecologia* **50**, 242–249 (1981).

27. W. R. Silva, *Patterns of Fruit-frugivores Interactions in two Atlantic Forest Bird Communities of South-eastern Brazil: Implications for Conservation* in *Seed Dispersal and Frugivory: Ecology, Evolution, and Conservation* (eds. Levey, D. J., Silva, W. R., Galetti, M.) 423–435 (CAB International, 2002).

28. Rodrigues, S. L. M. *Rede de Interações entre aves frugívoras e plantas em uma área de Mata Atlântica no Sudeste do Brasil*, thesis, Universidade Federal de São Carlos, Sorocaba, SP (2015).

29. Castro, E. R. *Fenologia reprodutiva do palmito Euterpe edulis (Arecaceae) e sua influência na abundância de aves frugívoras na floresta Atlântica*, thesis, UNESP, Rio Claro, SP (2007).

30. Correia, J. M. S. *Utilização de espécies frutíferas da Mata Atlântica na alimentação da avifauna da Reserva Biológica de Poços das Antas*, thesis, UNDB, Brasília, DF (1997).

31. Alves, K. J. F. *Composição da avifauna e frugivoria por aves em um mosaico sucessional na Mata Atlântica*, thesis, UNESP, Rio Claro, SP (2008).

32. Fadini, R. F.& de Marco Jr, P. Interações entre aves frugívoras e plantas em um fragmento de mata atlântica de Minas Gerais. *Ararajuba* **12**, 97–103 (2004).

33. Kindel, A. *Interações entre plantas ornitocóricas e aves frugívoras na Estação Ecológica de Aracuri, Muitos Capões, RS*, thesis, UFRGS, Porto Alegre, RS (1996).

34. Pizo, M. A. Frugivory and habitat use by fruit-eating birds in a fragmented landscape of southeast Brazil. *Ornitol. Neotrop*. **15**, 117–126 (2004).

35. Athiê, S. *Composição da avifauna e frugivoria por aves em um mosaico de vegetação*

secundária em Rio Claro, região centro-leste do estado de São Paulo, thesis, UFSCAR, São Carlos, SP (2009).

36. Ribeiro da Silva, F. *et al*. The restoration of tropical seed dispersal networks. *Restor. Ecol.* **23**, 852–860 (2015).

37. Hasui, E. *O papel das aves frugívoras na dispersão de sementes em um fragmento de floresta semidecídua secundária em São Paulo*, thesis, USP, São Paulo, SP (1994).

38. Robinson, V. *Índice de importância de diferentes espécies de plantas na atração de aves para uma área reflorestada em Piracicaba*, thesis, UNESP, Rio Claro, SP (2015).

39. Silva, R. F. M. *Interações entre plantas e aves frugívoras no campus da Universidade Federal do Rio de Janeiro*, thesis, UFRJ, Rio de Janeiro, RJ (2011).

40. Heleno, R. H., Ramos, J. A. & Memmott, J. Integration of exotic seeds into an Azorean seed dispersal network. *Biol. Invasions* **15**, 1143–1154 (2013).

41. Schleuning, M., Blüthgen, N., Flörchinger, M., Braun, J., Schaefer, M. H. & Böhning-gaese, K. Specialization and interaction strength in a tropical plant-frugivore network differ among forest strata. *Ecology* **92**, 26–36 (2011).

42. Schneiberg, I. *et al*. Urbanization homogenizes the interactions of plant-frugivore bird networks. *Urban Ecosyst.* **23**, 457–470 (2020).

43. Machado-de-Souza, T., Campos, R. P., Devoto, M. & Varassin, I. G. Local predictors of the structure of a tropical bird-seed dispersal network. *Oecologia* **189**, 421–433 (2019).

44. González-Castro, A., Traveset, A. & Nogales, M. Seed dispersal interactions in the Mediterranean Region: contrasting patterns between islands and mainland. *J. Biogeogr.* **39**, 1938–1947 (2012).

45. Faustino, T. C. & Machado, C. G. Frugivoria por aves em uma área de campo rupestre na

Chapada Diamantina, BA. *Rev. Bras. Ornitol.* **14**, 137–143 (2006).

46. Jordano, P. El ciclo anual de los paseriformes frugívoros en el matorral mediterráneo del sur de España: importancia de su invernada y variaciones interanuales. *Ardeola* **32**, 69–94 (1985).

47. Saavedra, F. *et al.* Functional importance of avian seed dispersers changes in response to human-induced forest edges in tropical seed-dispersal networks. *Oecologia* **176**, 837–848 (2014).

48. Noma, N. & Yumoto, T. Fruiting phenology of animal-dispersed plants in response to winter migration of frugivores in a warm temperate forest on Yakushima Island, Japan. *Ecol. Res.* **12**, 119–129 (1997).

49. Silva, G. B. M. & Pedroni, F. Frugivoria por aves em área de cerrado no município de Uberlândia, Minas Gerais. *Rev. Árvore* **38**, 433–442 (2014).

50. Vizentin-Bugoni, J. *et al.* Structure, spatial dynamics, and stability of novel seed dispersal mutualistic networks in Hawai‘i. *Science* **364**, 78–82 (2019).

51. Acosta-Rojas, D. C., Jiménez-Franco, M. V., Zapata-Pérez, V. M., De La Rúa, P. & Martínez-López, V. An integrative approach to discern the seed dispersal role of frugivorous guilds in a Mediterranean semiarid priority habitat. *PeerJ* **7**, e7609 (2019).

52. Naniwadekar, R., Chaplod, S., Datta, A., Rathore, A. & Sridhar, H. Large frugivores matter: insights from network and seed dispersal effectiveness approaches. *J. Anim. Ecol.* **88**, 1250–1262 (2019).

53. Montoya-Arango, S., Acevedo-Quintero, J. F. & Parra, J. L. Abundance and size of birds determine the position of the species in plant-frugivore interaction networks in fragmented forests. *Community Ecol.* **20**, 75–82 (2019).

54. García, D., Donoso, I. & Rodríguez-Pérez, J. Frugivore biodiversity and complementarity in interaction networks enhance landscape-scale seed dispersal function. *Funct. Ecol.* **32**, 2742–2752 (2018).

55. Casas, G., Bastazini, V. A. G., Debastiani, V. J. & Pillar, V. D. Assessing sampling sufficiency of network metrics using bootstrap. *Ecol. Complex.* **36**, 268–275 (2018).

56. Fricke, E. C., Tewksbury, J. J. & Rogers, H. S. Defaunation leads to interaction deficits, not interaction compensation, in an island seed dispersal network. *Glob. Chang. Biol.* **24**, e190–e200 (2018).

57. Rumeu, B. *et al.* Predicting the consequences of disperser extinction: richness matters the most when abundance is low. *Funct. Ecol.* **31**, 1910–1920 (2017).

58. Farwig, N., Schabo, D. G. & Albrecht, J. Trait-associated loss of frugivores in fragmented forest does not affect seed removal rates. *J. Ecol.* **105**, 20–28 (2017).

59. Gorchov, D. L., Cornejo, F., Ascorra, C. F. & Jaramillo, M. Dietary overlap between frugivorous birds and bats in the Peruvian Amazon. *Oikos* **74**, 235–250 (1995).

60. Carlo, T. A. & Morales, J. M. Generalist birds promote tropical forest regeneration and increase plant diversity via rare-biased seed dispersal. *Ecology* **97**, 1819–1831 (2016).

61. Ramos-Robles, M., Andresen, E. & Díaz-Castelazo, C. Temporal changes in the structure of a plant-frugivore network are influenced by bird migration and fruit availability. *PeerJ* **4**, e2048 (2016).

62. Sarmento, R., Alves-Costa, C. P., Ayub, A. & Mello, M. A. R. Partitioning of seed dispersal services between birds and bats in a fragment of the Brazilian Atlantic Forest. *Zoologia* **31**, 245–255 (2014).

63. García, D., Martínez, D., Stouffer, D. B. & Tylianakis, J. M. Exotic birds increase

generalization and compensate for native bird decline in plant-frugivore assemblages. *J. Anim. Ecol.* **83**, 1441–1450 (2014).

64. Cruz, J. C., Ramos, J. A., da Silva, L. P., Tenreiro, P. Q. & Heleno, R. H. Seed dispersal networks in an urban novel ecosystem. *Eur. J. For. Res.* **132**, 887–897 (2013).

65. Burns, K. C. What causes size coupling in fruit–frugivore interaction webs? *Ecology* **94**, 295–300 (2013).

66. Andrade, P. C., Mota, J. V. L. & de Carvalho, A. A. F. Interações mutualísticas entre aves frugívoras e plantas em um fragmento urbano de Mata Atlântica, Salvador, BA. *Rev. Bras. Ornitol.* **19**, 63–73 (2011).

67. Velho, N., Ratnam, J., Srinivasan, U. & Sankaran, M. Shifts in community structure of tropical trees and avian frugivores in forests recovering from past logging. *Biol. Conserv.* **153**, 32–40 (2012).

68. O'Donnell, C. F. & Dilks, P. J. Foods and foraging of forest birds in temperate rainforest, South Westland, New Zealand. *N. Z. J. Ecol.* **18**, 87–107 (1994).

69. Costa, J. M., da Silva, L. P., Ramos, J. A. & Heleno, R. H. Sampling completeness in seed dispersal networks: when enough is enough. *Basic Appl. Ecol.* **17**, 155–164 (2016).

70. Timóteo, S., Correia, M., Rodríguez-Echeverría, S., Freitas, H. & Heleno, R. Multilayer networks reveal the spatial structure of seed-dispersal interactions across the Great Rift landscapes. *Nat. Commun.* **9**, 140 (2018).

71. David, J. P., Murugan, B. S. & Manakadan, R. Frugivory by birds and mammals in Sriharikota Island, southern India. *J. Bombay Nat. Hist. Soc.* **108**, 24–40 (2011).

72. Medeiros e Silva, É. E., Paixão, V. H. F., Torquato, J. L., Lunardi, D. G. & Lunardi, V. de O. Fruiting phenology and consumption of zoochoric fruits by wild vertebrates in a

seasonally dry tropical forest in the Brazilian Caatinga. *Acta Oecologica* **105**, 103553 (2020).

73. Pratt, T. K. & Stiles, E. W. The Influence of fruit size and structure on composition of frugivore assemblages in New Guinea. *Biotropica* **17**, 314–321 (1985).

74. Brown, E. D. & Hopkins, M. J. G. Tests of disperser specificity between frugivorous birds and rainforest fruits in New Guinea. *Emu* **102**, 137–146 (2002).

75. Kopij, G. Winter diet of frugivorous birds in the suburbs of Bloemfontein, South Africa. *African J. Wildl. Res.* **30**, 163–165 (2000).

76. Stanley, M. C. & Lill, A. Avian fruit consumption and seed dispersal in a temperate Australian woodland. *Austral Ecol.* **27**, 137–148 (2002).

77. French, K. Evidence for frugivory by birds in montane and lowland forests in south-east Australia. *Emu* **90**, 185–189 (1990).

78. Williams, P. A. & Karl, B. J. Fleshy fruits of indigenous and adventive plants in the diet of birds in forest remnants, Nelson, New Zealand. *N. Z. J. Ecol.* **20**, 127–145 (1996).

79. Gomes, V. S. M. *Variação espacial e dieta de aves terrestres na restinga de Jurubatiba, RJ*, thesis, UFRJ, Rio de Janeiro, RJ (2006).

80. Motta Jr, J. C. *A exploração de frutos como alimento por aves de mata ciliar numa região do Distrito Federal*, thesis, UNESP, Rio Claro, SP (1991).

81. Argel-de-Oliveira, M. M. *Frugivoria por aves em um fragmento de floresta de restinga no estado do Espírito Santo, Brasil*, thesis, UNICAMP, Campinas, SP (1999).

82. Ikuta, K. G. & Martins, F. C. Interação entre aves frugívoras e plantas no Parque Estadual da Cantareira, estado de São Paulo. *Atualidades Ornitológicas* **172**, 33–36 (2013).

83. Donatti, C. I. *et al.* Analysis of a hyper-diverse seed dispersal network: modularity and

underlying mechanisms. *Ecol. Lett.* **14**, 773–781 (2011).

84. Gondim, M. J. C. *A exploração de frutos por aves frugívoras em uma área de Cerradão no Estado de São Paulo*, thesis, UNESP, Rio Claro, SP (2002).

85. Ruggera, R. A., Blendinger, P. G., Gomez, M. D. & Marshak, C. Linking structure and functionality in mutualistic networks: do core frugivores disperse more seeds than peripheral species? *Oikos* **125**, 541–555 (2016).

86. Blendinger, P. G. *et al.* Scale-dependent spatial match between fruits and fruit-eating birds in Andean mountain forests. *Biotropica* **47**, 702–711 (2015).

87. Blendinger, P. G. *et al.* Fine-tuning the fruit-tracking hypothesis: spatiotemporal links between fruit availability and fruit consumption by birds in Andean mountain forests. *J. Anim. Ecol.* **81**, 1298–1310 (2012).

88. Menezes Pinto, Í., Emer, C., Cazetta, E. & Morante-Filho, J. C. Deforestation simplifies understory bird seed-dispersal networks in human-modified landscapes. *Front. Ecol. Evol.* **9**, 640210 (2021).

89. Boyle, W. A., Conway, C. J. & Bronstein, J. L. Why do some, but not all, tropical birds migrate? A comparative study of diet breadth and fruit preference. *Evol. Ecol.* **25**, 219–236 (2011).

90. Crome, F. H. J. Foraging ecology of an assemblage of birds in lowland rainforest in northern Queensland. *Aust. J. Ecol.* **3**, 195–212 (1978).

91. Gopal, A., Mudappa, D., Raman, T. R. S. & Naniwadekar, R. Forest cover and fruit crop size differentially influence frugivory of select rainforest tree species in Western Ghats, India. *Biotropica* **52**, 871–883 (2020).

92. Li, H. *et al.* The functional roles of species in metacommunities, as revealed by

metanetwork analyses of bird–plant frugivory networks. *Ecol. Lett.* **23**, 1252–1262 (2020).

93. Herrera, C. M. A study of avian frugivores, bird-dispersed plants, and their interaction in Mediterranean scrublands. *Ecol. Monogr.* **54**, 1–23 (1984).

94. Plein, M. *et al.* Constant properties of plant-frugivore networks despite fluctuations in fruit and bird communities in space and time. *Ecology* **94**, 1296–1306 (2013).

95. Stiebel, H. *Frugivorie bei mitteleuropäischen Vögeln*, thesis, Universität Oldenburg (2003).

96. Muñoz, M. C., Schaefer, H. M., Böhning-Gaese, K. & Schleuning, M. Importance of animal and plant traits for fruit removal and seedling recruitment in a tropical forest. *Oikos* **126**, 823–832 (2017).

97. Quitián, M. *et al.* Elevation-dependent effects of forest fragmentation on plant-bird interaction networks in the tropical Andes. *Ecography* **41**, 1497–1506 (2018).

98. Dehling, D. M. *et al.* Functional relationships beyond species richness patterns: trait matching in plant-bird mutualisms across scales. *Glob. Ecol. Biogeogr.* **23**, 1085–1093 (2014).

99. Buitrón-Jurado, G. *Diversidad de aves frugívoras y árboles, redes de interacción e identificación de árboles magnetos en dos bosques nublados de Venezuela con distintas condiciones de fragmentación*, thesis, Instituto Venezolano de Investigaciones Científicas, Miranda, Venezuela (2012).

100. Balasubramanian, P. Interactions between fruit-eating birds and bird-dispersed plants in the tropical dry evergreen forest of Point Calimere, South India. *J. Bombay Nat. Hist. Soc.* **93**, 428–441 (1996).

101. Chimera, C. G. & Drake, D. R. Patterns of seed dispersal and dispersal failure in a

hawaiian dry forest having only introduced birds. *Biotropica* **42**, 493–502 (2010).

102. Githiru, M., Lens, L., Bennur, L. A. & Ogol, C. P. K. O. Effects of site and fruit size on the composition of avian frugivore assemblages in a fragmented Afrotropical forest. *Oikos* **96**, 320–330 (2002).

103. Malmborg, P. K. & Willson, M. F. Foraging ecology of avian frugivores and some consequences for seed dispersal in an Illinois woodlot. *Condor* **90**, 173–186 (1988).

104. Spotswood, E. N., Meyer, J. Y. & Bartolome, J. W. An invasive tree alters the structure of seed dispersal networks between birds and plants in French Polynesia. *J. Biogeogr.* **39**, 2007–2020 (2012).

105. Wolfe, J. D., Johnson, M. D. & Ralph, C. J. Do birds select habitat or food resources? Nearctic-neotropic migrants in northeastern Costa Rica. *PLoS One* **9**, e86221 (2014).

106. Chen, C. C. & Chou, L. S. The diet of forest birds at Fushan Experimental Forest. *Taiwan J. For. Sci.* **14**, 275–287 (1999).

107. Kamruzzaman, M. & Asmat, G. S. M. Seasonal variations of fruit preference among frugivorous birds in Chittagong, Bangladesh. *Bangladesh J. Zool.* **36**, 187–206 (2008).

108. Palmeirim, J. M., Gorchov, D. L. & Stoleson, S. Trophic structure of a neotropical frugivore community: is there competition between birds and bats? *Oecologia* **79**, 403–411 (1989).

109. Blake, J. G. & Loiselle, B. A. Fruits in the diets of neotropical migrant birds in Costa Rica. *Biotropica* **24**, 200–210 (1992).

110. Traveset, A. Resultats preliminars sobre el consum de fruits per ocells a l'illa de Cabrera (Illes Balears). *Anu. Ornitològic les Balear* **7**, 3–9 (1992).

111. Fortuna, M. A., Ortega, R. & Bascompte, J. The web of life. Preprint at

https://arxiv.org/abs/1403.2575 (2014).

112. Schleuning, M. *et al.* Specialization of mutualistic interaction networks decreases toward tropical latitudes. *Curr. Biol.* **22**, 1925–1931 (2012).

113. Dalsgaard, B. *et al.* Opposed latitudinal patterns of network-derived and dietary specialization in avian plant–frugivore interaction systems. *Ecography* **40**, 1395–1401 (2017).

114. Chao, A., Colwell, R. K., Lin, C. & Gotelli, N. J. Sufficient sampling for asymptotic minimum species richness estimators. *Ecology* **90**, 1125–1133 (2009).